

**ENGINEERING TARGET TISSUE IN LAB-ON-A-
CHIP DEVICES FOR PREDICTING HOMING
CHOICES OF METASTATIC CANCER**

**A Thesis Submitted to
The Graduate School of Engineering and Sciences of
İzmir Institute of Technology
in Partial Fulfillment of the Requirements for the Degree of**

DOCTOR OF PHILOSOPHY

in Bioengineering

**by
Gizem BATI AYAZ**

**December 2020
İZMİR**

ACKNOWLEDGEMENTS

First and foremost I would like to express my sincere gratitude to my supervisor Prof. Devrim Pesen Okvur for her guidance, encouragement, and endless support throughout my PhD. This work would not be possible without her. I would also like to thank my co-supervisor Assit. Prof. Yavuz Oktay for his support. I am grateful to Assoc. Prof. Özden Yalçın Özuysal for her invaluable suggestions and scientific guidance over the course of the work. I would also like to thank Prof. Ataç Sönmez for his advice during the thesis progression.

Furthermore, my thanks go to friends and colleagues especially my group mates, Müge Bilgen, İsmail Tahmaz, Burcu Fıratlıgil Yıldırım, Aslı Kısım, Begüm Gökçe. As teamwork is essential, I am very thankful to the members of the Controlled *in vitro* Microenvironments (CivMs) laboratory for their team spirit, help and support. I would like to thank to my friends and colleagues Eyüp Yöndem, Güncem Ocak, Deniz Cemre Turgut, Helin Giriş, Elif Sıla Tanaydın, Abdurehman Eshete for their support, help and friendship.

I would also like to gratefully acknowledge TÜBİTAK through the project number of 115E057, TÜBİTAK BİDEB 2211-C scholarship and YÖK 100/2000 scholarship for the financial support during this PhD research.

My special thanks go to my parents for their constant support and encouragements in every step of my way. The last but not the least, my sincere appreciation goes to my beloved husband, Umur Ayaz. He has always shown his patience and love for me through difficult times.

ABSTRACT

ENGINEERING TARGET TISSUE IN LAB-ON-A-CHIP DEVICES FOR PREDICTING HOMING CHOICES OF METASTATIC CANCER

The metastatic cascade of cancer results in the extravasation of the tumor to other parts of the body. Metastasis is the leading cause of cancer related deaths. Breast cancer is the most common cancer in women, and lung is one of the organs with the most metastasis. For this reason, it is critical to engineer a tissue microenvironment that includes complex cell-cell interactions with co-culture of endothelial, epithelial and stromal cells, and the invasion and extravasation steps of metastasis can be observed for early diagnosis of metastasis. Vascularization is the critical step for engineering the tissues. The *in vitro* models used today are insufficient to create the tissue environment closest to *in vivo* conditions. Recently developed lab-on-a-chip platforms provide suitable environments for mimicking the *in vivo* structure in tissue engineering studies.

In this research:

- ✓ Different lab-on-a-chip devices fabricated to engineer breast and lung target tissues.
- ✓ For the first time, epithelial, fibroblast and endothelial cells were tri-cultured and breast and lung tissue environments were engineering with microvasculature.
- ✓ Different gel, media and cell numbers have been optimized for engineering of breast and lung tissue environments with microvascularization.
- ✓ Different matrix environments have been optimized to observe invasion and/or extravasation steps separately or together.

ÖZET

METASTATİK KANSERİN HEDEFLENME SEÇİMLERİNİN TAHMİNİ İÇİN YONGA-ÜSTÜ-LABORATUVAR AYGITLARI İÇİNDE HEDEF DOKU MÜHENDİSLİĞİ

Kanserin metastatik kaskadı, tümörün vücudun diğer bölgelerine yayılması ile sonuçlanır. Metastaz, kansere bağlı ölümlerin önde gelen nedenidir. Meme kansere kadınlarda en sık görülen kanser olup akciğer, metastazının en çok görüldüğü organlardan biridir. Bu sebeple metastazın erken tanısı için metastazın invazyon ve ekstrasvazyon basamaklarının gözlenebileceği, endotel, epitel ve stromal hücrelerinin ko-kültürü ile kompleks hücre-hücre etkileşimlerini içerecek doku mikroçevresinin oluşturulabilmesi kritik önem taşımaktadır. Damarlanma doku mühendisliği için kritik bir adımdır. Günümüzde kullanılan *in vitro* modeller, *in vivo* koşullara en yakın doku ortamının oluşturulması için yetersiz kalmaktadır. Son yıllarda gelişen yonga-üstü-labratuvar ortamları *in vivo* yapıyı taklit etmek ve doku mühendisliği çalışmaları için uygun ortamlar sağlamaktadır.

Bu çalışmada:

- ✓ Meme ve akciğer hedef dokularının üretilmesi için farklı yonga-üstü-laboratuvar cihazları üretilmiştir.
- ✓ İlk defa epitel, fibroblast ve endotel hücrelerinin tri-kültürü gerçekleştirilerek mikrodamarlanma ile birlikte meme ve akciğer doku ortamları oluşturulmuştur.
- ✓ Meme ve akciğer doku ortamlarının mikrodamarlanma ile birlikte oluşturulması için farklı jel ortamları ve hücre sayıları optimize edilmiştir.
- ✓ İnvazyon ve ekstrasvazyon basamaklarının ayrı ayrı ve birlikte gözlemlenebilmesi için matriks ortamları optimize edilmiştir.

TABLE OF CONTENTS

LIST OF FIGURES	x
LIST OF TABLES	xvi
CHAPTER 1	1
1. Objectives	1
CHAPTER 2	2
2.1. Cancer	2
2.1.1. Homing Choices of Metastatic Breast Cancer	3
2.2. Structure of Normal and Malignant Breast Tissue	4
2.3. Structure of Normal Lung Tissue and The Pulmonary Metastatic Niche	6
2.4. Mesenchymal Stem Cells (MSCs)	8
2.5. Lab-on-a-chip Technology.....	9
2.6. Tissue Engineering and Organotypic Microfluidic 3D <i>in vitro</i> Models	12
CHAPTER 3	14
3.1. Fabrication of Lab-on-a-chip Devices for Construction of Target Tissues	14
3.1.1. UV Lithography and 3D Printing for the Fabrication of Molds ...	14
3.1.2. Soft Lithography	15
3.1.2.1. Cleaning of PDMS LOC Device.....	15
3.1.2.2. Bonding of PDMS LOC Device	16
3.2. Coating of PDMS LOC Device	17
3.3. Cell Culture	18
3.3.1. Maintenance of b.End3	18
3.3.2. Maintenance of HUVEC-C	18

3.3.3. Maintenance of MCF-10A	19
3.3.4. Maintenance of WI38.....	19
3.3.5. Maintenance of Beas-2B	19
3.3.6. Maintenance of MDA-MB-231.....	20
3.3.7. Maintenance of Raw264.7	20
3.3.8. Maintenance of 3T3-L1.....	20
3.3.9. Maintenance of MCF-7	20
3.3.10. Labeling of Cell Lines.....	21
3.4. Preparation of Fibrin Gel	22
3.5. Media Preparation for Target Tissue for Acini Structure	23
3.6. LOC Device Gradient Characterization.....	23
3.7. Generation of Endothelial Monolayer	24
3.8. Endothelial Monolayer Integrity Assay	24
3.9. Invasion Assay	25
3.10. Extravasation Assay.....	25
3.11. Analysis of Extravasation Assay	26
CHAPTER 4	28
4.1. Generation of Microvascular Network	28
4.1.1. Low and High Concentrations of Endothelial Cells.....	28
4.1.2. Different Endothelial Cell Lines	30
4.1.3. Use of Fibroblasts as Stromal Cells	32
4.1.4. Different Fibrin Gel Compositions	37
4.1.5. Use of Fibroblasts in Co-culture with Endothelial Cells	41
4.1.6. Use of Matrigel and Collagen in Fibrin Gel.....	43
4.2. Engineering Breast and Lung Tissue	45
4.2.1. Co-culture of Raw264.7 and MCF-10A in Fibrin Gel.....	45
4.2.2. Tri-culture of HUVEC-C, Raw264.7 and MCF-10A in Fibrin Gel.....	46
4.2.3. Co-culture of HUVEC-C with 3T3-L1 or MCF-10A Cells in	

Fibrin Gel.....	48
4.2.4. Tri-culture of b.End3, 3T3-L1 and MCF-10A Cells in Fibrin gel for Generation of Breast Tissue.....	58
4.2.5. Testing the Effect of Different Mediums and Combination of Cells for Induction of Microvascular Sprouting.....	66
4.2.5.1. Laminin Coated and Non-Coated Surfaces to Test Vascular Sprouting in Breast Tissue.....	68
4.2.5.2. Test of Low Height and Thin Post Gaps of LOC for MVN Formation and Sprouting of Endothelial Cells.....	70
4.2.5.3. The Effect of Matrigel Containing Media on Structure of Breast Epithelial Cells.....	72
4.2.5.4. Low Height and Thin Post Gaps of LOC for Generation of MVN in Lung Tissue.....	74
4.2.5.5 Test of the Formation of MVN in the Presence of Mesenchymal Stem cells (MSCs) in the Matrix for Lung Tissue.....	76
4.2.5.6 Use of Matrigel and Collagen Containing Fibrin Gel for Generation of Lung Tissue.....	84
4.2.5.7. The Effect of Matrigel Containing Media on Structure of Lung Epithelial Cells.....	85
4.3. Invasion of Different Cell Lines in Fibrin Gel and GFR Matrigel and Mixture of Fibrin and GFR-matrigel (FM).....	86
4.3.1. Invasion of Cells into Breast and Lung Tissue Mimics Laden GFR-Matrigel.....	88
4.3.2. Invasion of Cells into Breast and Lung Tissue Mimics Laden Mixture of Fibrin Gel and GFR-Matrigel (FM).....	92
4.4. Extravasation of Different Cell Lines into Breast and Lung Tissue Mimics.....	97
4.4.1. Formation of Endothelial Monolayer.....	97
4.4.1.1. Characterization of Endothelial Monolayer.....	99

4.4.1.2. Extravasation into Lung Tissue Mimics	101
4.4.2. Formation of MVN in Tissue Mimics.....	102
CHAPTER 5	106
REFERENCES	109



LIST OF FIGURES

<u>Figure</u>	<u>Page</u>
Figure 2.1. Hallmarks of cancer ¹	2
Figure 2.2. Metastatic choices of breast cancer in the different organs.....	3
Figure 2.3. Most common metastasis sites of breast cancer at autopsy ³	3
Figure 2.4. Structure of normal and malignant breast tissue ⁵	5
Figure 2.5. Structure of mammary gland <i>in vivo</i> and MCF10A <i>in vitro</i> ⁶	5
Figure 2.6. Structure of alveoli.	7
Figure 2.7. The multipotentiality of MSCs ¹⁰	9
Figure 2.8. Fabrication of the master mold by UV lithography ¹⁴	11
Figure 3.1. a) Polymerized PDMS b) LOC devices c) Different size of punctures.....	15
Figure 3.2. Permanent bonding of PDMS LOC devices onto glass slide a) Cleaning of dusts b) Placement of glass slides and LOC devices c) UV Ozone treatment d) Permanent bonding e) LOC devices.....	16
Figure 3.3. Hydrophobicity of glass and PDMS surfaces.....	16
Figure 3.4. Different lab-on-a-chip devices for distinct experimental setups.	17
Figure 3.5. Preperation of fibrin gel.	23
Figure 3.6. The formula to calculate the permeability of the endothelial monolayer....	24
Figure 3.7. a) Invasion and b) Extravasation procedure.	27
Figure 4.1. Experimental conditions for generation of MVN.....	28
Figure 4.2. Confocal images of 3.5×10^6 /ml HUVEC-C in fibrin gel day by day.....	28
Figure 4.3. Confocal images of 3.5×10^6 /ml HUVEC-C for day2.....	29
Figure 4.4. Confocal images of 6×10^6 /ml HUVEC-C in fibrin gel day by day.....	29
Figure 4.5. Confocal images of 6×10^6 /ml b.End3 in fibrin gel day by day.....	30
Figure 4.6. Confocal images of 6×10^6 /ml b.End3 in fibrin gel for day 7.	30
Figure 4.7. Confocal images of 65×10^4 /ml b.End3 in fibrin gel for day 2 and day 6. ...	31
Figure 4.8. Experimental setup to observe the effect of fibroblasts.	32
Figure 4.9. Confocal images of 4.9×10^6 /ml HUVEC-C in fibrin gel day by day.....	33
Figure 4.10. Confocal images of LOC device containing 4.9×10^6 /ml HUVEC-C in fibrin.....	34
Figure 4.11. Confocal images of LOC device containing 4.9×10^6 /ml HUVEC-C in fibrin.....	35

<u>Figure</u>	<u>Page</u>
Figure 4.12. Confocal images of 4.5×10^6 /ml HUVEC- in fibrin gel by day.	36
Figure 4.13. Confocal images of 6×10^6 /ml b.End3 in fibrin gel day by day.	37
Figure 4.14. Confocal images of 6×10^6 /ml b.End3 in fibrin gel for day 2.	38
Figure 4.15. Confocal images of 6×10^6 /ml b.End3 in fibrin gel for day 2 and day 5.	39
Figure 4.16. Confocal images of 4.5×10^6 /ml b.End3 and 0.163×10^6 /ml D1-ORL- UVA	40
Figure 4.17. Confocal images of 4.5×10^6 /ml b.End3 in fibrin gel for day 1, day 2 and day 6.	41
Figure 4.18. Confocal images of 7.9×10^6 /ml b.End3 and 1×10^6 /ml 3T3-L1 cells in fibrin gel for day 1.	42
Figure 4.19. Comparison of confocal images of 7.9×10^6 /ml b.End3 and 1×10^6 /ml 3T3-L1 cells in fibrin gel for day 1 and day 2.	43
Figure 4.20. Confocal images of 3×10^6 /ml b.End3 and 1.8×10^6 /ml 3T3-L1 cells in fibrin gel for day 1 and day 2.	44
Figure 4.21. Confocal images of 3×10^6 /ml b.End3 and 1.8×10^6 /ml 3T3-L1 cells in fibrin gel after dextran diffusion at day 2.	44
Figure 4.22. Confocal images of Raw264.6, MCF-10A in fibrin gel for day 4.	45
Figure 4.23. Confocal images of Raw264.6, MCF-10A in fibrin gel for day 4.	46
Figure 4.24. Confocal images of HUVEC-C, Raw264.6, MCF-10A in fibrin gel day by day.	46
Figure 4.25. Confocal images of HUVEC-C, Raw264.6, MCF-10A in fibrin gel for day 4.	47
Figure 4.26. Confocal images of HUVEC-C, Raw264.6, MCF-10A in fibrin gel for day 5.	47
Figure 4.27. Confocal images of HUVEC-C and 3T3-L1 in fibrin gel the day by day.	48
Figure 4.28. Confocal images of HUVEC-C and MCF-10A in fibrin gel the day by day.	49
Figure 4.29. Confocal images of HUVEC-C and MCF10A cells in concentration of 0.325×10^6 /ml at day 2 and day 7.	50

<u>Figure</u>	<u>Page</u>
Figure 4.30. Confocal images of 4.9×10^6 /ml HUVEC-C and 0.75×10^6 /ml MCF-10A in fibrin gel and 2×10^6 /ml 3T3-L1 in reservoirs away from endothelial cells day by day.....	51
Figure 4.31. Confocal images of 4.9×10^4 /ml HUVEC-C and 0.75×10^6 /ml MCF-10A in fibrin gel day by day.	52
Figure 4.32. Confocal images of 4.9×10^6 /ml HUVEC-C and 3.4×10^6 /ml MCF-10A in fibrin gel and 2×10^6 /ml 3T3-L1 at the lateral channels.	53
Figure 4.33. Confocal images of 4×10^6 /ml HUVEC-C and 2×10^6 /ml MCF-10A in fibrin gel in fibrin gel and 1×10^6 /ml 3T3-L1 at the lateral medium channels.....	54
Figure 4.34. Confocal images of 4×10^4 /ml HUVEC-C and 2×10^6 /ml MCF-10A in fibrin gel in fibrin gel day.	55
Figure 4.35. Confocal images of 4×10^6 /ml HUVEC-C and 4×10^6 /ml MCF-10A in fibrin gel in fibrin gel and 1×10^6 /ml 3T3-L1 at he lateral channels.....	56
Figure 4.36. Confocal images of 4×10^6 /ml /ml HUVEC-C and 4×10^6 /ml MCF-10A in fibrin gel day by day.	57
Figure 4.37. Comparison of high and low concentrations of co-culture conditions for b.End3, 3T3-L1, MCF-10A cells in fibrin gel for day 1 and day 5.	59
Figure 4.38. Confocal images of b.End3, 3T3-L1, and MCF-10A cells in fibrin gel with the different cell concentrations.....	61
Figure 4.39. Confocal photos of 3×10^6 /ml b.End3, 0.9×10^6 /ml MCF-10A, and 0.9×10^6 /ml 3T3-L1 in fibrin gel day by day.	62
Figure 4.40. Confocal photos of 3×10^6 /ml b.End3, 1.3×10^6 /ml MCF-10A, and 0.5×10^6 /ml 3T3-L1 in fibrin gel day by day.	63
Figure 4.41. Confocal photos of 3×10^6 /ml b.End3, 1.35×10^6 /ml MCF-10A, and 0.45×10^6 /ml 3T3-L1 in fibrin gel with different gel concentration day by day.....	64
Figure 4.42. Brightfield Z-stack images of target tissue in 2 mg/ml fibrin gel at day 4.....	65
Figure 4.43. Fluorescence Z-stack images of endothelial cells in 2 mg/ml fibrin gel at day 4.....	65

<u>Figure</u>	<u>Page</u>
Figure 4.44. Fluorescence Z-stack images of dextran 70kDa in 2 mg/ml fibrin gel at day 4.....	66
Figure 4.45. Test of different VEGF doses in vasculature.	66
Figure 4.46. 50ng/ml VEGF and 100ng/ml Ang-1.....	67
Figure 4.47. 0 and 100ng/ml VEGF in the absence of MSCs.	67
Figure 4.48. 50ng/ml VEGF conditions with endothelial cells at the lateral channels...	68
Figure 4.49. Breast tissue with 2% matrigel containing media in APTES coated or uncoated LOC devices (m: matrix, r: reservoir).	69
Figure 4.50. Confocal images of mimicking breast tissue in fibrin gel in one post LOC devices for day 1, day 3.	70
Figure 4.51. Confocal images of mimicking breast tissue in fibrin gel in three posts LOC devices for day 1, day 3.	71
Figure 4.52. Confocal photos of mimicking breast tissue in fibrin gel in five posts and high height LOC devices for day 1, day 3.....	72
Figure 4.53. Acinus structure of MCF-10A epithelial cells in matrigel containing media at day 6.	73
Figure 4.54. Lobular unit (a) and acinar structure (b) of MCF-10A cells.	73
Figure 4.55. Confocal images of mimicking lung tissue in fibrin gel in one post LOC devices for day 1, day 3.	74
Figure 4.56. Confocal images of mimicking lung tissue in fibrin gel in five posts LOC devices for day 1, day 3.	75
Figure 4.57. Confocal images of mimicking lung tissue in fibrin gel in five posts LOC devices for day 2, 3 and 6 in the presence of MSCs.	77
Figure 4.58. Confocal images of mimicking lung tissue in fibrin gel in five posts LOC devices for day 2, 3 and 6 in the absence of MSCs.	77
Figure 4.59. Confocal images of mimicking lung tissue in fibrin gel in five posts LOC devices for day 2, 3 and 6 in the presence of MSCs.	78
Figure 4.60. Confocal images of mimicking lung tissue in fibrin gel in five posts LOC devices for day 2, 3 and 6 in the absence of MSCs.	78
Figure 4.61. Confocal images of lung tri-culture in fibrin gel according to Wisco numbers in high height of LOC device.....	79

<u>Figure</u>	<u>Page</u>
Figure 4.62. Confocal images of lung tri-culture in fibrin gel according to Wisco numbers in low height of LOC device.	80
Figure 4.63. Confocal images of lung tri-culture in fibrin gel according to Wisco numbers in high height of LOC device in the absence of MSCs.	81
Figure 4.64. Confocal images of lung tri-culture in fibrin gel according to Wisco numbers in low height of LOC device in the absence of MSCs.	82
Figure 4.65. Confocal images of lung tri-culture in fibrin gel according to Jeon numbers in high height of LOC device.	82
Figure 4.66. Confocal images of lung tri-culture in fibrin gel according to Jeon numbers in low height of LOC device.	83
Figure 4.67. Confocal images of lung tissue in matrigel and collagen containing fibrin gel.	84
Figure 4.68. Confocal images after application of dextran 70kDa of lung tissue in matrigel and collagen containing fibrin gel.	84
Figure 4.69. Images of alveolar ducts.	85
Figure 4.70. Structure of Beas-2B epithelial cells in fibrin gel at day 7.	85
Figure 4.71. Invasion of breast cancer cells in only containing fibrin gel structure.	86
Figure 4.72. Invasion capacity of cells in GFR-matrigel.	86
Figure 4.73. Invasion capacity of cells in mixture of fibrinogen and GFR matrigel.	87
Figure 4.74. Invasion index of different cells into GFR-matrigel.	87
Figure 4.75. Invasion index of different cells into FM.	87
Figure 4.76. Invasion of cells into lung fibroblast laden within GFR-matrigel.	89
Figure 4.77. Invasion of cells into breast fibroblast laden within GFR-matrigel.	89
Figure 4.78. Invasion of cells into lung epithelial cell laden within GFR-matrigel.	90
Figure 4.79. Invasion of cells into breast epithelial cell laden within GFR-matrigel.	90
Figure 4.80. Invasion of cells into lung tissue mimic laden within GFR-matrigel.	91
Figure 4.81. Invasion of cells into breast tissue mimic laden within GFR-matrigel.	91
Figure 4.82. Invasion of cells into lung fibroblast cell laden within FM.	92
Figure 4.83. Invasion of cells into breast fibroblast cell laden within FM.	93
Figure 4.84. Invasion of cells into lung epithelial cell laden within FM.	93
Figure 4.85. Invasion of cells into breast epithelial cell laden within FM.	94
Figure 4.86. Invasion of cells into lung tissue mimic laden within FM.	94

<u>Figure</u>	<u>Page</u>
Figure 4.87. Invasion of cells into breast tissue mimic laden within within FM.....	95
Figure 4.88. Invasion index of distinct cells into epithelial cells, fibroblasts or breast and lung tissue mimics laden within GFR-matrigel seperately day by day.....	95
Figure 4.89. Invasion index of distinct cells into epithelial cells, fibroblasts or breast and lung tissue mimics laden within FM seperately day by day.	96
Figure 4.90. Summary of invasion into distinct matrices.	96
Figure 4.91. Dextran ensured homogeneous distribution of endothelial cells.....	98
Figure 4.92. Laminin coating resulted in efficient intact endothelial monolayer formation. (a) Representative 3D images of extravasation LOC showing endothelial cells (green) on laminin (LAM) coated surfaces from different views (top, side 1 and side 2). (b) The endothelial monolayer between the post gaps are represented with two-sided arrows (Scale bar: 200 μ M).....	98
Figure 4.93. Staining of endothelial monolayer composed of different sources of endothelial cells.....	99
Figure 4.94. (a) Confocal images of 70 kDa dextran, (b) fluorescence intensity of 70 kDa dextran, (c) permeability of 70 kDa dextran in the absence and the presence of HUVEC (Scale bar: 500 μ M).	100
Figure 4.95. Permeability values of different gel componenet with or without endothelial cells.....	100
Figure 4.96. Extravasation of MDA-MB-231 breast cancer cells into generated lung tissue.....	101
Figure 4.97. Lung tissue in fibrin and GFR matrigel mixture at day 2.	102
Figure 4.98. Confirmation of MVN formation at day 2.	102
Figure 4.99. Lung tissue laden within fibrin and GFR matrigel mixture after dextran loading and staining.	103
Figure 4.100. Extravasation of breast cancer cells into lung and breast tissue mimics with MVN.	104
Figure 4.101. Analysis of extravasation in MVN tissue mimics.	104
Figure 4.102. Extravasation of breast cancer cells for breast and lung tissue mimics.	105

LIST OF TABLES

<u>Table</u>	<u>Page</u>
Table 1. Typical sites of metastatic relapse for solid tumours ⁴	4
Table 2. Componentes of acinus generating medium ⁶	23
Table 3. Cell lines for breast and lung tissue.....	58
Table 4. The gel components containing high concentration of fibrinogen without aprotinin.	59
Table 5. Cell concentrations ³⁷	74
Table 6. Cell concentrations and doubling times.....	76
Table 7. Cell concentrations from different sources.....	79

CHAPTER 1

INTRODUCTION

1. Objectives

The goal of the study is to engineer different target tissues in lab-on-a-chip devices that will be used for predicting homing choices of metastatic cancer. Specific aims are:

- ✓ To fabricate lab-on-a-chip devices.
- ✓ To optimize tri-culture of cell types namely, endothelial cells, fibroblasts, and epithelial cells that are relevant to breast and lung tissues.
- ✓ To determine homing choices of different breast cancer cells in lab-on-a-chip devices containing the engineered tissues.

CHAPTER 2

LITERATURE REVIEW

2.1. Cancer

Cancer is the worldwide disease which has incidence on both men and woman in different organs such as brain, liver, lung, and breast. This disease has been arised the result of the uncontrolled cell proliferation. It uses mainly six properties for the multistep progression and the growth of tumor. The features of cancer cells can be listed in here: 1) Sustaining proliferative signaling: In the normal tissue, the growth signals are controlled during the cell cycle for both the maintenance of the cell number and the structure of the tissue. But the cancer cells get out of control in the non-observant manner. 2) Evading growth suppressors: Cancer cells can achieve the maintenance of the cell proliferation via the tumor suppressor genes. 3) Resisting cell death: Programmed cell death is known as apoptosis. These cells limit the apoptosis via the antiapoptotic factors. 4) Enabling replicative immortality 5) Inducing angiogenesis: Cancer cells form new blood vessels since they need more nutrient and oxygen supply during the tumor growth 6) Activating invasion and metastasis: Cancer cells invade into extracellular matrix (ECM) by the degradation of the basement membrane. Then they can reach and enter the blood vessels (intravasation). The next step reveals via the escape of cancer cells from the blood vessels (extravasation). At the end, they can form new tumor at the distant sites of the body in the different organs (metastasis) ¹.

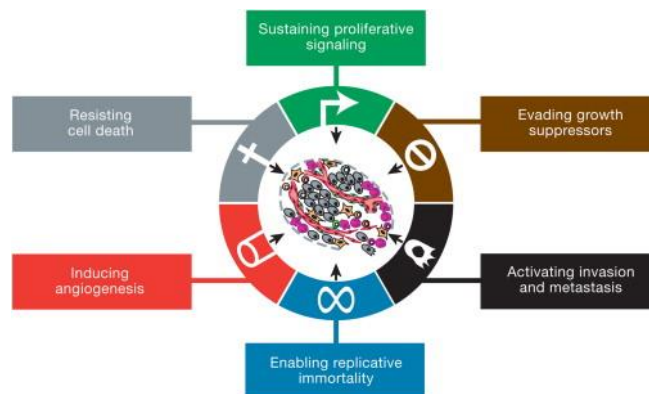


Figure 2.1. Hallmarks of cancer ¹.

2.1.1. Homing Choices of Metastatic Breast Cancer

Metastasis doesn't occur randomly in the organs. This situation was made sense of "seed and soil" hypothesis by Stephan Paget. It explains that tumor cells choose the certain microenvironments (the "seed") in the specific organs (the "soil") during the metastasis of cancer ².

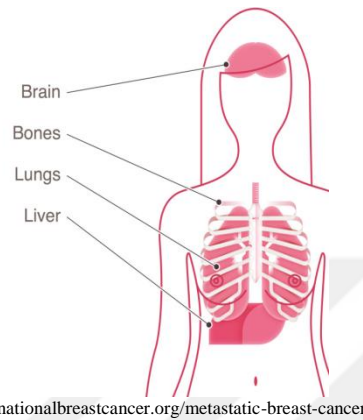


Figure 2.2. Metastatic choices of breast cancer in the different organs.

The dissemination of the breast cancer carcinoma is resulted in metastases in the different organs such as bone, lung, liver that are listed below depending on the common sites from the breast cancer autopsy ³.

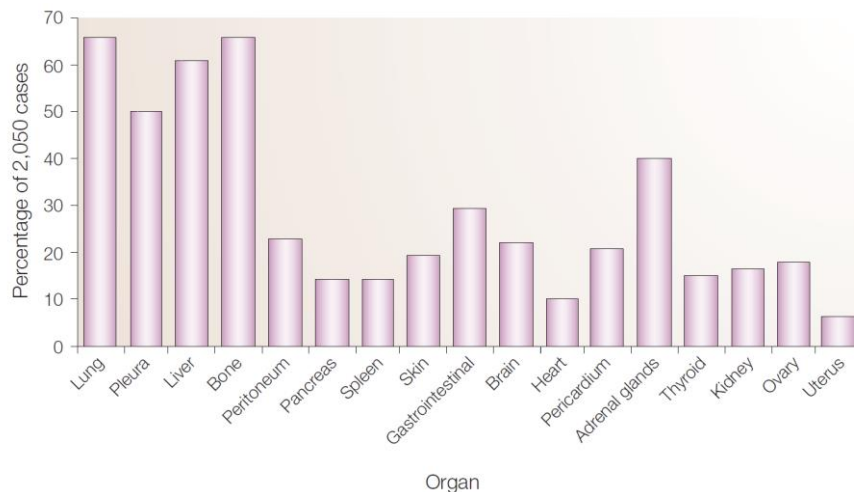


Figure 2.3. Most common metastasis sites of breast cancer at autopsy ³.

90% of cancer death is because of the metastasis. Lung, liver, brain, bone are important organs for the dissemination of the breast cancer. Prominent property of different kinds of metastatic cancers is the formation of new tumor at the different sites of the body or organs ⁴.

Table 1. Typical sites of metastatic relapse for solid tumours ⁴.

Tumour type	Principal sites of metastasis
Breast	Bone, lungs, liver and brain
Lung adenocarcinoma	Brain, bones, adrenal gland and liver
Skin melanoma	Lungs, brain, skin and liver
Colorectal	Liver and lungs
Pancreatic	Liver and lungs
Prostate	Bones
Sarcoma	Lungs
Uveal melanoma	Liver

2.2. Structure of Normal and Malignant Breast Tissue

The mammary gland occurs in only mammals for the supplement of nutrition to living newborn creature. Development of mammary progresses in the developmental process and this gland is immature at birth. Production of high levels of hormones such as estrogen and progesterone is the sign of the puberty beginning. After puberty, growth cycle and involution is controlled by the menstrual cycles of pregnancy and lactation. Structure of the mammary gland consists of immature branches duct system locating with a fat pad. Enhancement of ductal branching occurs after the pubertal developmental process and this ductal tree overspread the fat pad. After weaning, mammary gland transforms into pre-pregnancy form via apoptosis. Production and release of milk is realized by continuous epithelial cells in the ductal structure of breast into the lumen. Myoepithelial cells are in contact with the basement membrane in the layer. Fibroblasts cover these two layer as the basis of the ducts ⁵.

Figure 2.4 shows the structure of normal and malignant breast tissue. At the a) part of the figure, the anatomy of the human mammary gland is shown. Branching ducts in 15-20 lobes form mammary glands in contact with nipple. b) Epithelial cells as a

layer accompany with each duct that plays a role in milk production. This structure is covered by contractible myoepithelial cells. The embedded glandular ducts take place in fibroblast stroma. c) This structure is destroyed in breast cancer with the presence of an epithelial cell mass (Staining antibodies ER: brown stained nuclei, Low ER positive epithelial cells present in the normal breast).

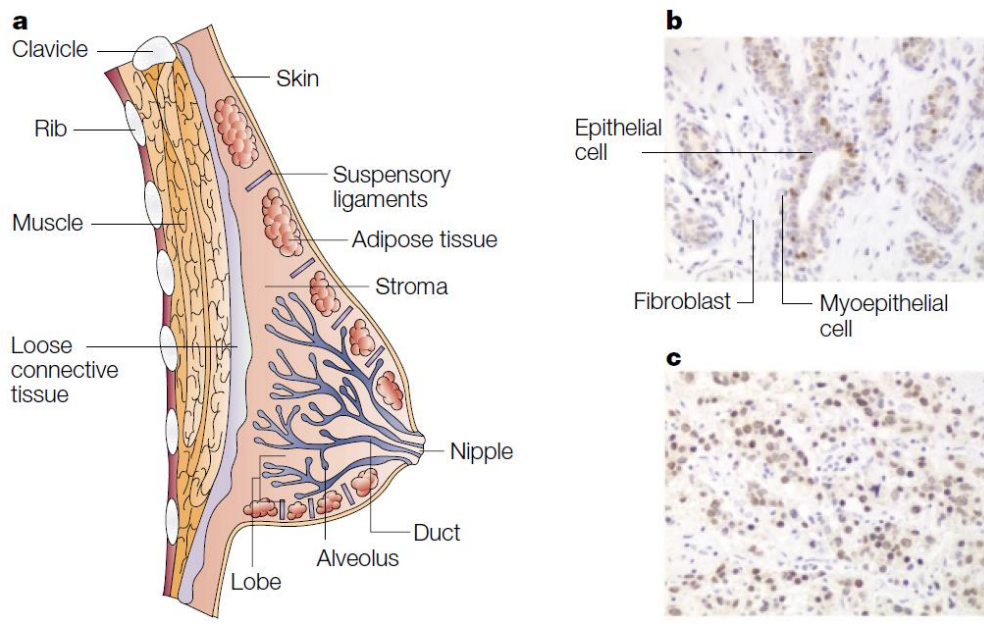


Figure 2.4. Structure of normal and malignant breast tissue ⁵.

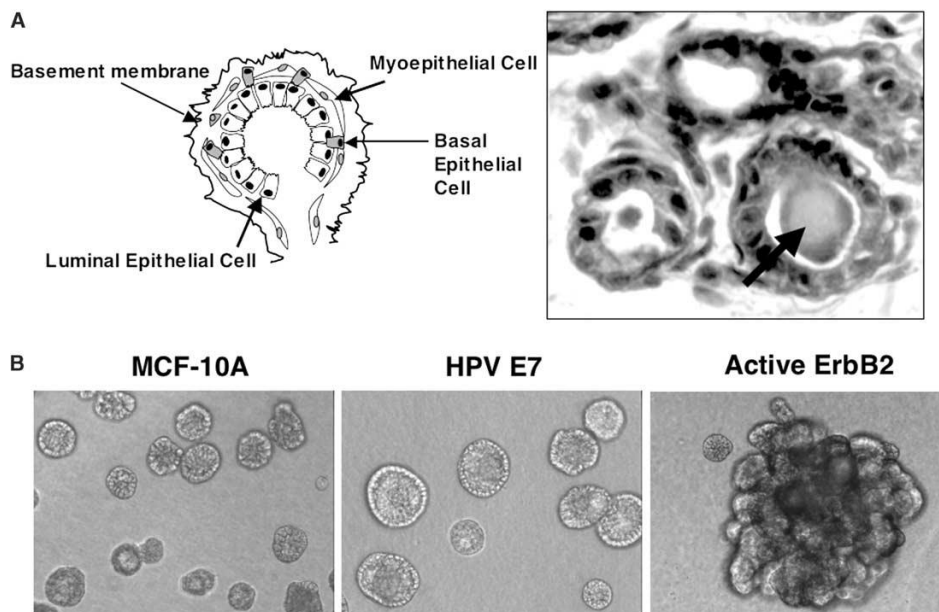


Figure 2.5. Structure of mammary gland *in vivo* and MCF10A *in vitro* ⁶.

Figure 2.5 shows the architecture of mammary gland. In schematic, polarized epithelium rounds a hollow lumen, that consists of luminal epithelial, myoepithelial and basal epithelial cells are located in inner and outer layer, respectively. In the part A, acini of mammary tissue section stained with hematoxylin & eosin. Black arrow indicates the lumen which contains secretory materials, generally. In the part B, normal and oncogene expressing MCF-10A cultured during 20 days on the basement membrane. MCF-10A and HPV E7 show more *in vivo* like acini structure with hollow lumen within different sizes while ErB2 generates multiacinar structures.

2.3. Structure of Normal Lung Tissue and The Pulmonary Metastatic Niche

Lungs contain respiratory membranes 0.5 to 1 mm thick size that provides the appropriate gas exchange. Total surface reaches 40 times greater than the individual's skin about 60m² in males. Air-blood barrier contains alveolar and capillary walls. These alveoli walls are composed of three cell types: Type1 (alveolar) cells, type2 (septal) cells alveolar macrophages (dust cells). Predominant type1 cells have squamous epithelial origin and they are located in the alveolar wall line in a continuous manner for providing the gas exchange. Type2 cells are located among type1 cells with low numbers. Microvilli containing alveolar cells are rounded and cuboidal cells as type2 (septal) cells. Secreted alveolar fluid is located between the cells and air moist by type2 cells. One of the components of this alveolar fluid is surfactant that contains the mixture of phospholipid and lipoproteins. The main role of the surfactant is the decrease of the surface tension of the alveolar fluid that leads to decrease the possibility of alveoli collapse. Alveolar macrophages interact with the alveolar wall. They are mobile phagocytes. Their work resulted in distracting dust particles and debris in the alveolar spaces and engulfing stranger particles ⁷ (Figure 2.6).

Metastasis is based on the molecules that secreted in ECM in metastatic home site. Tenascin C (TnC), is one of the negative regulated molecules via suppressing microRNA (miR-335) providing screen of metastatic factor in lung niche. Although knockdown of TnC don't provide tumor growth in breast cancer, it causes the lung metastasis in mice. There are two genes related with Wnt and Notch signaling, LGR5 and Musashi1 (MSI1) respectively.

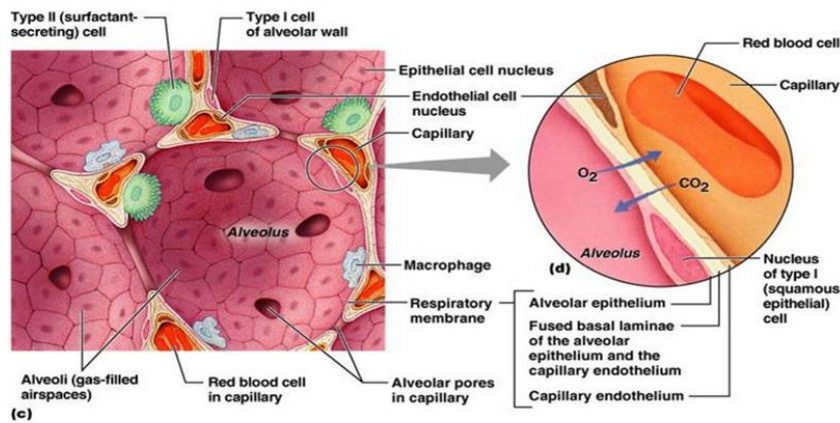
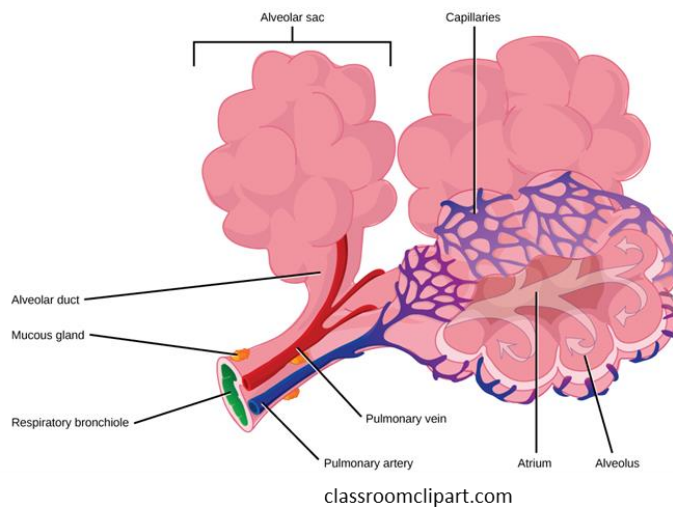


Figure 2.6. Structure of alveoli.

These genes are down-regulated at the consequence of the absence of TnC. They have an effect on metastasis additionally besides each one of its' lung metastasis formation effect. One of the ECM molecules, Periostin (POSTN), is associated with TnC in the metastatic niche of lung. Studies showed the knock down of POSTN caused 90% inhibition of lung metastasis by non-effected the growth of cancer in mice breast. Causation of POSTN activity is realized via $TGF\beta$ at the high level in breast cancer cells and also primary lung fibroblasts. The characteristics of CSCs (cancer stem cells) population showed $CD24^+CD90^+$ have ability to form metastais in lungs. In addition, population is very close to the periostin-rich stromal niche. POSTN is a metastatic niche factor effect the tumor growth via Wnt signaling in CSCs. Another important factor is VCAM-1 receptor which is located in the breast cancer related with lung metastasis and

presents a place for binding of metastasis-associated macrophages. This binding leads to PI3K/Akt activation and gives a chance to escape from TRAIL-induced apoptosis in cancer cells ⁸.

2.4. Mesenchymal Stem Cells (MSCs)

Mesenchymal stem cells have ability differentiate into osteoblasts, chondrocytes and adipocytes thanks to their multipotent characteristic. They have positive surface markers such as CD44, CD73, CD105 and CD90. They can be isolated from the bone marrow, adipose tissue, dental pulp. They can enter the blood from the vessel and reach the inflammatory sites in the body. This property may be the sign of their regenerative function in different organs such as lung, liver, brain and heart ⁹. These cells are also contact with innate and adaptive immune systems. They can achieve the induction of releasing pro-inflammatory cytokines by providing survival in the inflammatory sites of injured tissues. Transplantation of MSCs into the bone marrow in non-obese diabetic–severe combined immunodeficiency (NOD–SCID) mice resulted in the differentiation into pericytes, myofibroblasts, bone-marrow stromal cells, osteocytes, osteoblasts and endothelial cells. All of them contribute the formation of hematopoietic stem cell niche that is the critical for the maintenance of the hematopoiesis. In the absence of appropriate stimulation, they are inactive in the bone marrow. They are differentiated and transferred in the sinusoidal vascular system by the stimulation ¹⁰. The contribution of MSCs has been shown in tumor growth and progression. The occurrence of MSCs has been shown in the prostate tumor at the range between 0.01-1.1%. MSCs have an effect on the enhancement of the metastatic potential by effecting the motility and invasiveness. In addition, they have a role in the construction of secondary site. The tumor suppression effect of MSCs has been shown in the breast cancer, hepatoma, and melanoma in contrast to the tumor growth effect. Human MSCs were isolated from the umbilical cord and adipose tissue. Their metastatic inhibition effect for lung was shown after the implantation into a breast cancer metastasis mouse model. In addition, the induction of tumor growth and proliferation has been shown by poly (ADP-ribose) polymerase (PARP) and caspase-3 cleavage that causes apoptosis ¹¹. MSCs have different functionalities depending on their sources so replication of other MSCs sources related studies cannot be realized

with bone marrow derived MSCs. Different MSCs have distinct protein markers for example, Oct4, Nanog, alkaline phosphatase, SSEA-4 for bone marrow derived; Oct4, Nanog, SOX2, alkaline phosphatase, SSEA4 for adipose and dermis derived; Oct4, Nanog, SOX2, SSEA4 for heart derived MSCs. Cancer associated fibroblasts (CAFs) have an effect on the induction tumor formation. Their heterogeneity characteristic may be associated with having different kinds of cell derivatives. Their origin comes from bone marrow MSCs, fibroblasts and trans differentiation of epithelial and endothelial cells ⁹.

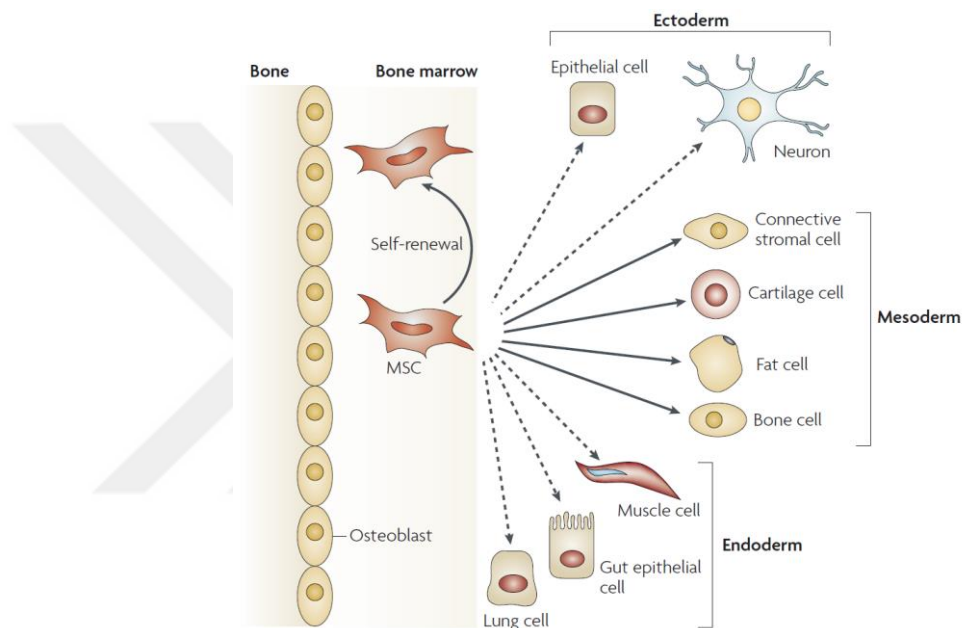


Figure 2.7. The multipotentiality of MSCs ¹⁰.

This figure shows the differentiation capacity of MSCs in the bone marrow cavity. They have also self-renewal feature as all stem cells. Here, dashed and straight arrows show the trans differentiation of cells for different lineages; ectoderm, endoderm and mesoderm.

2.5. Lab-on-a-chip Technology

Microfluidic systems give a valuable technology to work and handle small quantities of fluids changing ranges from 10^{-9} to 10^{-18} liters via different sizes of channels reach a few micrometers. The main advantage of these systems is working

with small amount of fluids/specimens by providing high resolutions and sensitivity. Another output of this advance is taking short times and low cost for analysis. This technology provides also transfer the inner incident to signals with presenting many advantages compares to previous methodologies in cell biology.

- ✓ Small volume requirement and miniaturize platform
- ✓ Controlled *in vitro* microenvironment conditions
- ✓ Non-invasive methodology
- ✓ High spatial resolution
- ✓ High temporal resolution (real time and fast analysis)
- ✓ Principle based on fluid mechanics
- ✓ Low cost due to provide label free detection and study with small volume of liquid

This chip technology is widely used in many different areas such as biomedicine, drug screening, cancer biology, environmental monitoring with distinct topics; adhesion, cell sorting, migration, toxicity, signaling mechanisms. This technology can be thought as a miniaturized cell biology laboratory with respect to meet all needs are described above ¹².

UV lithography technique is also known as photolithography based on a parallel writing method that is useful for the fabrication of patterns by using photoresist in micrometer size. Two kinds of photoresist are used as negative/positive photoresist depending on their dissolution/degradation property via exposure to UV respectively. SU-8 is commonly used for both 2D and 3D fabrication of master molds as a negative photoresist. It contains eight epoxy groups and thus is named SU-8. Different SU-8 series are commercially available depending on their viscosity.

All steps in UV lithography can be performed in the clean room conditions. We need three consecutive days for the fabrication of master mold. UV lithography steps can be listed in the three main titles as spin coating of SU-8, exposure to UV light onto the SU-8 coated wafer, development of the SU-8 master ¹³.

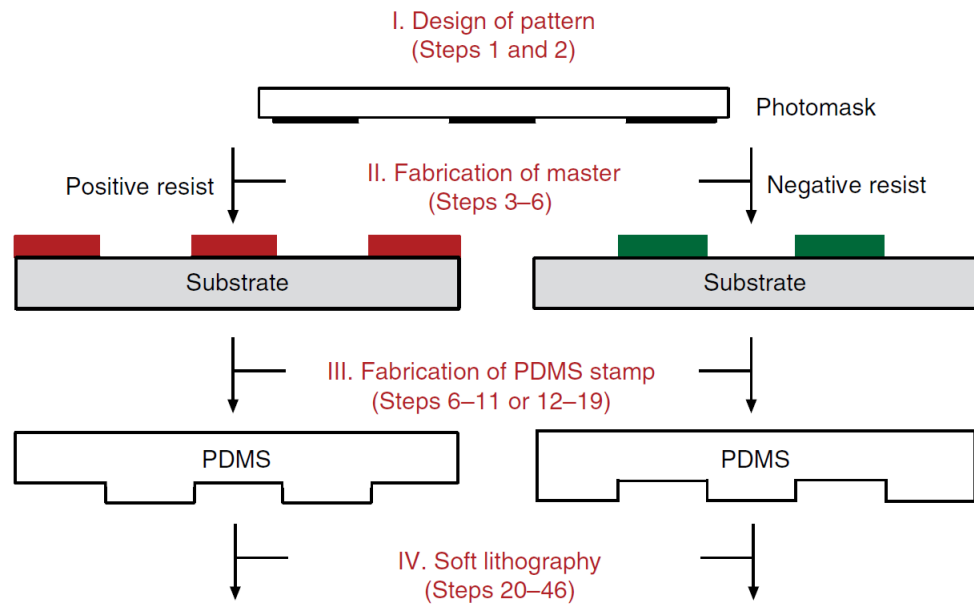


Figure 2.8. Fabrication of the master mold by UV lithography¹⁴.

Figure 2.8 shows the main steps of the fabrication of the master mold by using different photomasks as negative/positive. The next step is the preparation of lab-on-a-chip devices by using PDMS via soft lithography.

Micro machining and microfabrication based on silicon are not easy and cost effective techniques to work. The alternative technology has been advanced by using silicon rubber, poly (dimethylsiloxane) (PDMS). This technology gives many advantages/disadvantages for researchers in fabrication and cost. They can be listed as below^{14,15}.

Advantages:

- ✓ Gas permeability: There is no need for any oxygenator system for O₂ supply in contrast to silicon, glass plastic devices.
- ✓ Optical transparency: It gives an opportunity for real-time measurements or morphology, motility analysis in tissue repair and organization studies.
- ✓ Non-toxic and commercially available
- ✓ Hydrophobic: Its' surface can be transformed into hydrophobic property with oxygen plasma treatment.

Disadvantages:

- Adsorbs hydrophobic molecules.
- Mechanical properties can change in time.
- Sensitive to some chemicals.
- Its' water permeability causes the evaporation in PDMS.

2.6. Tissue Engineering and Organotypic Microfluidic 3D *in vitro*

Models

The tissue engineering was defined as the combination of engineering principles and life sciences for repair and regeneration applications related with tissue or organ functions by Langer and Vacanti in 1993. This interdisciplinary field generates the option for tissue/organ transplantation. Three components of the tissue engineering are cells, scaffolds, growth factors. Cells are critical factor of them by having important features such as repair/proliferation capacity (e.g stem cells), cell-cell interaction (construction of tissue), ECM production. Scaffolds are also essential for adhesion of cells to give their structure. In addition, porosity structure of the scaffolds is the key player that provides the penetration of nutrient and gases. Different kinds of degradable scaffolds are used such as natural materials (collagen, fibrin) or synthetic polymers (polyglycolide, polylactide) ¹⁶.

Co-cultures approaches are important for tissue modeling studies for drug screening and cancer metastasis, respiratory disease. Drug screening studies provide to see the effect of drug in co-cultures of cancer cells. Co-culture of lymphoma cancer cells and neonatal stroma cells in 3D polystyrene scaffold to construct a blood cancer model to test the drugs. "Lung-on-a-chip" system was used to see the effect of drugs for respiratory disease by co-culture of lung alveolar epithelial cells and endothelial cells. Another drug toxicity study is the co-culture of hepatocytes and endothelial cells in nylon scaffolds in the basis of creation 3D liver for drug tests ¹⁷. Co-culture platforms are applicable for studying several diseases. Three co-culture study of epithelial cells, macrophages and dendritic cells is one of the example to form a platform to study the alveolar epithelial barrier and infectious disease ¹⁸. The other tissue model was developed by using circulating breast cancer cells in the endothelial cells coated microfluidic channels to show the different adhesion, angiogenesis tendencies response

to various chemokines related to induce cancer metastasis¹⁹. To mimic natural microenvironment, the choice of the experimental platform is so important for taking a real-like response. 3D co-culture systems are more appropriate than 2D co-culture systems because of having different topographical patterns that differentiate the cell response. Cell culture in 2D causes the differentiation of phenotypic character of cells as well as cell response¹⁷. Cell response and related analysis are affected by the interaction between structure and function. 3D co-cultures contain different kinds of cells in terms of proliferation, viability heterogeneously so they provide more realistic microenvironments and conditions to study many diseases such as cancer. 3D co-cultures set suitable environment for the interaction of epithelial and stromal cells²⁰. Huh et. al, fabricated a biomimetic system for alveolar-capillary interface of the human lung to see the organ like responses to bacteria and inflammatory cytokines²¹. Another application is the developed “the human lung-on-a-chip” to form a disease model for pulmonary edema in human lungs. This disease causes the vascular leakage across the alveolar-capillary barrier. They tested the cytotoxic effect of interleukin-2 (IL-2) and therapeutics (angiopoietin-1) and inhibitor vanilloid 4 (TRPV4) in the presence of mechanical breathing in the human disease model in lung-on-a-chip²². In addition, Jeon et. al, developed human 3D vascularized organotypic microfluidic system to study the organ-specific extravasation of breast cancer cell into bone and muscle microenvironments by forming microvascular network that presents a platform for drug screening²³. Bischel et. al, developed another microfluidic platform to study angiogenesis in vitro conditions by the fabrication of 3D endothelial monolayer as blood vessel lumen²⁴.

Distribution or gradient of growth factors have an affect on microvascular function. The main regulator of vascular angiogenesis is vascular endothelial growth factor (VEGF) in the presence of multile growth factors such as platelet-derived growth factor B, transforming growth factor beta 1, fibroblast growth factor 2 (FGF2) having mitogenic effect, Angiopoietins (Ang1, Ang2). Formation of networks and tube-like structures of endothelial cells had been studied by Folkman & Haudenschild in 1980²⁵.

CHAPTER 3

MATERIAL AND METHODS

3.1. Fabrication of Lab-on-a-chip Devices for Construction of Target Tissues

Molds were fabricated by using 3D printers (Formlabs) and UV lithography. Fabrication of PDMS chips was accomplished by a soft lithography method, then following PDMS pouring, cleaning and punching of the inlets and outlets of PDMS chip and the permanent glass bonding steps respectively. Cylindrical biopsy punches were used for creating inlets and outlets. The PDMS chips were then permanently bonded with cover glass slides by UV/Ozone treatment (Bioforce, Nanosciences, ProCleaner™). The bonded chips were held on a hot plate for 15 minutes. The LOCs were sterilized with UV for 15 or 30 minutes before use.

3.1.1. UV Lithography and 3D Printing for the Fabrication of Molds

LOC devices are fabricated by UV lithography or 3D printing. The fabrication of master mold is ongoing process during 3 days in the clean room conditions for UV lithography technique. First day, the heater is set to 65 °C and wafer is waited onto the heater for 5 minutes. 5-6 ml of SU-8 photoresist is poured and spread onto silicon wafer by hand at first. Spinner is used to spread SU-8 on the surface of wafer by certain speed homogenously and more favourable way. And then, it is heated on the hot plate. The height of wafer is depending on the speed of spinner and the amount of the poured SU-8. Wafer is heated at 65 °C for 5 minutes and 95 °C for 30 minutes, respectively. Protection of wafer against rapid change of heat is important point to prevent the fracture. Second day, the heating process are checked by re-heating of wafer at 95°C. This process is repeated until the disappearance of wrinkles on the wafer. Desired mask of design is placed onto wafer and UV is exposed at certain second according to the width of poured SU-8 such as 30-45 seconds. Heating is realized at 65°C for 5 minutes and 95°C for 10 minutes, respectively following of exposure step. The wafer is waited until the next day for cooling. Third day, the process is applied to remove from non-

cross-link parts of wafer. Developer solution is used for this process. Then wafer is washed with isopropanol solution. Master mold is ready for the fabrication of PDMS lab-on-a-chip (LOC) devices.

3.1.2. Soft Lithography

Silicon elastomer is cured with curing agent at 1:10 ratio. 60 grams of total PDMS is prepared for each of master molds. Mixture is mixed until formation of bubbles. The removal of bubbles from mixture is realized by the vacuum desiccator before polymerization. PDMS (Polydimethylsiloxane) are poured into the molds on the smooth surface. Molds are placed at room temperature or 37°C for 24 hours for polymerization.

3.1.2.1. Cleaning of PDMS LOC Device

At the end of the polymerization of PDMS, it is peeled from the surface of the master mold with the help of ethanol gently. First of all, the lab-on-a-chip (LOC) devices are cut and punched with the certain diameter of punchers for the appropriate loading of fluids. Inlet and outlets are punched with 2mm diameter puncher. The dusts are cleaned by the scotch tape. And then devices are placed into glass petri dishes for the cleaning process. LOC devices are rinsed with upH₂O and 70% Et-OH respectively. The sonication is applied for 10 minutes in upH₂O. They are rinsed with upH₂O for 3 times and then they are sonicated with 70% Et-OH for 5 minutes. Finally, they are rinsed with upH₂O. At the end of the cleaning process, the water is aspirated from the inlets & outlets and all posts and parts are checked for drying.

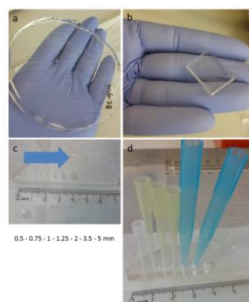


Figure 3.1. a) Polymerized PDMS b) LOC devices c) Different size of punctures for loading d) Different pipette tips for loading.

3.1.2.2. Bonding of PDMS LOC Device

UV/Ozone treatment is crucial for the disposal of any organic materials and permanent bonding of LOC devices onto the glass slide surface. Firstly, dusts are cleaned by using scotch tape on PDMS LOC devices. UV/Ozone is applied onto both surface of glass slides and devices for 5 minutes. At the last step, UV is applied for 15-30 minutes to sterilize LOC devices before usage of LOC devices in the experiments.

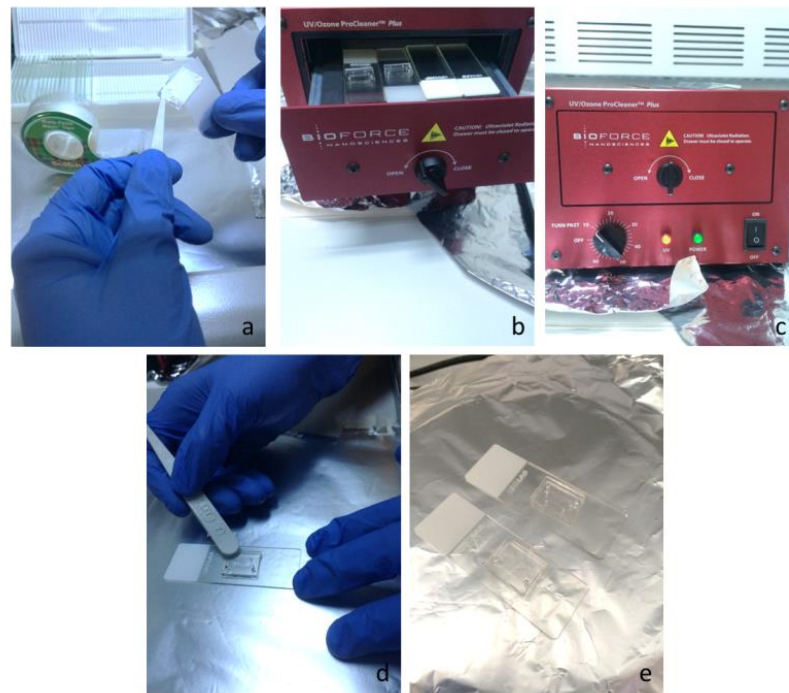


Figure 3.2. Permanent bonding of PDMS LOC devices onto glass slide a) Cleaning of dusts b) Placement of glass slides and LOC devices c) UV Ozone treatment d) Permanent bonding e) LOC devices.

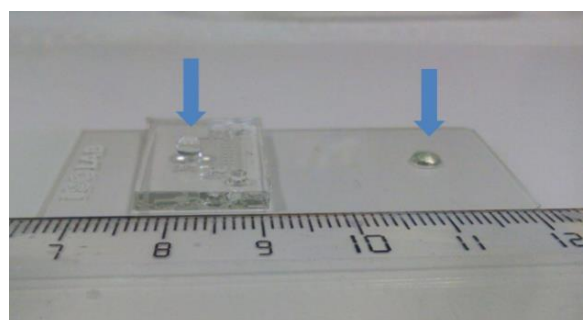


Figure 3.3. Hydrophobicity of glass and PDMS surfaces.

Left arrow shows the hydrophobic surface after UV Ozone treatment while right arrow shows the hydrophilic surface in Figure 3.3.

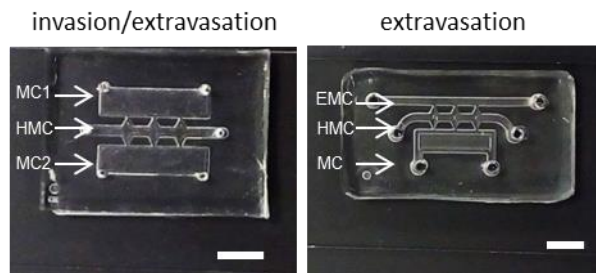


Figure 3.4. Different lab-on-a-chip devices for distinct experimental setups.

Figure 3.4 shows the lab-on-a-chip devices that are used in invasion and extravasation experiments. Scale bar is 5mm. The dimensions of invasion chip: the homing matrix channel (HMC) 3 mm width x 12 mm length x 200 μ m height and medium channels (MC1/MC2) 3 mm width x 12 mm length x 200 μ m height, extravasation chip: the homing matrix channel (HMC) 3 mm width x 15 mm length x 200 μ m height, endothelial monolayer channel (EMC) 3 mm width x 20 mm length x 200 μ m height and medium channel (MC) 3 mm width x 10 mm length x 200 μ m height.

3.2. Coating of PDMS LOC Device

Coating step was performed with Poly-L-lysine (PLL, P2682, Sigma Aldrich) or 3-aminopropyltriethoxysilane (APTES, A3648, Sigma Aldrich) to provide more intact endothelial monolayer structure before cell loading. 0.01 mg/ml concentration of PLL was used and LOC devices were incubated at 37⁰C, 5% CO₂ incubator overnight. They were washed with ultra-pure water for 3 times the following day. They were then placed at 80⁰C for 24 hours to gain hydrophobicity. 2% of APTES in acetone was also used for pre-coating steps. APTES was loaded to the channels of LOC devices and then washed with 1X PBS for 3 times and ultra-pure autoclaved H₂O after 15 minutes of incubation in the cell culture laminar cabinet. Laminin (0.0125 mg/ml, L2020, Sigma Aldrich) and fibronectin (0.0125 mg/ml, F2006, Sigma Aldrich) were mixed with 1X Universal Buffer, while serum-free DMEM high glucose media (Biological Industries, 01-055-

1A) was used for collagen type I (0.0125 mg/ml, 354249, Corning) suspension. Each protein solution was loaded to LOC devices and they were incubated at 37°C, 5% CO₂ for 1 hour. Laminin and fibronectin were first washed with 1X Universal Buffer and then with ultra-pure autoclaved H₂O for 3 times, while collagen was first washed with serum-free DMEM high glucose medium and then with ultra-pure autoclaved H₂O for 3 times. Remained liquids were aspirated by a vacuum. Devices are stored in vacuum desiccators at least one day before experimental set-ups.

3.3. Cell Culture

In this study b.End3 and HUVEC-C cell lines as endothelial cells, MCF-10A and Beas-2B cell lines for epithelial cells, WI-38 and 3T3-L1 cells as fibroblasts and MDA-MB-231, LM-231 (Bone metastatic clones) and MCF-7 cell lines as breast cancer cells were used in the experiments.

3.3.1. Maintenance of b.End3

Cell culture medium is composed of DMEM High Glucose (Biological Industries), 10% fetal bovine serum, 1% L-glutamine, 1% Penicillin-Streptomycin. 60 or 100 mm treated petri dishes are used for culture. Passage number 6-30 is used for experiments. Trypsin Edta-C is used for splitting of cells. It is applied for 4-5 minutes for detachment of cells from the surface of petri dish. After the collection of cells with complete medium, cells are centrifuged at 1000 rpm 5 minutes. At the end, they are re-suspended and passage ratio is 1/2 or 1/4 for 100% confluency in 2-3 days.

3.3.2. Maintenance of HUVEC-C

Endothelial cell growth medium (EGMTM-2 BulletKitTM) is used for culture of HUVECs. Passage number 5-11 is used for experiments. 60 mm treated cell culture petri dishes are coated with 1ml of 0.1% fibronectin (FN) and incubated at 37°C, 5% CO₂ for 1 hour. Then cells are seeded into treated FN coated petri dishes. Trypsin Edta-C is used for splitting of cells. It is applied for 4-5 minutes for detachment of cells from the surface of petri dish. After the collection of cells with complete medium of

HUVECs, cells are centrifuged at 1000 rpm 5 minutes. At the end, they are re-suspended and passage ratio is 1/2 or 1/3 for 100% confluency in 2-3 days.

3.3.3. Maintenance of MCF-10A

Cell culture medium is composed of DMEM:F12 (Biological Industries), 10% donor horse serum, 1% L-glutamine, 1% Penicillin-Streptomycin. Passage number 6-25 is used for experiments. Trypsin Edta-C is used for splitting of cells. It is applied for 17 minutes for detachment of cells from the surface of petri dish. After the collection of cells with complete medium, cells are centrifuged at 1000 rpm 5 minutes. At the end, they are re-suspended and passage ratio is 1/4 or 1/8 for 100% confluency in 2-3 days.

3.3.4. Maintenance of WI38

Cell culture medium is composed of MEM- α (Sigma Aldrich), 10% fetal bovine serum, 1% L-glutamine, 1% Penicillin-Streptomycin. 60 treated petri dishes are used for culture. Passage number 3-15 is used for experiments. Trypsin Edta-C is used for splitting of cells. It is applied for 3-4 minutes for detachment of cells from the surface of petri dish. After the collection of cells with complete medium, cells are centrifuged at 1000 rpm 5 minutes. At the end, they are re-suspended and passage ratio is 1/2 or 1/3 for 100% confluency in 2-3 days.

3.3.5. Maintenance of Beas-2B

Cell culture medium is composed of DMEM High Glucose (Biological Industries), 10% fetal bovine serum, 1% L-glutamine, 1% Penicillin-Streptomycin. 60 or 100 mm treated petri dishes are used for culture. Passage number 6-30 is used for experiments. Trypsin Edta-C is used for splitting of cells. It is applied for 4-5 minutes for detachment of cells from the surface of petri dish. After the collection of cells with complete medium, cells are centrifuged at 1000 rpm 5 minutes. At the end, they are re-suspended and passage ratio is 1/2 or 1/4 for 100% confluency in 2-3 days.

3.3.6. Maintenance of MDA-MB-231

Cell culture medium is composed of DMEM High Glucose (Biological Industries), 10% fetal bovine serum, 1% L-glutamine, 1% Penicillin-Streptomycin. 60 or 100 mm treated petri dishes are used for culture. Passage number 6-30 is used for experiments. Trypsin Edta-C is used for splitting of cells. It is applied for 4-5 minutes for detachment of cells from the surface of petri dish. After the collection of cells with complete medium, cells are centrifuged at 1000 rpm 5 minutes. At the end, they are re-suspended and passage ratio is 1/2 or 1/4 for 100% confluency in 2-3 days.

3.3.7. Maintenance of Raw264.7

Cell culture medium is composed of RPMI (Biological Industries), 10% fetal bovine serum, 1% L-glutamine, 1% Penicillin-Streptomycin. Passage number 6-23 is used for experiments. Medium of cells were collected from non-treated petri dish After the collection of cells with complete medium, cells are centrifuged at 400 rcf for 5 minutes. At the end, they are re-suspended and passage ratio is 1/5 or 1/10 for 100% confluency in 2-3 days.

3.3.8. Maintenance of 3T3-L1

Cell culture medium is composed of DMEM High Glucose (Biological Industries), 10% Calf serum, 1% L-glutamine, 1% Penicillin-Streptomycin. 100 mm treated petri dishes are used for culture. Passage number 3-13 is used for experiments. Pre-adipocytes are recommended until 12-13 passage numbers. 11×10^4 cells are seeded into 100 mm treated petri dishes. Cells are sub-cultured for 2-3 days with 70% confluency.

3.3.9. Maintenance of MCF-7

Cell culture medium is composed of DMEM High Glucose (Biological Industries), 10% fetal bovine serum, 1% L-glutamine, 1% Penicillin-Streptomycin. 60 or 100 mm treated petri dishes are used for culture. Passage number 6-30 is used for experiments. Trypsin Edta-C is used for splitting of cells. It is applied for 10 minutes for detachment of cells from the surface of petri dish. After the collection of cells with

complete medium, cells are centrifuged at 1000 rpm 5 minutes. At the end, they are re-suspended and passage ratio is 1/4 for 100% confluency in 2-3 days.

3.3.10. Labeling of Cell Lines

Cell tracker dyes (Thermo Fisher Scientific) are used for observation of co-culture of cells by using confocal microscopy. Cells are labeled with green (CellTracker™ Green CMFDA), red (CellTracker™ Red CMTPX), deep red (CellTracker™ Deep Red) and blue (CellTracker™ Blue CMAC) tracker dye a day before experiment. Final tracker concentrations are 10 μ M, 5 μ M, 1 μ M, 10 μ M, 25 μ M for red, deep red, green and blue trackers respectively. Cells are washed with serum free DMEM then tracker was suspended in serum free DMEM and applied onto cells. Incubation was 30 minutes for green, red, deep red trackers and 1 hour for blue tracker at 37°C 5% CO₂. After the incubation dye was aspirated and cells were washed with serum free DMEM for three times. At the end, own medium of cells was placed onto cells in petri dishes. Cells were placed into 37°C and 5% CO₂ incubator until experiment.

This tracker procedure is applicable for b.End3, 3T3-L1, MCF10A except Raw264.7. Raw264.7 cells are scraped from the surface and collect into 15ml of falcon tube with supernatant. After 1000rpm and 5minutes centrifuge, cells are re-suspended in serum free DMEM high glucose and seeded onto non-treated petri dish. And then, cells are incubated in the incubator (37°C and 5% CO₂) for 30 minutes or 60 minutes for green, red, deep red or blue tracker, respectively. At the end of the incubation time, cells are scraped and the centrifuge is applied again. Finally, cells are re-suspended in serum containing medium and seeded onto non-treated petri dish. Cells are used in the experiments the day after this procedure.

In invasion and extravasation experiments, MDA-MB-231, MCF-7 cancer cell lines and MCF10A normal epithelial cells were used which were labeled with cell tracker dyes (Thermo Fisher Scientific, CellTracker™ Red CMTPX, 10 μ M) before experiment or stably labelled with red fluorescent protein (dsRED).

Phalloidin staining was performed to engineering tissues seeded to the EMC. 4% paraformaldehyde was added to the EMC and fixation was performed. After overnight incubation at +4°C, the EMC was washed with PBS for 3 times and 5% BSA, 0,1%

Triton-X-100 containing PBS solution was added to the EMC for permeabilization and left at RT for 15 minutes. Then, the channel was again washed with PBS for 3 times and 1:40 diluted Phalloidin (Alexa Fluor™ 647) for actin-filament staining and 1:500 diluted DAPI for nuclei staining were loaded to the EMC and the chip was incubated for one hour at RT and dark. After 1 hour, the channel was washed again, the mounting medium was added and the chip was kept at +4°C. The next day, the samples were imaged by confocal microscopy.

3.4. Preparation of Fibrin Gel

All cell lines are removed from the surface according to each of their passage procedure. And they are re-suspended in EGM™-2 BulletKit™ or DMEM complete medium (450 ml DMEM high glucose, 5 ml penicillin-streptomycin, 5ml L-glutamine). Then, thrombin is added into cell re-suspension mix on ice. Fibrin gel matrix protocols were used in the experiments. The protocols are given below:

- Thrombin was added into cell re-suspension mix on ice. 8µl of this mixture and 8µl of fibrinogen are mixed by pipetting for 3-4 times. And it is loading into channel of LOC devices immediately. Fibrin gel polymerization is completed by waiting for 15 minutes in the laminar flow cabinet. LOC devices are placed on two surfaces (PDMS-glass) and held for 7.5 minutes for each position in humidity conditions. Concentration of fibrinogen was set to 2, 2.5, 3, 3.5 mg/ml changing thrombin concentrations (4, 2 and 0.83 U/ml).
- 5 µl matrigel (9.2 mg/ml), 5 µl collagen (4 mg/ml), 10 µl endothelial cells (b.End3/HUVEC-C), 6 µl fibroblasts (3T3-L1/WI38) + 6 µl epithelial cells (MCF10-A/BEAS-2B), 8 µl fibrinogen (15 mg/ml) were mixed according to this order. Mixture was loaded into middle matrix channel rapidly. Fibrin gel polymerization is completed by waiting for 15 minutes at 37°C and 5% CO₂ in humidity conditions.
- Fibrin gel and Growth factor reduced matrigel (GFR-matrigel) were mixed with 1:1 ratio. The final concentrations of each gel are 3 mg/ml. Thrombin concentration is set to 0.83U/ml.

LOC devices are placed on two surfaces (PDMS-glass) and held for 7.5 minutes for each position. At the end of polymerization, LOC devices are placed into glass petri dishes in humidity conditions providing 2-3 ml upH₂O for incubation at 37°C and 5% CO₂. Medium is changed every day during the experiment.

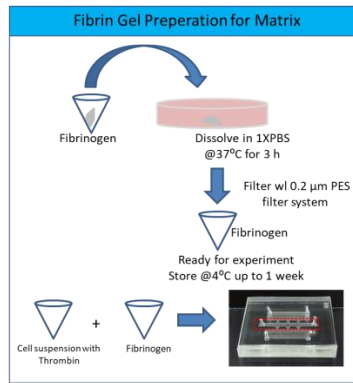


Figure 3.5. Preparation of fibrin gel.

3.5. Media Preparation for Target Tissue for Acini Structure

Table 2 shows the components of the media that is used to induce the generation of acinus structure.

Table 2. Components of acinus generating medium ⁶.

Component	Final concentration
DMEM/F12	500ml
Horse serum	10ml
EGF	5ng/ml
Hydrocortisone	0.5µg/ml
Cholera Toxin	100ng/ml
Pen/Strep	1:100
L-glutamine	1:100
Insulin	100µg/ml
Matrigel	%2

3.6. LOC Device Gradient Characterization

3 kDa (D34681, Alexa FluorTM 680, anionic, InvitrogenTM), 10 kDa (D7170, Oregon GreenTM 488, anionic, InvitrogenTM), 40 kDa (D1842, tetramethylrhodamine, neutral, InvitrogenTM) and 70 kDa (D1830), Texas RedTM, InvitrogenTM) (25 mg/ml)

dextran conjugated dyes were used for gradient characterization. Both reservoirs and endothelial monolayer channels (EMC) were loaded with each dextran dye in 1:250 dilutions. Images showed the diffusion of dyes were taken by Leica DMI8 confocal microscopy with 10X objective. Analyses were done using the FIJI/ImageJ program.

3.7. Generation of Endothelial Monolayer

HUVEC-C or b.End3 cells labeled with Green Cell Tracker CMFDA, were collected from culture dishes following 0,25% Trypsin EDTA Solution A (03-050-1B, Biological Industries) treatment for 5 minutes. After centrifugation, they were resuspended in 8% 450-650 kDa dextran (31392, Sigma Aldrich) in HUVEC-C or b.End3 media. The final concentration of endothelial cells was 3.85×10^6 /ml. The HUVEC-C or b.End3 cells were loaded to EMC of APTES-LAM coated extravasation LOCs. LOCs were incubated vertically at 37°C in a humidified incubator with 5% CO₂ overnight. Endothelial monolayer formation was confirmed by 3D imaging at a Leica SP8 confocal microscope with a 10X objective and 7.52 μm z- intervals.

3.8. Endothelial Monolayer Integrity Assay

3 kDa (D34681, Alexa Fluor™ 680, anionic, Invitrogen™), 10 kDa (D7170, Oregon Green™ 488, anionic, Invitrogen™), 40 kDa (D1842, tetramethylrhodamine, neutral, Invitrogen™) and 70kDa (D1830, Texas Red™, neutral, Invitrogen™) (25 mg/ml) dextran conjugated dyes loaded into device to check the integrity of endothelial monolayer. EMC was loaded with each dye in 1:250 dilutions. The images showed the diffusion of dyes were taken by Leica DMI8 confocal microscope with 10X objective. Analyses were done using the FIJI/ImageJ program.

$$P_{app}(\text{cm/s}) = \frac{dQ}{dt} \cdot \frac{1}{A \cdot C_{donor}} \cdot \frac{\text{Flux}}{\text{Initial fluorescent intensity}}$$

$$P_{app}(\text{cm/s}) = \frac{d\left(\frac{I_{gel}}{I_{perfusion}}\right)}{dt} \cdot \frac{V_{gel}}{A} \cdot \frac{1}{\text{Area of post gap}}$$

Ratio of intensity between matrix and endothelial channel
Volume of gel

Figure 3.6. The formula to calculate the permeability of the endothelial monolayer.

3.9. Invasion Assay

The invasion capacity of MDA-MB-231, LM-231, MCF-10A, MCF-7 cells into the breast and lung microenvironment generated by MCF-10A, 3T3-L1 and Beas2B, WI-38 cells respectively within the only GFR-matrigel or fibrin-GFR matrigel mixture (1:1) was checked. First, invasion capacity was tested only gel conditions without cells in the matrix by using different gel contents. Second, each cell lines (2×10^6 cells/ml) was embedded into matrix by mixing 1:1 dilution with different gel. Third, couple of two cell lines (Beas-2B: 4×10^6 cells/ml and WI-38: 4×10^6 cells/ml for lung, MCF-10A: 4×10^6 cells/ml and 3T3-L1: 4×10^6 cells/ml for breast) was mixed together 1:1 dilution and then mixed with 6 mg/ml GFR-matrigel (Corning, 354230) in 1:1 dilution in pre-cooled serum free medium and they were loaded to the middle channel (HMC) of LOC system. 30 minutes polymerization was performed in 37°C , 5% CO_2 in a humidified incubator. After polymerization, serum-free medium was loaded to the MC1 and the media channel 2 (MC2) and chips were incubated overnight. Afterwards, MDA-MB-231, LM-231, MCF-10A and MCF-7 cells were seeded to MC1 at a density of 1×10^6 cells/ml in serum free medium for each condition and left for incubation vertically for three days. The invasion ability of four cell lines was detected via Leica DMI8 confocal microscope.

Images of chips were taken each day and Z-stacks were combined via ImageJ application. The analysis of the acquired images was performed by Image J and Excel. Briefly, the sum of all Z-sections and thresholds of images were taken and the distance of each bright pixel to the starting point of the invasion was determined. And then, the distances of each pixels from the position which is the start line of cells after loading into channel. The invasion capacity of the cells was determined by the normalization of Day 2 and Day 3 to Day 1. Invasion index shows the day 1 normalized values for each days.

3.10. Extravasation Assay

The extravasation capacity of MDA-MB-231 cells into lung and breast microenvironments generated by WI-38, Beas-2B and 3T3-L1 and MCF-10A cells within the GFR-matrigel was checked. Each microenvironment cells concentrations is 4×10^6 cells/ml was mixed with 1:1 in serum free media then mixed with 6 mg/ml

growth factor reduced matrigel in 1:1 dilution in pre-cooled serum free medium and they were loaded to the HMC of LOC system. 30 minutes polymerization was performed in a 37⁰C, 5% CO₂ incubator. Meanwhile, b.End3 cells (labelled with Green Cell Tracker) were prepared within 8% of 450-650 kDa dextran (31392, Sigma Aldrich) containing medium.

After polymerization, the optimized number of b.End3 cells (19.736 cells/μm for height of channel) and serum-free media was loaded to the EMC and MC2 channels respectively and chips were vertically incubated overnight. The day after, the monolayer formation by b.End3 cells was checked by confocal microscopy and once the monolayer was formed, MDA-MB-231 cells were seeded to the EMC at a density of 1x10⁶ cells/ml in serum free medium for each condition and left for incubation vertically for 3 days. The integrity of endothelial monolayer was again confirmed by confocal microscopy after addition of MDA-MB-231 cells. The extravasation ability of them into the generated lung and breast microenvironments was detected by confocal microscopy for 3 days and extravasated and endothelial barrier-associated cells were calculated.

3.11. Analysis of Extravasation Assay

Region of interests (ROIs) were selected from the gaps of posts to observe the extravasation. Only the ROIs endothelial monolayer formed in the gaps among all posts were included into analysis. The ROIs in the EMC that did not touch the gel region were excluded from extravasation analysis. Cancer cells were entitled as “extravasated” or “associated” depending on their passage through endothelial monolayer or being in contact with endothelial monolayer, respectively. Cancer cells were counted in both 2D and 3D views by confocal microscopy software (LAS X Life Science). In addition to quantification of extravasated cells, extravasation metric was developed to eliminate leaked cancer cells during loading of them. Extravasation metric defines the ratio of number of extravasated posts where extravasation occurred to number of total posts in a LOC. All ROIs extravasation analyses were done using merged images consisting of 488 (endothelial cells), 555 (cancer cells) and brightfield channels. Applying following steps for migration analyses, distances of extravasated cancer cells calculated. 1) Z position is adjusted when an extravasated particle is visible. 2) A line was drawn from the center of the extravasated particle to the endothelial monolayer and LAS_X_Small_3.7.0_20979 (Leica software) automatically gave its length.

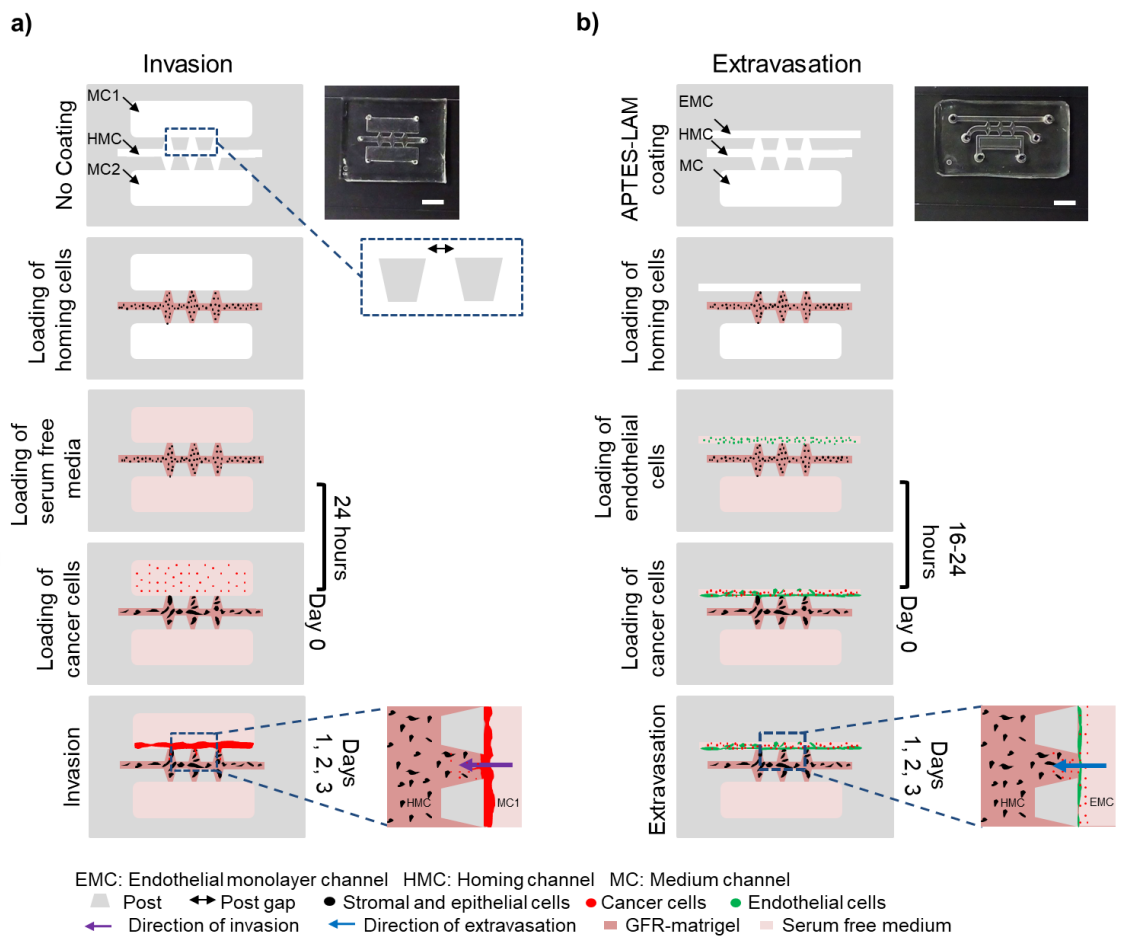


Figure 3.7. a) Invasion and b) Extravasation procedure.

CHAPTER 4

RESULTS and DISCUSSION

4.1. Generation of Microvascular Network

For this purpose, b.End3 and HUVEC-C cell lines are used in the experiments. The formation of the microvascular network (MVN) is a critical step of engineering target tissues to functionalize the target tissues. Different concentrations of endothelial cells were used to optimize the generation of MVN in gel containing only endothelial cells (HUVEC-C or b.End3). In addition, the content of the gel were optimized by changing the concentrations of fibrinogen, thrombin and aprotinin. Fibrinogen, thrombin concentrations were set 3.5mg/ml and 4U/ml ⁷.

4.1.1. Low and High Concentrations of Endothelial Cells

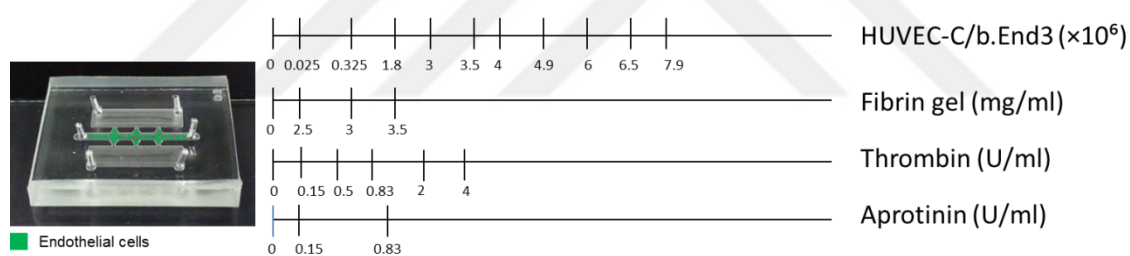


Figure 4.1. Experimental conditions for generation of MVN.

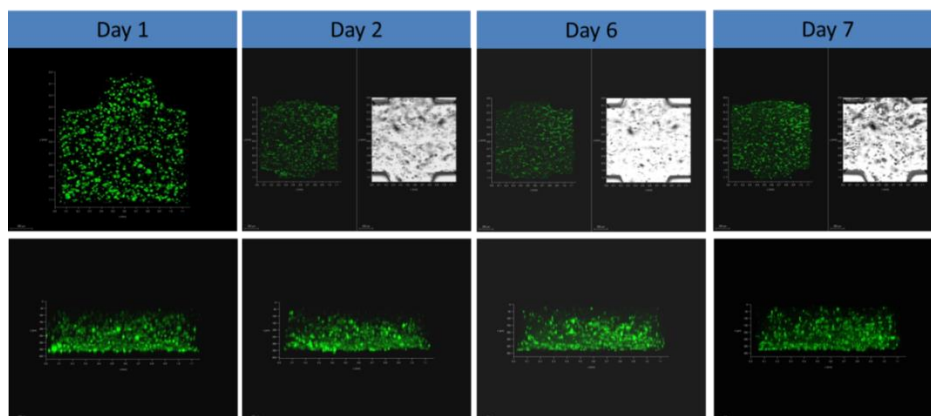


Figure 4.2. Confocal images of 3.5×10^6 /ml HUVEC-C in fibrin gel day by day.

Figure 4.1 shows the different concentrations for the distinct endothelial cells in the presence of changing gel components in terms of fibrinogen, thrombin and aprotinin. 3.5 mg/ml fibrinogen, 4 U/ml thrombin, 0 U/ml aprotinin were used in the gel composition for Figure 4.2-Figure 4.11.

10 μ M Green tracker was used as a dye for HUVEC-C a day before experiment. Numbers of endothelial cells were increased day by day. But the interactions of cells were not enough for the formation of MVN from the upper side of channel into bottom side of channel through the 3D structure. Initial concentration of HUVEC-C was not enough to see the vascular network in whole 3D structure in 7 days. Photos were taken by 10X objective.

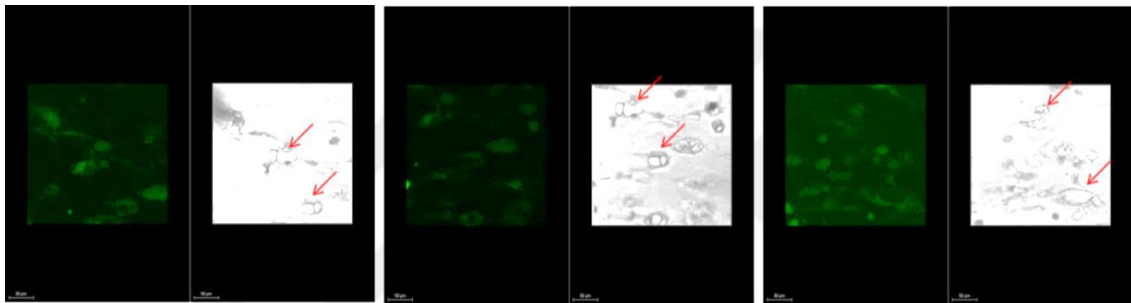


Figure 4.3. Confocal images of 3.5×10^6 /ml HUVEC-C for day 2.

Arrows show the vascularization of endothelial cells with different photos which were taken by confocal microscope with 20X objective.

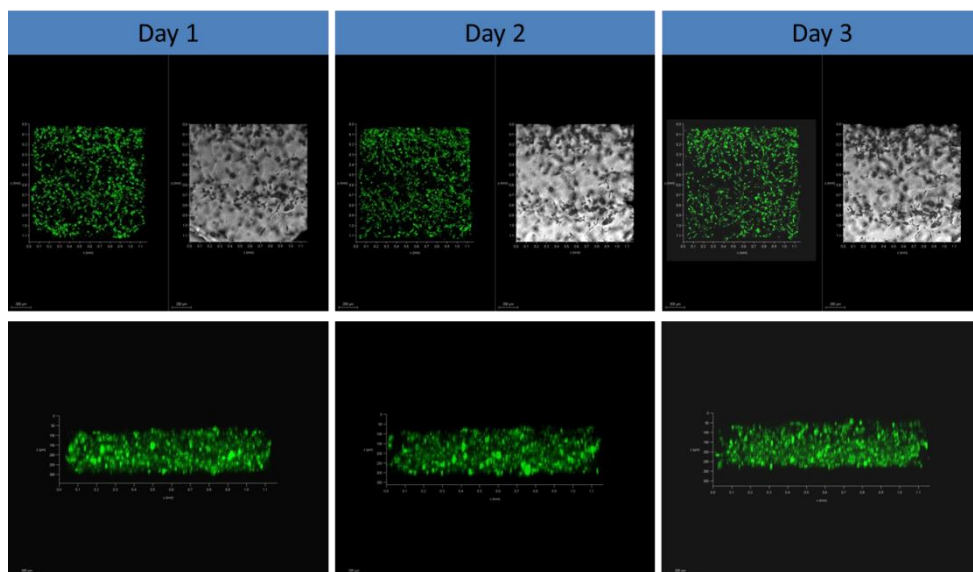


Figure 4.4. Confocal images of 6×10^6 /ml HUVEC-C in fibrin gel day by day.

10 μ M Green tracker was used as a dye for HUVEC-C a day before experiment. Concentration of endothelial cells was increased from 3.5×10^6 to 6×10^6 . The increment of number of cells was observed. Medium was changed every day. Images were taken by 10X objective. But the connections of endothelial cells were not enough not to form vascular network.

4.1.2. Different Endothelial Cell Lines

Same numbers of different endothelial cell lines were used to form MVN. In the literature, final concentration is 6×10^6 HUVEC-C were used for the formation of MVN in fibrin gel in 4-5 days ²⁹.

b.End3 cell line was used as another endothelial cell to observe the effect of distinct endothelial cell lines to induce the generation of MVN.

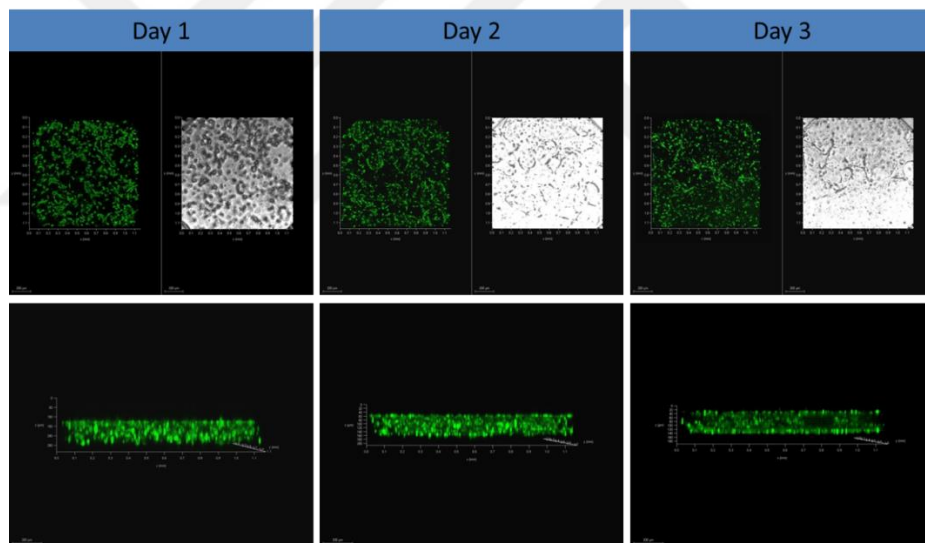


Figure 4.5. Confocal images of 6×10^6 /ml b.End3 in fibrin gel day by day.

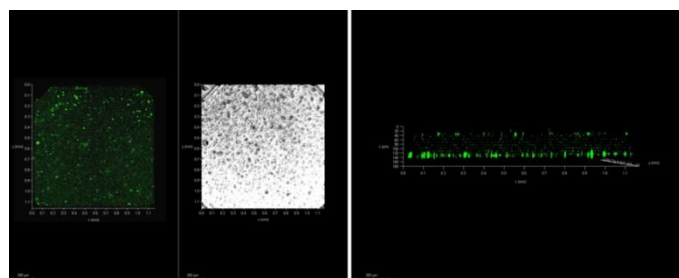


Figure 4.6. Confocal images of 6×10^6 /ml b.End3 in fibrin gel for day 7.

10 μM Green tracker was used as a dye for HUVEC-C a day before experiment. Numbers of b.End3 cells were increased day by day. Medium was changed every day. Images were taken by 10X objective. The increment of cell numbers was stopped after 2 days and also the disruption of 3D structure cells was observed at day 7. The growth rate of b.End3 is faster than HUVEC-C cells so the initial numbers of cells might be decreased for b.End3 cells to protect 3D structure in a long term.

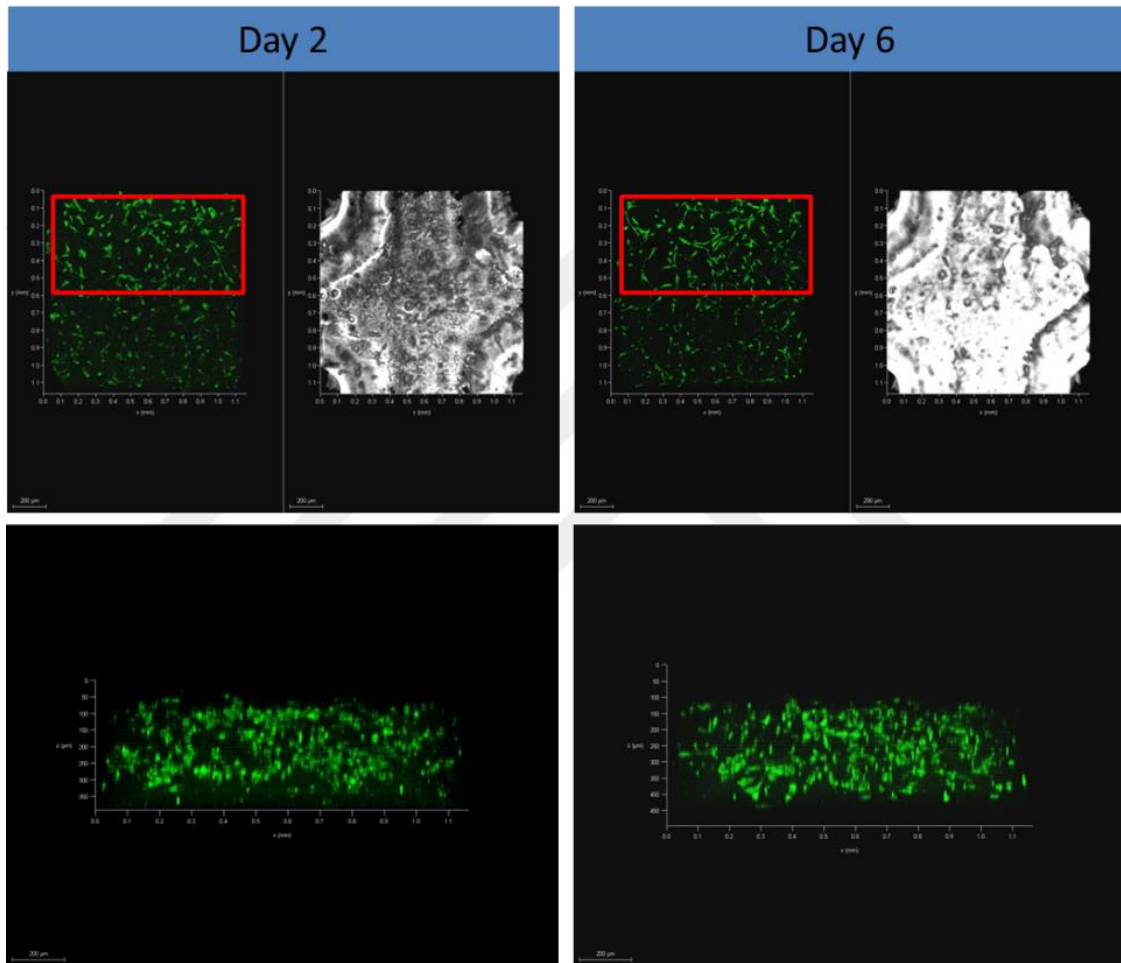


Figure 4.7. Confocal images of $65 \times 10^4/\text{ml}$ b.End3 in fibrin gel for day 2 and day 6.

10 μM Green tracker was used as a dye for HUVEC-C a day before experiment. Numbers of HUVEC-C were increased day by day. Red rectangular shows the increment of cell number. Here, we see the cells are elongated in fibrin gel from day 2 to day 6.

The results showed that the different concentrations of endothelial cells effected the alignment of the cells at the beginning days of the culture in the matrix the

regardless of endothelial cell type. Cell-cell interaction and alignment took time at low beginning concentrations

(Figure 4.2 and Figure 4.7). In the light of the results, the beginning concentration of cells is the critical step to provide efficient cell-cell interaction and also in a short culture time. In the literature different approaches have been used in the terms of both cell and gel concentrations for the vasculature or angiogenesis research^{7, 26, 27}. For this purpose, $4.9 \times 10^6/\text{ml}$ concentration was determined as a beginning concentration. The rich microenvironment condition that contains fibroblast, myoblast and also the cell-cell signalling are crucial to mimic the *in vivo* like conditions where the invasion and extravasation occurs in the extent of organ specific homing stromal cells. MVN formation was shown in a paracrine signaling of fibroblast in lab-on-a-chip devices by preventing the regression of the network⁷.

4.1.3. Use of Fibroblasts as Stromal Cells

We tested the presence and absence of fibroblasts to improve the formation of MVN by using different cell loading setup into chips (Figure 4.8). The concentrations of endothelial cells and fibroblast were set to $4.9 \times 10^6/\text{ml}$ and $2 \times 10^6/\text{ml}$, respectively.

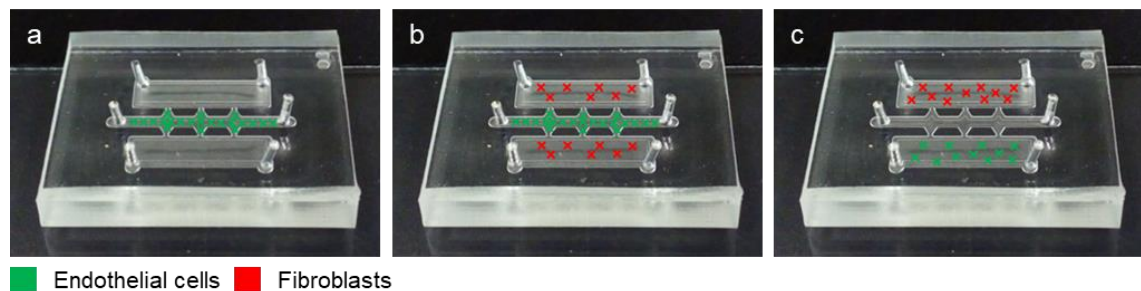


Figure 4.8. Experimental setup to observe the effect of fibroblasts.

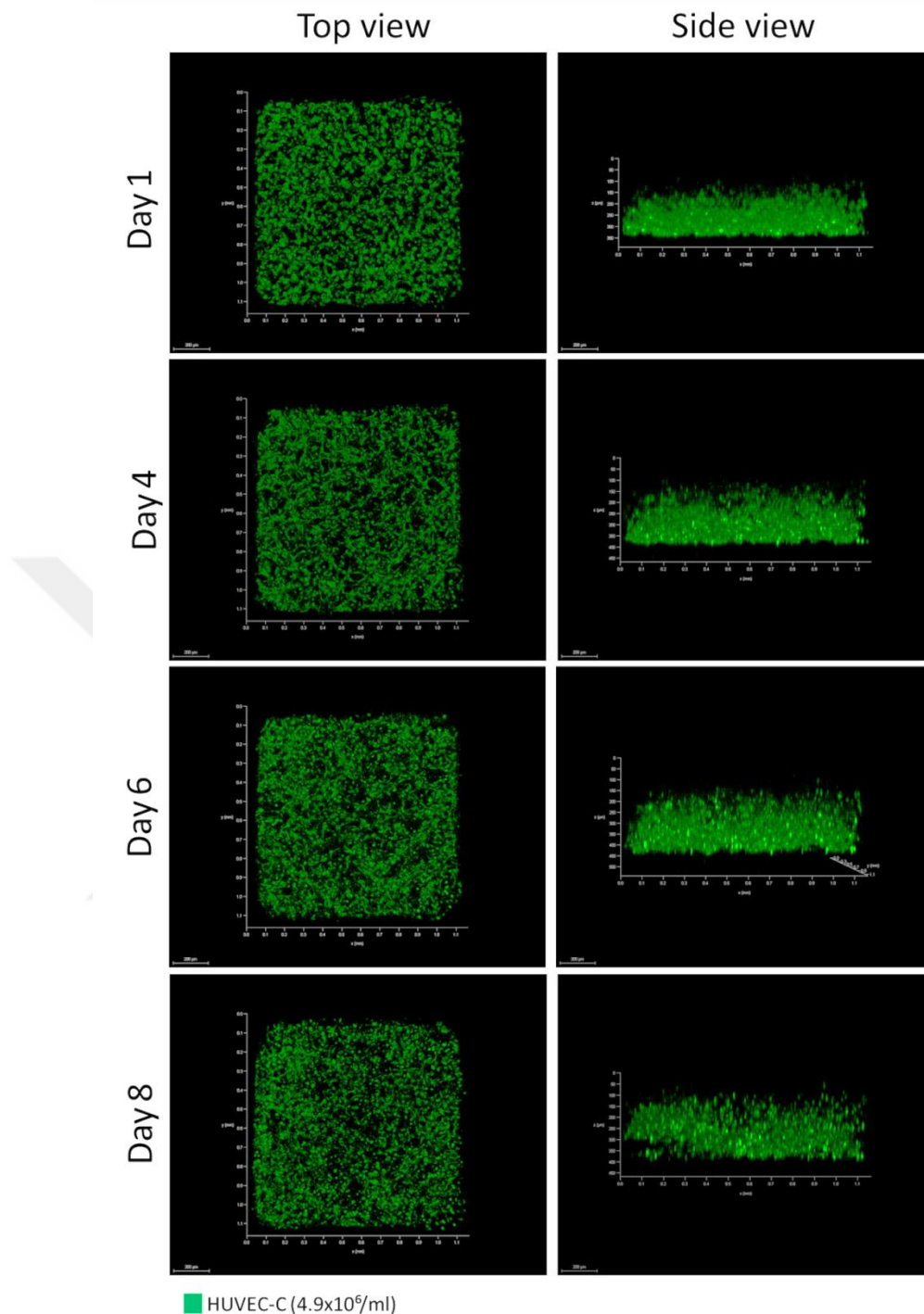


Figure 4.9. Confocal images of 4.9×10^6 /ml HUVEC-C in fibrin gel day by day.

10 μ M Green tracker was used as a dye for HUVEC-C a day before experiment. Concentration of endothelial cells was set to 4.9×10^6 /ml. The increment of number of cells was observed. Medium was changed every day. Images were taken by 10X objective. But the connections of endothelial cells were not enough to form vascular network. The lumen formation and the vascularization were not observed at the 8th day.

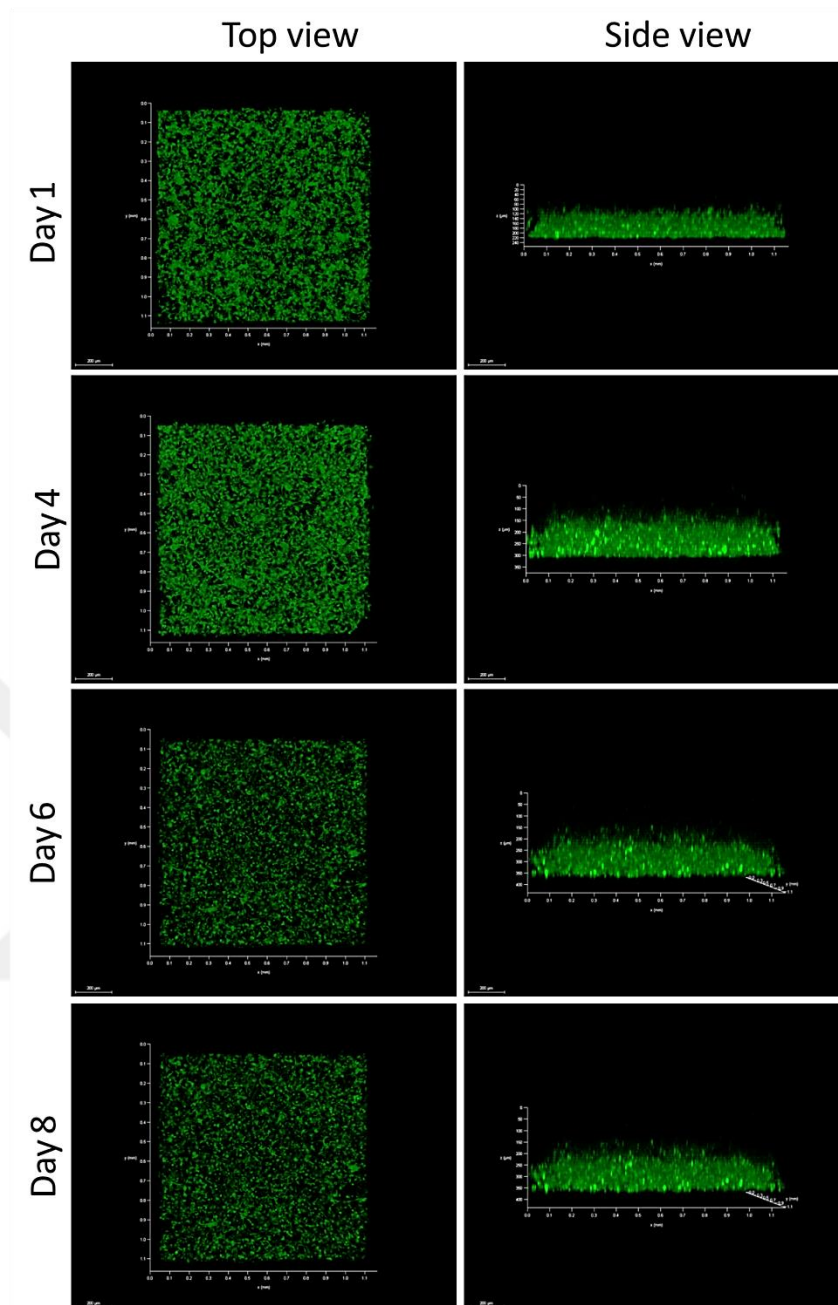


Figure 4.10. Confocal images of LOC device containing 4.9×10^6 /ml HUVEC-C in fibrin gel and 2×10^6 /ml 3T3-L1 in reservoirs day by day.

10 μ M Green tracker was used as a dye for HUVEC-C a day before experiment. Fibrinogen concentration was set as 3.5 mg/ml and cells were dissolved in 4U/ml thrombin containing medium according to first fibrin gel protocol. Concentration of endothelial cells was used as 4.9×10^6 /ml. Medium was changed every day. Images were taken by 10X objective. Increment of cell number or alignment of endothelial cells was not observed in the presence of 3T3-L1 (2×10^6 /ml) in reservoirs.

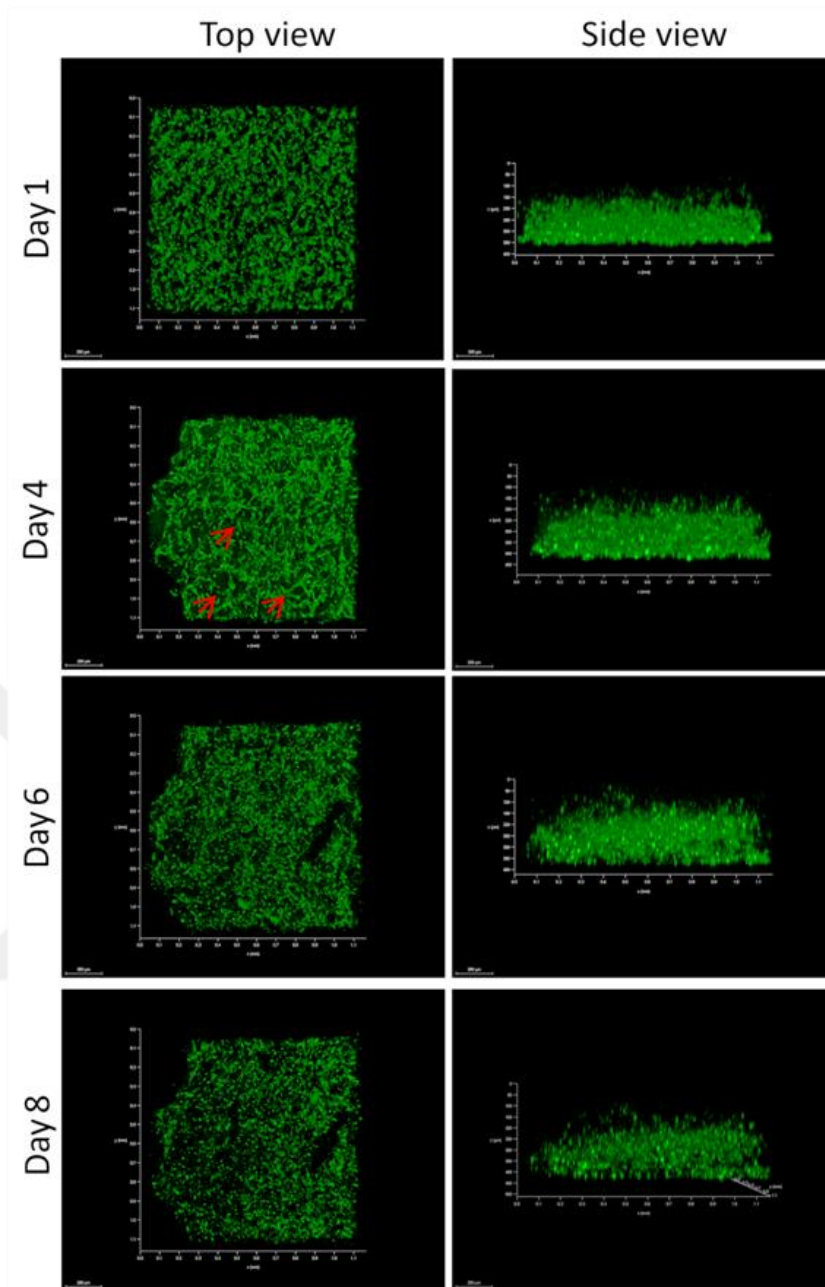


Figure 4.11. Confocal images of LOC device containing 4.9×10^6 /ml HUVEC-C in fibrin gel and 2×10^6 /ml 3T3-L1 in reservoirs away from endothelial cells day by day.

10 μ M Green tracker was used as a dye for HUVEC-C a day before experiment. Fibrinogen concentration was set as 3.5 mg/ml and cells were dissolved in 4U/ml thrombin containing medium. 3T3-L1 cells were loaded into reservoir which was one channel away from the matrix channel. Medium was changed every day. Images were taken by 10X objective.

The results showed that more alignment of cells was observed in Figure 4.11 compare to Figure 4.9 and Figure 4.10. Alignment of cells showed the presence of fibroblasts that affected the microvasculature in a paracrine way when we compare the day 4 images. The endothelial cells were rounded themselves and formed circular shaped as lumen structure resemble with vein structure *in vivo*. Red arrows show the MVN formation.

But even more alignment was observed, the lumen formation and the structure was not completely enough for the vascularization of endothelial cells. At day 6 and day 8, the significant difference was not observed for the alignment and the connection of cells.

A high concentration of fibrinogen was resulted in more compact structure which affects the pore size and diffusion ²⁸. In the results, the concentrations of fibrinogen might limit the diverse parameters such as the connection, alignment and lumen diameter. To observe effect of low concentration of fibrinogen, we decreased the concentration of gel. In addition, we added the aprotinin which inhibits the fibrinolysis in the matrix to control the culture of cells at the long term. Another approach is changing the thrombin concentration which also affects the pore size and diffusion of gel ²⁹.

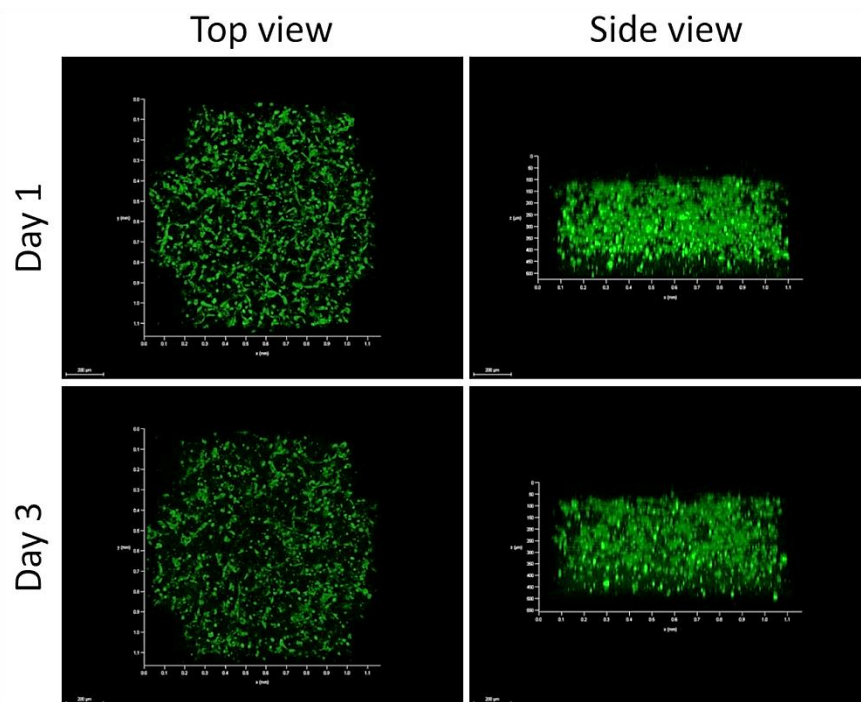


Figure 4.12. Confocal images of 4.5×10^6 /ml HUVEC- in fibrin gel by day.

10 μM Green tracker was used as a dye for HUVEC-C a day before experiment. Fibrinogen concentration was set as 2.5 mg/ml and cells were dissolved in 0.5U/ml thrombin and aprotinin (0.15U/ml) containing medium according to first fibrin gel protocol. Aprotinin was used as a proteinase inhibitor to provide the maintenance of the structure in a long term²⁹. Concentration of HUVEC-C cells is $4.5 \times 10^6/\text{ml}$. Low concentration of fibrinogen and the nearly the same number of HUVEC-C provided the more alignment and connection of cells at the beginning of day 1 compare to the conditions containing higher concentration fibrinogen (Figure 4.2, Figure 4.4, Figure 4.6, Figure 4.9).

4.1.4. Different Fibrin Gel Compositions

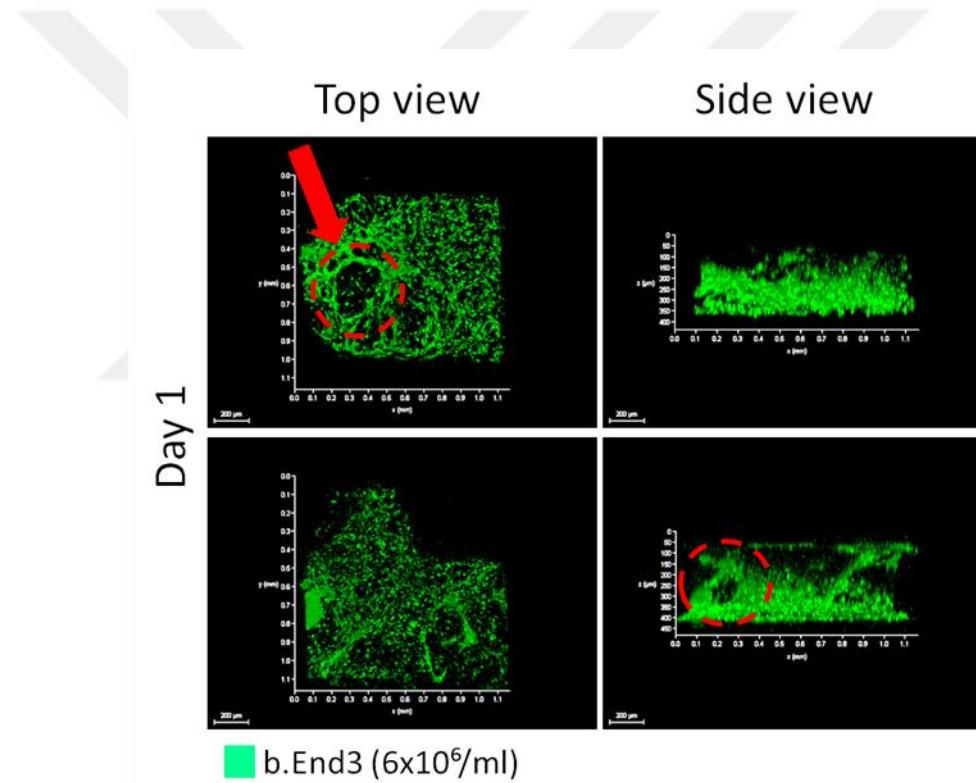


Figure 4.13. Confocal images of $6 \times 10^6/\text{ml}$ b.End3 in fibrin gel day by day.

10 μM Green tracker was used as a dye for b.End3 a day before experiment. Fibrinogen concentration was set as 3 mg/ml and cells were dissolved in 0.5 U/ml thrombin and 0.15 aprotinin containing medium. Figure 4.13, Figure 4.14, Figure 4.15 show the confocal images of vascularization and the structure of the endothelial cells for day 1, day 2 and day 5. Red circular areas and arrow show the lumens at the different positions of images.

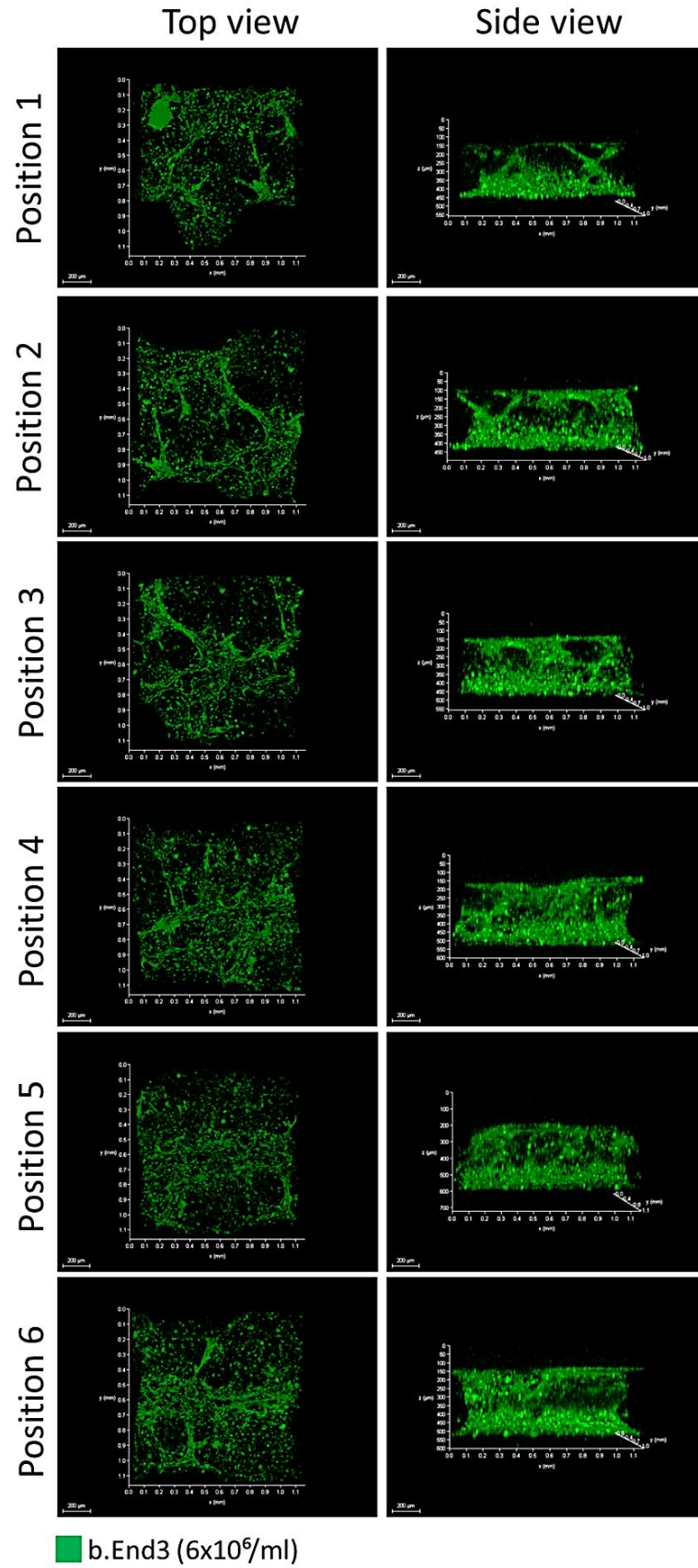


Figure 4.14. Confocal images of $6 \times 10^6/\text{ml}$ b.End3 in fibrin gel for day 2.

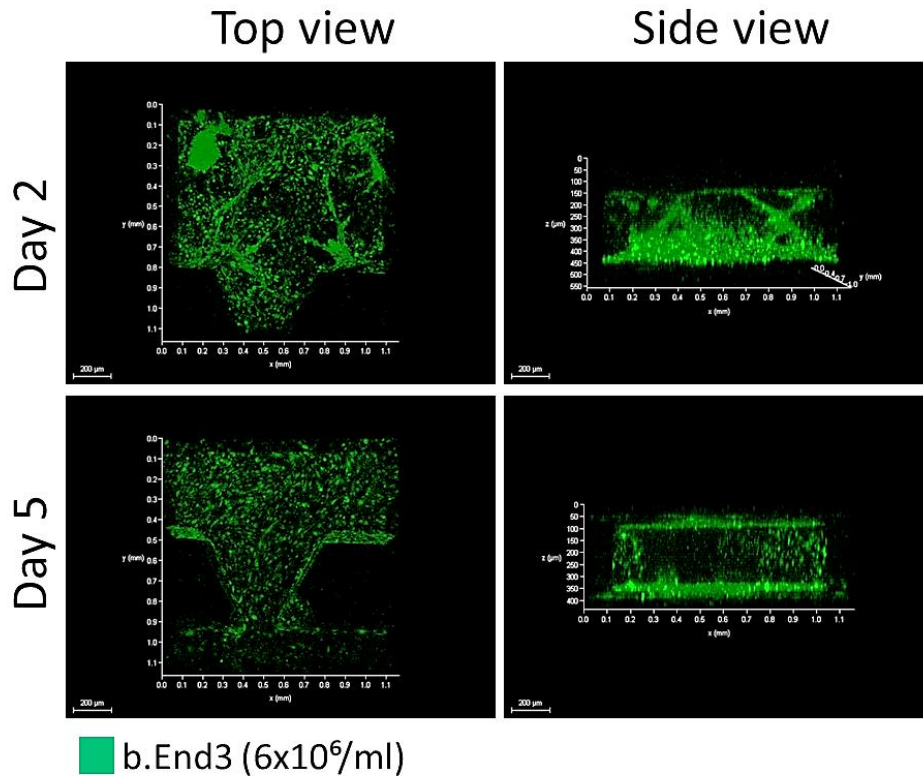


Figure 4.15. Confocal images of $6 \times 10^6/\text{ml}$ b.End3 in fibrin gel for day 2 and day 5.

10 μM Green tracker was used as a dye for b.End3 a day before experiment. Fibrinogen concentration was set as 3 mg/ml and cells were dissolved in 0.5 U/ml thrombin and 0.15 U/ml aprotinin containing medium according to first fibrin gel protocol (Figure 4.14 and Figure 4.15).

The results show that 3D structure, the integrity and the connections of the endothelial cells were provided lower concentration of fibrinogen. The low concentration of fibrinogen let the cells being more alignment and convenient medium diffusion in long term compare to higher concentration of gel. But the connections of cells were destroyed at day 5. The usage of aprotinin was determined to inhibit fibrinolysis activity of gel. Lower concentrations of thrombin (0.5 U/ml) in 3 mg/ml fibrin gel in the presence of aprotinin supported the formation of MVN better at day 2. However, MVN structure was disrupted at day 5.

In another approach is usage of mesenchymal stem cells to provide the MVN formation. The effect of different seeding ratios of mesenchymal stem cells was shown that the MVN formation occurred by stabilizing the endothelial cells which regulates angiogenic sprouting in microfluidic device ³⁰. In another research, the presence of mural cell-like human bone marrow mesenchymal stem cells showed the effect on

increase of network branches and decrease of vessel diameter compare to conditions only culture of endothelial cells in the microfluidic system³¹. We combined the usage of aprotinin and mesenchymal stem cells (D1-ORL-UVA: bone marrow mesenchymal stem cells) to control the degradation of gel.

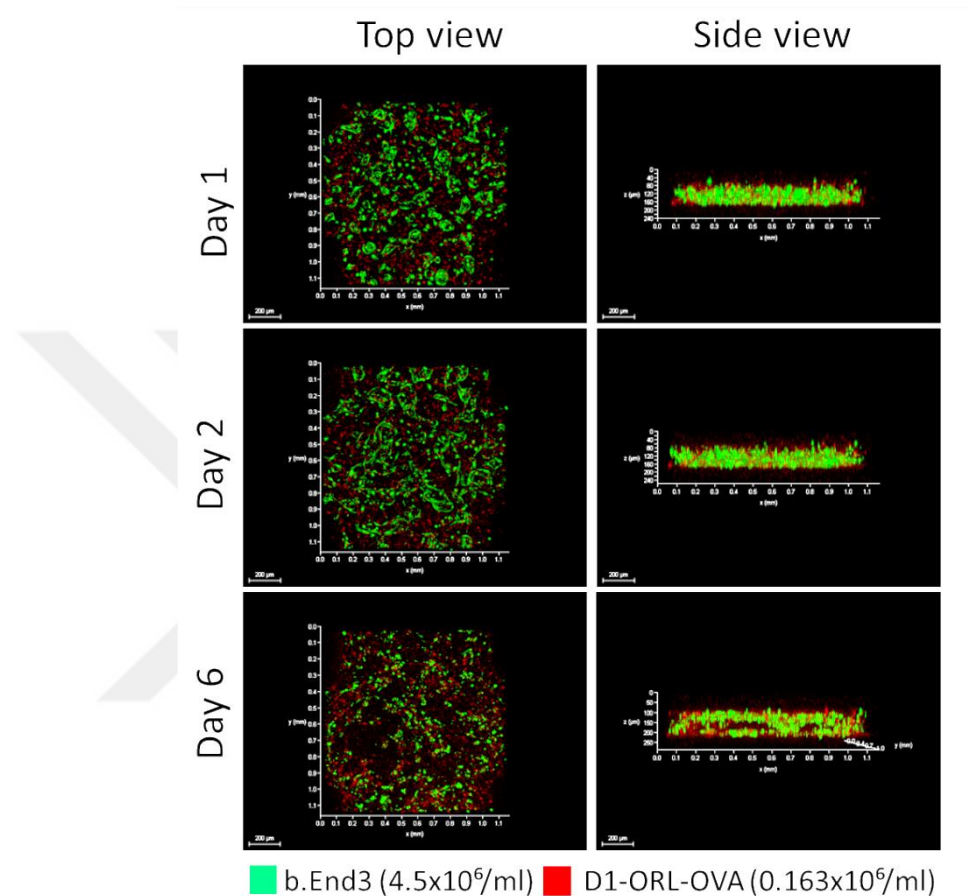


Figure 4.16. Confocal images of $4.5 \times 10^6/\text{ml}$ b.End3 and $0.163 \times 10^6/\text{ml}$ D1-ORL-OVA in fibrin gel.

10 μM Green tracker and 5 μM Deep red tracker was used as a dye for b.End3 and D1-ORL-OVA cells a day before experiment. Fibrinogen concentration was set as 3 mg/ml and cells were dissolved in 4 U/ml thrombin and 0.15 U/ml aprotinin containing medium according to first fibrin gel protocol. Vascularization of endothelial cells was observed in presence or absence of mesenchymal stem cells to understand the effect of stem cells for the construction of vascular tissue (Figure 4.16 and Figure 4.17).

In the presence of mesenchymal stem cells, both the connection and the alignment of endothelial cells were shown. In Figure 4.17, at day 6 endothelial cells lost their cell-cell connection by forming two different phases like structure which lines up and down in the chip. In Figure 4.16, endothelial cells were prone to be more aligned in

the chip by keeping the connections up and down of the cells in device. But the duration of culture is long.

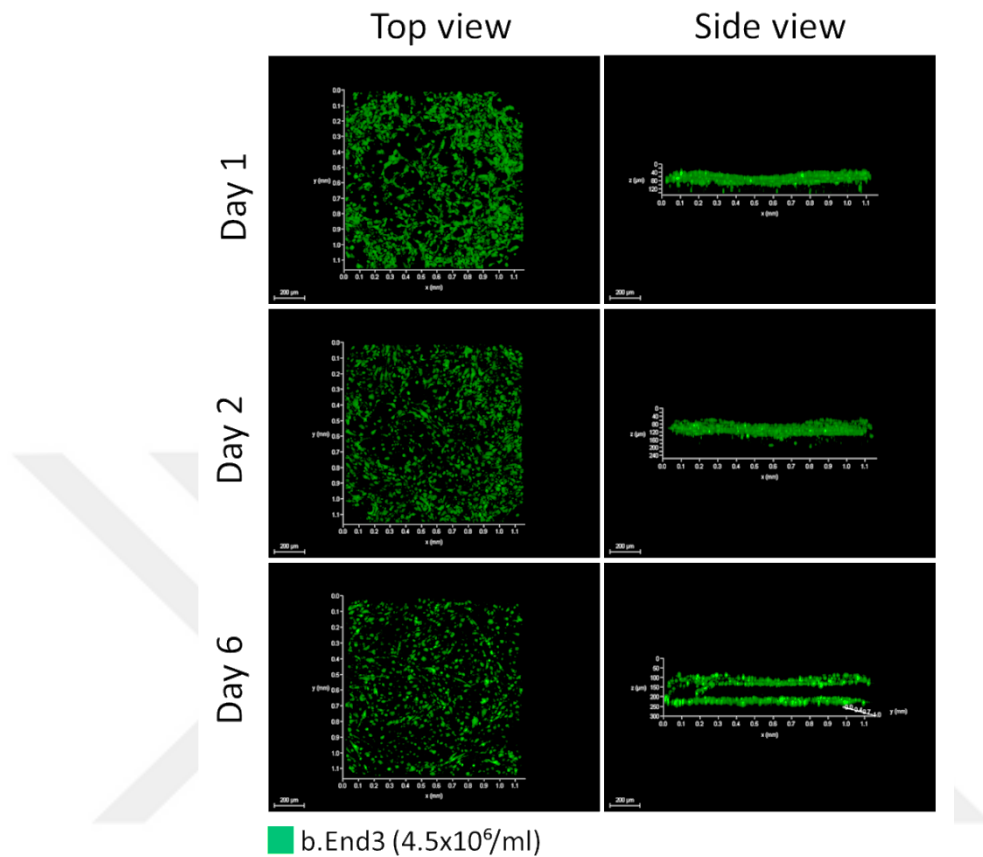


Figure 4.17. Confocal images of $4.5 \times 10^6/\text{ml}$ b.End3 in fibrin gel for day 1, day 2 and day 6.

We decided to continue with using fibroblasts which are main regulators of generating homing microenvironment. In addition, we decided to use co-culture of fibroblasts with endothelial cells rather than providing paracrine signalling Figure 4.10 and Figure 4.11 to decrease the long term culture by achieving generation of MVN formation at the same time. For this purpose, we used low concentration of gel and high concentration of endothelial cells in the absence of aprotinin.

4.1.5. Use of Fibroblasts in Co-culture with Endothelial Cells

High concentration of b.End3 endothelial cells in co-culture with fibroblasts to improve the MVN formation. In addition, the concentration of thrombin was increased into 0.83 U/ml.

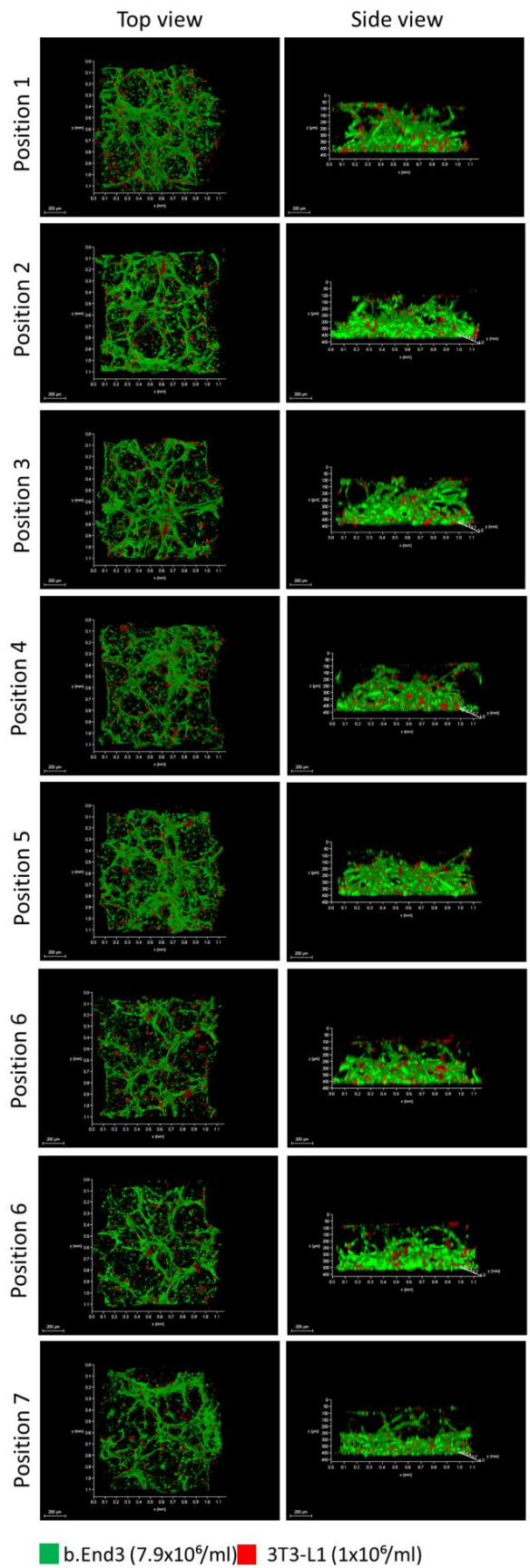


Figure 4.18. Confocal images of $7.9 \times 10^6/\text{ml}$ b.End3 and $1 \times 10^6/\text{ml}$ 3T3-L1 cells in fibrin gel for day 1.

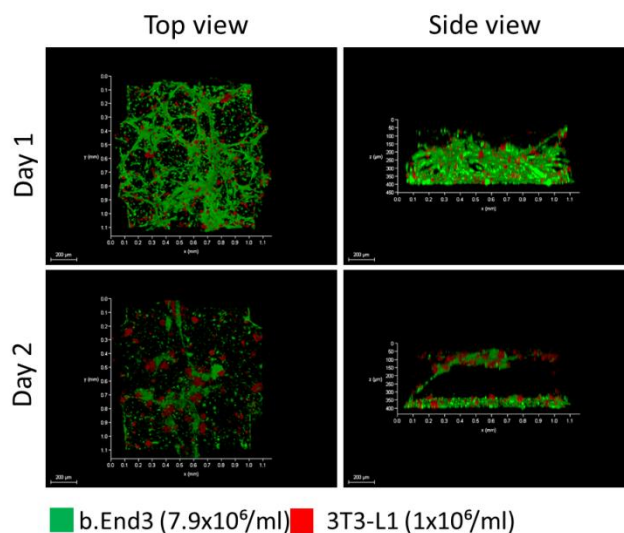


Figure 4.19. Comparison of confocal images of $7.9 \times 10^6/\text{ml}$ b.End3 and $1 \times 10^6/\text{ml}$ 3T3-L1 cells in fibrin gel for day 1 and day 2.

10 μM Green tracker and 5 μM Deep red tracker was used as a dye for b.End3 and 3T3-L1 cells a day before experiment. Fibrinogen concentration was set as 3 mg/ml and cells were dissolved in 0.83 U/ml thrombin containing medium without aprotinin. Vascularization of endothelial cells was observed in the presence of fibroblasts. Figure 4.18 shows the different parts and positions of chip. But, the structure of tissue disrupted at day 2. Cell-cell connections between PDMS and glass surfaces did not observe at day 2. It might be cause of the high concentration of endothelial cells with the absence of aprotinin in the gel composition which is more tents to degradation. We decided to decrease of endothelial cell concentration to prolong the maintenance of structure as an intact form.

The results showed that higher concentration of thrombin (0.83 U/ml) in 3 mg/ml fibrin gel in the absence of aprotinin supported the formation of MVN at day 1. However, MVN structure was disrupted at day 2.

4.1.6. Use of Matrigel and Collagen in Fibrin Gel

In another approach is usage of collagen type 1 (0.2 mg/ml) in the gel composition, was shown that has an effect on enhancing lumen formation of developing tubular structures²⁶.

10 μM Green tracker and 5 μM Deep red tracker was used as a dye for b.End3 and 3T3-L1 cells a day before experiment. Fibrinogen, matrigel and collagen concentrations were set as 3 mg/ml, 1.15 mg/ml and 0.5 mg/ml. Cells were dissolved in 0.83 U/ml thrombin containing medium according to third fibrin gel protocol. Vascularization of endothelial cells was observed in the presence of fibroblasts. The structure of tissue was still intact at day 2. It provided more convenient conditions compare to Figure 4.19.

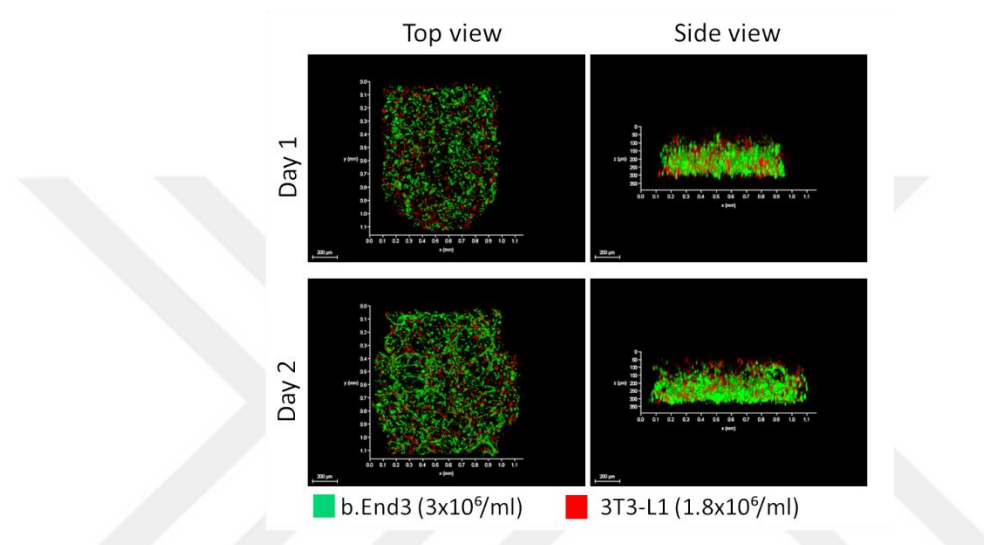


Figure 4.20. Confocal images of $3 \times 10^6/\text{ml}$ b.End3 and $1.8 \times 10^6/\text{ml}$ 3T3-L1 cells in fibrin gel for day 1 and day 2.

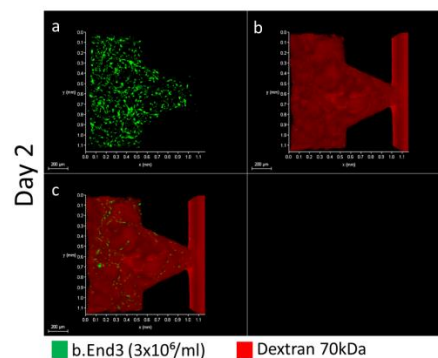


Figure 4.21. Confocal images of $3 \times 10^6/\text{ml}$ b.End3 and $1.8 \times 10^6/\text{ml}$ 3T3-L1 cells in fibrin gel after dextran diffusion at day 2.

We used dextran molecule to observe the perfusion of the structure. Figure 4.21 shows the permeability results. Dextran 70kDa was used in 1:50 dilution with complete DMEM media. Dextran 70kDa diffused into both matrix and cells.

The invasion of endothelial cells might be the inefficient towards the media channels. Usage of b.End3, MCF-10A, and 3T3-L1 cells are planned to engineer the target breast tissue in this experimental setup. The total concentration of MCF-10A, and 3T3-L1 was set to 1.8×10^6 /ml not to inhibit the vascularization of endothelial cells.

4.2. Engineering Breast and Lung Tissue

To engineer breast tissue, mimicking the complex microenvironmental conditions is the critical beginning step. Mammary gland is consisting of enrich microenvironment and diversity of cell types containing fibroblasts, adipocytes, epithelial cells and vasculature related cells³². Both of myoepithelial and luminal cells is the main generators of the stroma which their activity is resulted in formation of branching ducts. The luminal epithelial cells are known as the polarized characteristic morphology generating constant layer that builds duct and alveolus. Each ductal branching is connecting with small spheroid shaped acini or alveoli³³.

4.2.1. Co-culture of Raw264.7 and MCF-10A in Fibrin Gel

We co-cultured macrophages (Raw264.7) and epithelial cells (MCF-10A) cells to optimize the engineering breast tissue by using different cell concentrations. Macrophages and epithelial cells were used in 1:1 dilution 12.5×10^4 /ml or 2.5×10^4 /ml as final concentrations. Fibrin gel components and concentrations were used according to Figure 4.1 (Fibrinogen: 3.5 mg/ml, Thrombin: 4 U/ml).

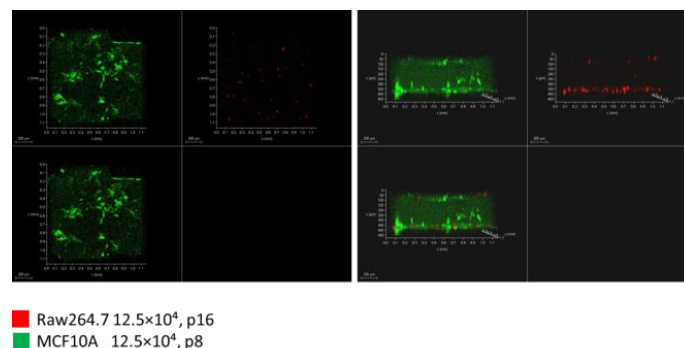


Figure 4.22. Confocal images of Raw264.6, MCF-10A in fibrin gel for day 4.

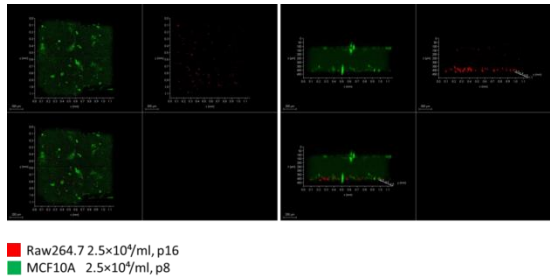


Figure 4.23. Confocal images of Raw264.6, MCF-10A in fibrin gel for day 4.

Co-culture of low concentrations of cells ($12.5 \times 10^4/\text{ml}$) provided more suitable environment to find each other of epithelial cells in the matrix during four-day culture. But the homogeneous distribution of epithelial cells did not observe. At the right part of each figures, cells generated phase like structure lining up-down in the channel no filling the middle side of the structure (Figure 4.22 and Figure 4.23). Optimization of co-culture was continued with the addition of epithelial cells as forming tri-culture conditions by changing concentrations of cells.

4.2.2. Tri-culture of HUVEC-C, Raw264.7 and MCF-10A in Fibrin Gel

We began to optimize the generation of breast tissue by using endothelial cells, macrophages and epithelial cells in different concentrations.

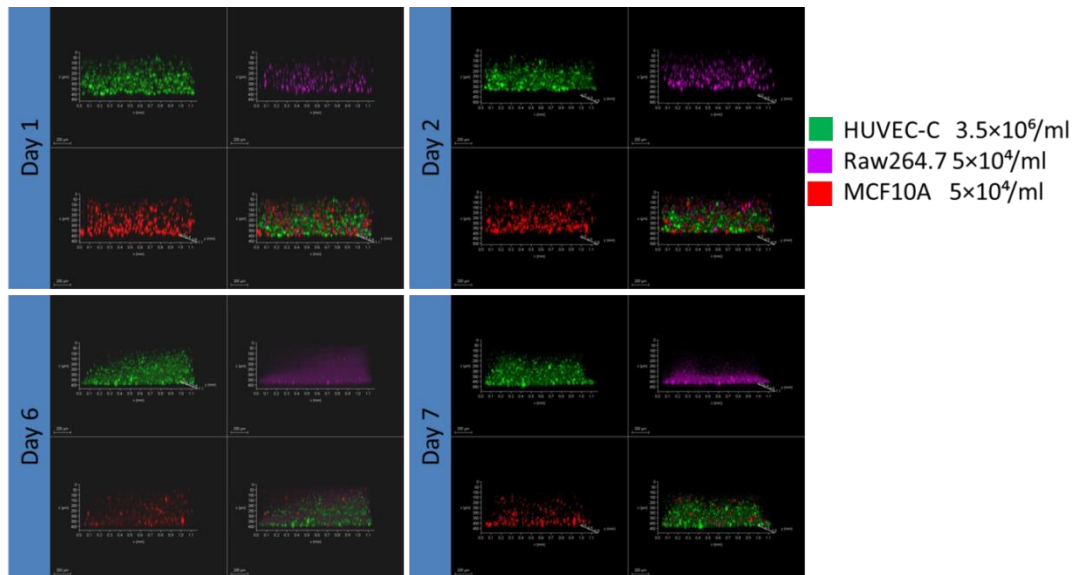


Figure 4.24. Confocal images of HUVEC-C, Raw264.6, MCF-10A in fibrin gel day by day.

10 μM Green tracker, 25 μM Blue tracker and 5 μM Red tracker were used as a dye for HUVEC-C, Raw264.7 and MCF-10A, respectively a day before experiment. The 3D structure was protected until 6 days. But the morphological changes and the decrease in cell numbers were observed all of endothelial cells, macrophages and epithelial cells. Especially, Raw264.7 and MCF10-A cells precipitated at the bottom with the 6th and 7th day.

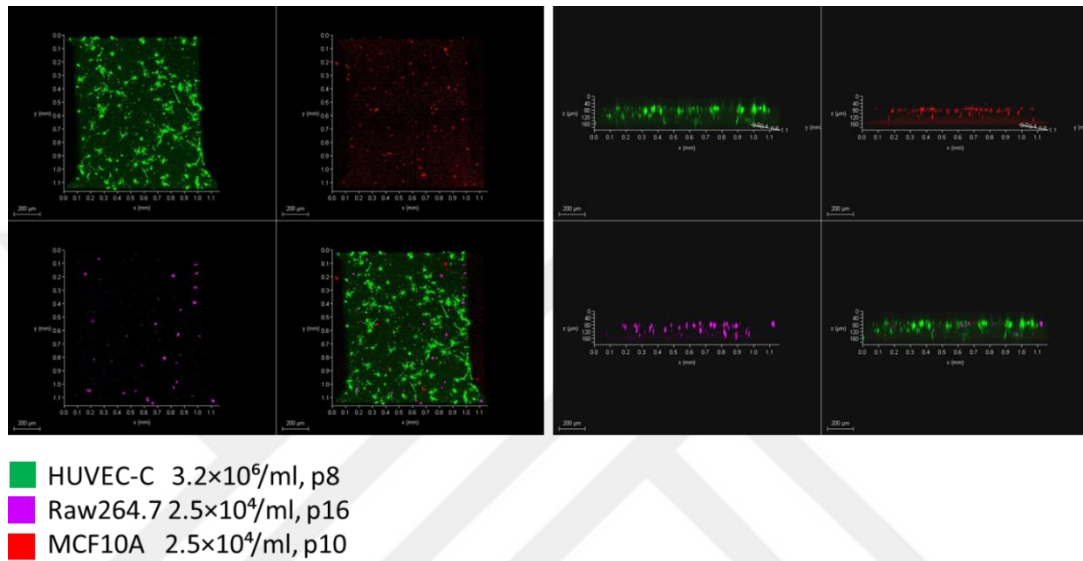


Figure 4.25. Confocal images of HUVEC-C, Raw264.6, MCF-10A in fibrin gel for day 4.

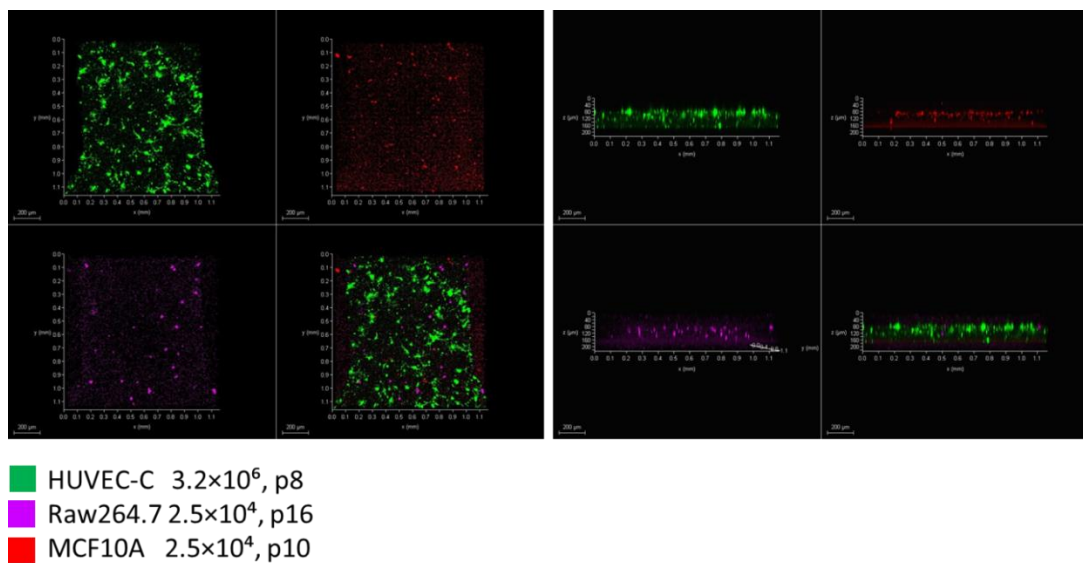


Figure 4.26. Confocal images of HUVEC-C, Raw264.6, MCF-10A in fibrin gel for day 5.

10 μ M Green tracker, 25 μ M Blue tracker and 5 μ M Red tracker were used as a dye for HUVEC-C, Raw264.7 and MCF-10A, respectively a day before experiment. Confocal images were taken for day 4 and day 5. Cell ratios of Raw264.7 and MCF-10A cells did not inhibit the growth of HUVEC-C, but the MVN was not observed at day 5.

Macrophages and fibroblasts are known as key players in the tumor microenvironment. Macrophages have a heterogeneous cell population taking role in immune system, repair mechanism and also homeostasis in the microenvironment of tissue³⁴. We decided not to use macrophages in the matrix. Because of our primary aim is to generate healthy tissue not in the state of inflammation.

4.2.3. Co-culture of HUVEC-C with 3T3-L1 or MCF-10A Cells in Fibrin Gel

We tested low number of endothelial cells with fibroblasts in a long term culture.

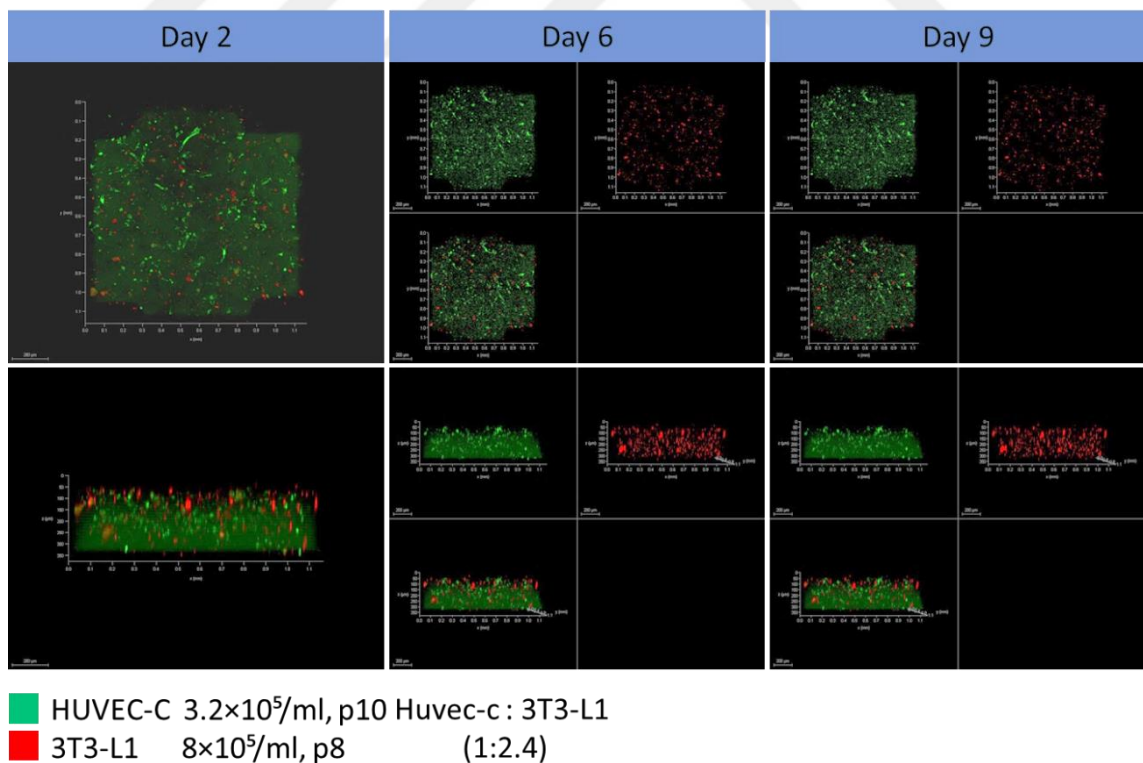


Figure 4.27. Confocal images of HUVEC-C and 3T3-L1 in fibrin gel the day by day.

10 μ M Green tracker, 5 μ M Red tracker were used as a dye for HUVEC-C and 3T3-L1 cells respectively a day before the experiment. Confocal photos were taken for day 2, day 6 and day 9. Fibroblast are the main component of stroma since we used higher concentration of fibroblast, but higher concentration might inhibit the connection of endothelial cells to form MVN. The structure did not disrupt. In addition, it is a long period for the formation of vascularization and the construction of target tissue. We decided to test also the same cell concentration with epithelial cells (MCF-10A).

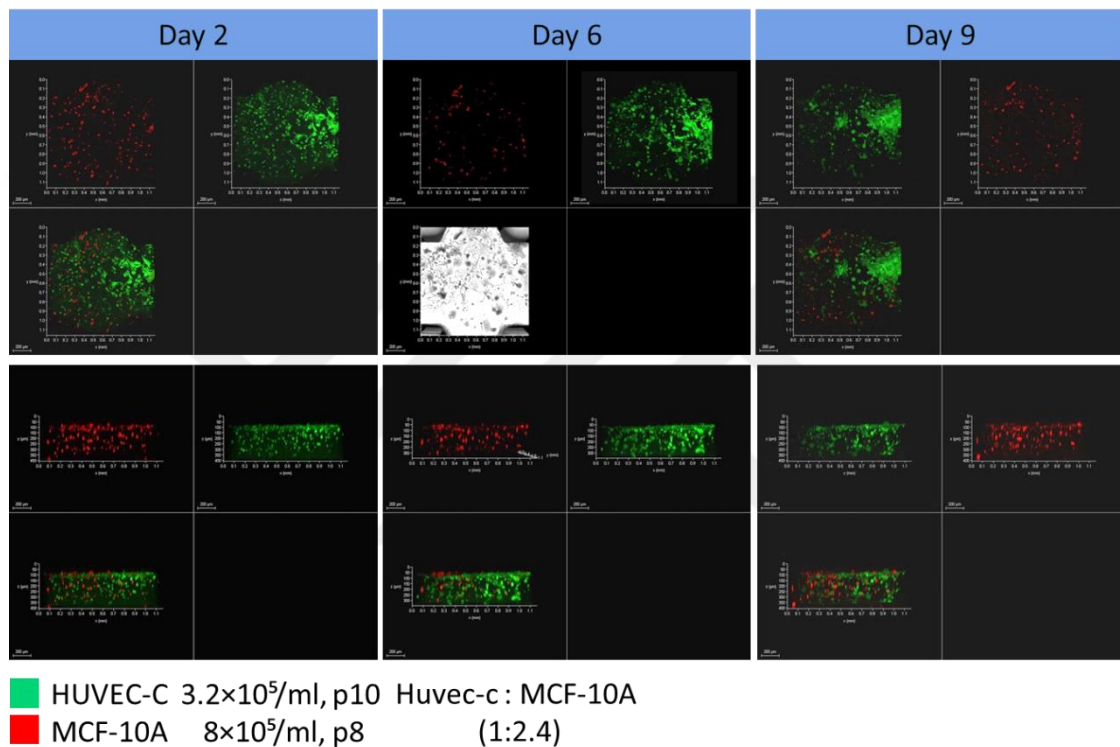


Figure 4.28. Confocal images of HUVEC-C and MCF-10A in fibrin gel the day by day.

10 μ M Green tracker, 5 μ M Red tracker were used as a dye for HUVEC-C and MCF-10A respectively a day before the experiment. Confocal photos were taken for day 2, day 6 and day 9. The concentration of MCF-10A cells did not inhibit the growth of HUVEC-C. The structure was conserved until 9th day.

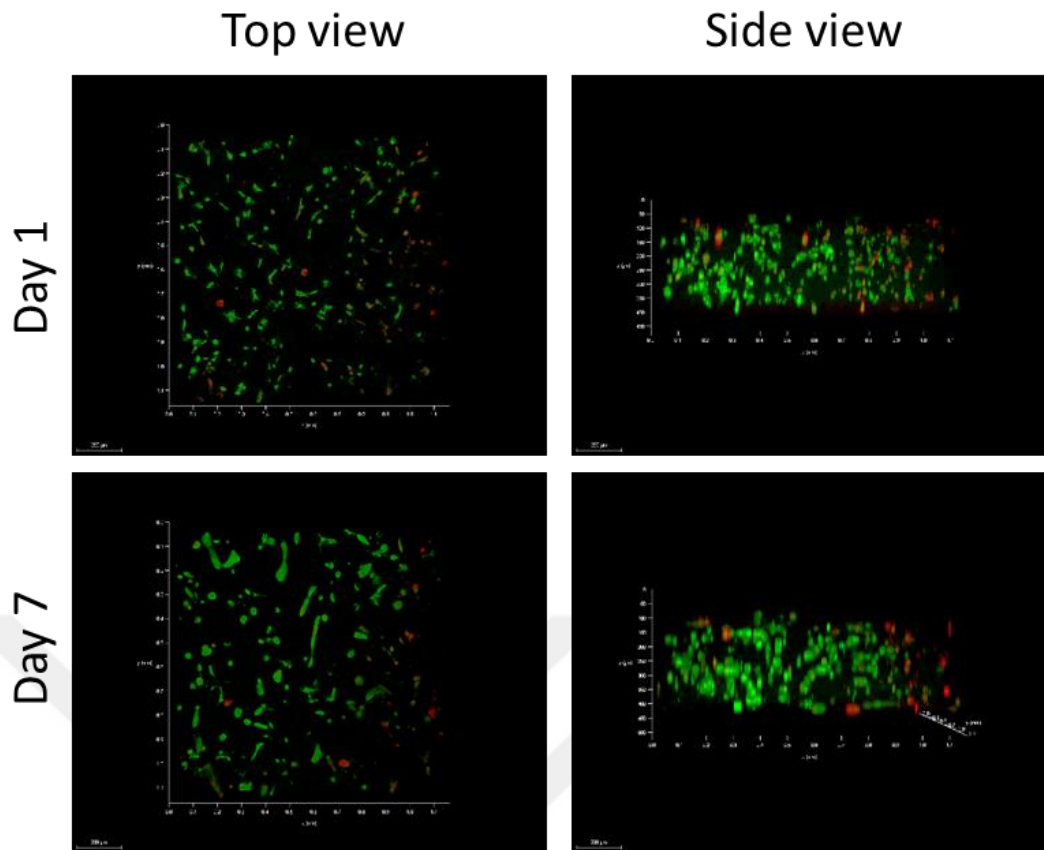


Figure 4.29. Confocal images of HUVEC-C and MCF10A cells in concentration of $0.325 \times 10^6/\text{ml}$ at day 2 and day 7.

Images show the conditions which contains fibroblasts (4166/ml) at the lateral medium channels. $10 \mu\text{M}$ Green, $5 \mu\text{M}$ Deep red tracker were used as dyes for HUVEC-C and MCF-10A, respectively. Fibrinogen concentration was set as 2.5 mg/ml and cells were dissolved in 4U/ml thrombin containing medium. Final concentration of each cell (HUVEC-C, MCF-10A) is $0.325 \times 10^6/\text{ml}$. Medium was changed every day. Images were taken by 10X objective. Low numbers of HUVEC-C and MCF-10A cells were used for the formation of target tissue. Because high numbers of cells might cause the disruption of the tissue structure rapidly. In addition, fibroblasts were loaded into lateral channels to observe the effects of fibroblast which provides the lumen formation or not via their soluble factors in the microenvironment. We observed that the lumen formation and vascularization did not form at the end of a week. We decided to increase the beginning concentrations of endothelial cells with co-culture conditions with epithelial cells.

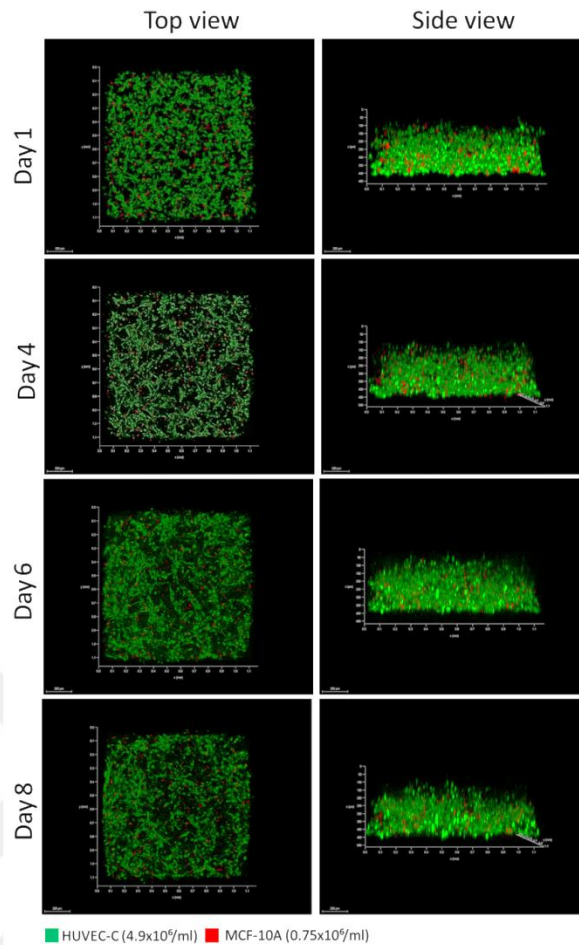


Figure 4.30. Confocal images of $4.9 \times 10^6/\text{ml}$ HUVEC-C and $0.75 \times 10^6/\text{ml}$ MCF-10A in fibrin gel and $2 \times 10^6/\text{ml}$ 3T3-L1 in reservoirs away from endothelial cells day by day.

$10 \mu\text{M}$ Green tracker and $5 \mu\text{M}$ deep red tracker were used as a dye for HUVEC-C and MCF-10A a day before experiment, respectively. Fibrinogen concentration was set as 3.5 mg/ml and cells were dissolved in 4 U/ml thrombin containing medium. Concentration of endothelial cells and MCF-10A cells were $4.9 \times 10^6/\text{ml}$ and $0.75 \times 10^6/\text{ml}$.

3T3-L1 cells were loaded into reservoirs which were one channel away from the matrix channel (Figure 4.8b). The reason of this loading position is that the prevention of 3T3-L1 invasion providing the soluble factors from 3T3-L1 to endothelial cells. Medium was changed every day. Images were taken by 10X objective. More alignment of cells was observed at fourth day. Addition of MCF-10A cells did not inhibit the alignment and connection of endothelial cells compare to Figure 4.29. But, the MVN

formation and the structure was not still completely enough for the vascularization of endothelial cells.

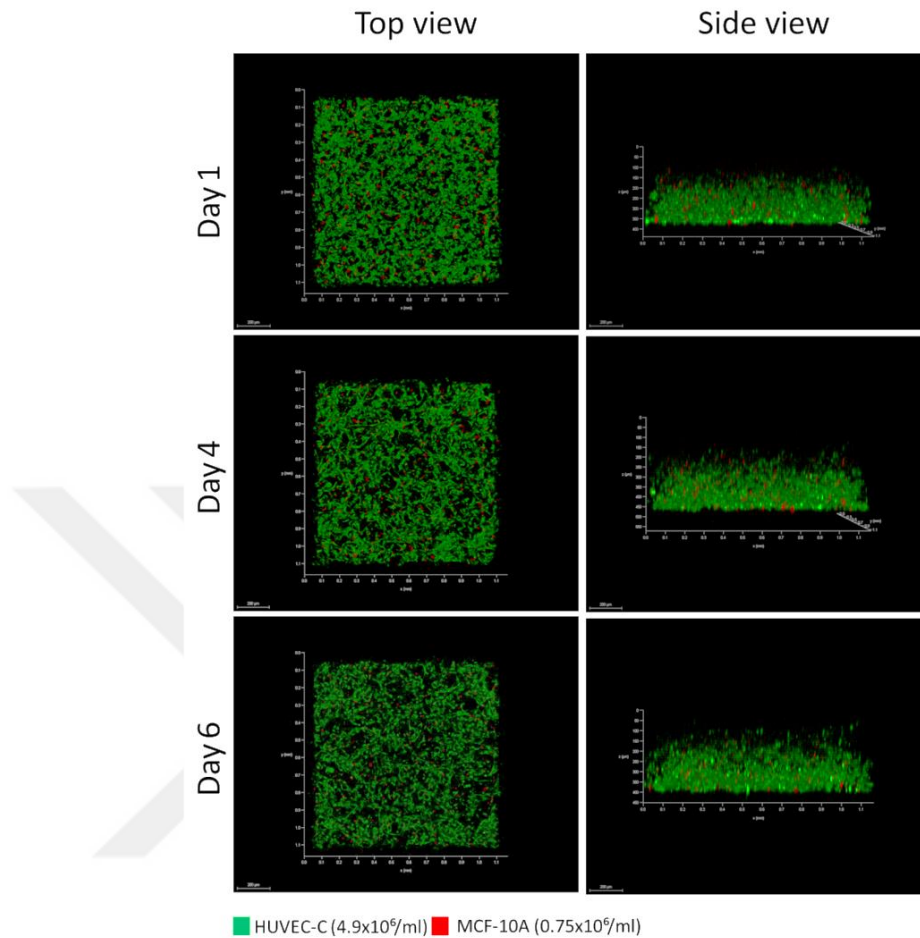


Figure 4.31. Confocal images of 4.9×10^4 /ml HUVEC-C and 0.75×10^6 /ml MCF-10A in fibrin gel day by day.

10 μ M Green tracker and 5 μ M deep red tracker were used as a dye for HUVEC-C and MCF-10A a day before experiment, respectively. Fibrinogen concentration was set as 3.5 mg/ml and cells were dissolved in 4U/ml thrombin containing medium according to first fibrin gel protocol. Concentration of endothelial cells and MCF-10A cells were 4.9×10^6 /ml and 0.75×10^6 /ml.

Only HUVEC-C media was loaded into reservoirs. Medium was changed every day. Images were taken by 10X objective. More alignment of cells was observed at fourth day. There was not any big difference in the terms of endothelial cell alignment or vascularization in the axis morphological changes compare to Figure 4.30. In Figure 4.31, endothelial cells began to form rounded shapes to form lumen like structure at day 4, while in Figure 4.30 we observed a more compact and tight connection of endothelial

cells. Organizations of endothelial cells were effected via fibroblast, but the vascularization did not observe in a long term culture. We tested the higher concentration of epithelial cells in the presence of fibroblasts at the lateral channels.

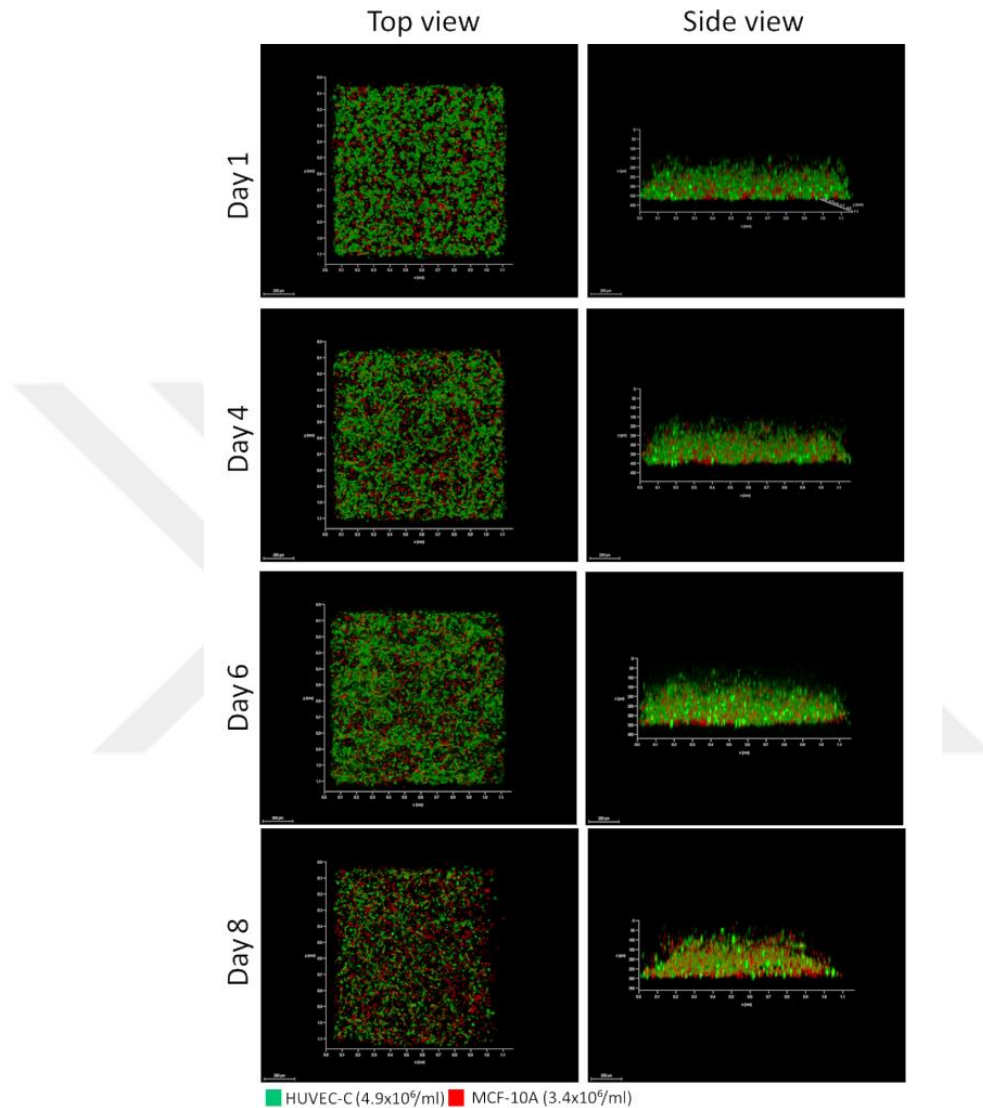


Figure 4.32. Confocal images of 4.9×10^6 /ml HUVEC-C and 3.4×10^6 /ml MCF-10A in fibrin gel and 2×10^6 /ml 3T3-L1 at the lateral channels.

10 μ M Green tracker and 5 μ M deep red tracker were used as a dye for HUVEC-C and MCF-10A a day before experiment, respectively. Fibrinogen concentration was set as 3.5 mg/ml and cells were dissolved in 4U/ml thrombin containing medium. Concentration of HUVEC-C and MCF-10A cells were 4×10^6 /ml and 2×10^6 /ml, respectively. In addition, fibroblasts (3T3-L1) were loaded into lateral channels with 1×10^6 /ml.

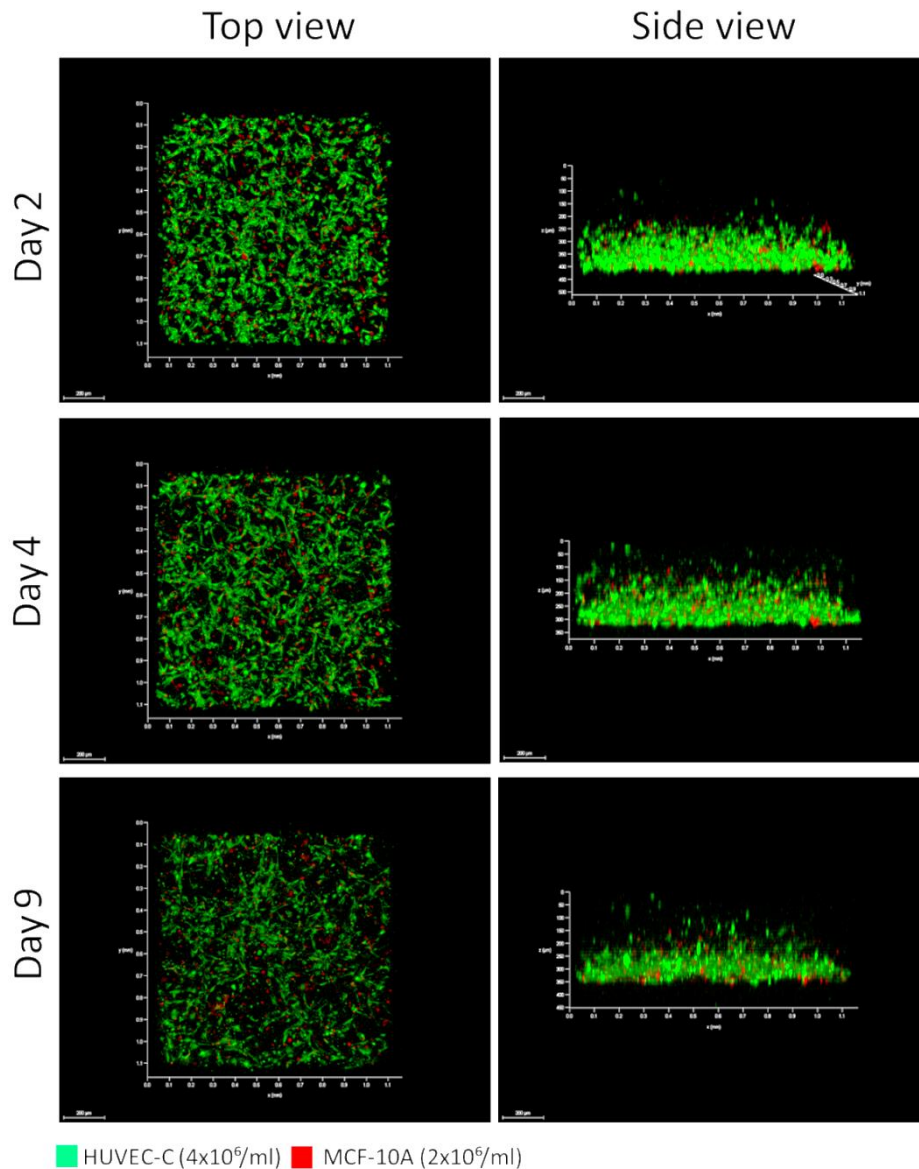


Figure 4.33. Confocal images of $4 \times 10^6/\text{ml}$ HUVEC-C and $2 \times 10^6/\text{ml}$ MCF-10A in fibrin gel in fibrin gel and $1 \times 10^6/\text{ml}$ 3T3-L1 at the lateral medium channels.

To understand the effect of 3T3-L1 for the construction of cells by providing optimum epithelial cell number, $2 \times 10^6/\text{ml}$ and $4 \times 10^6/\text{ml}$ of MCF-10A cells were used in the presence and absence of 3T3-L1 cells at the lateral channels. The results were shown at Figure 4.33 and Figure 4.34. $10 \mu\text{M}$ Green tracker and $5 \mu\text{M}$ deep red tracker were used as a dye for HUVEC-C and MCF-10A a day before experiment, respectively. Fibrinogen concentration was set as 3.5 mg/ml and cells were dissolved in 4U/ml thrombin containing medium according to first fibrin gel protocol. Concentration of HUVEC-C and MCF-10A cells were $4 \times 10^6/\text{ml}$ and $2 \times 10^6/\text{ml}$, respectively.

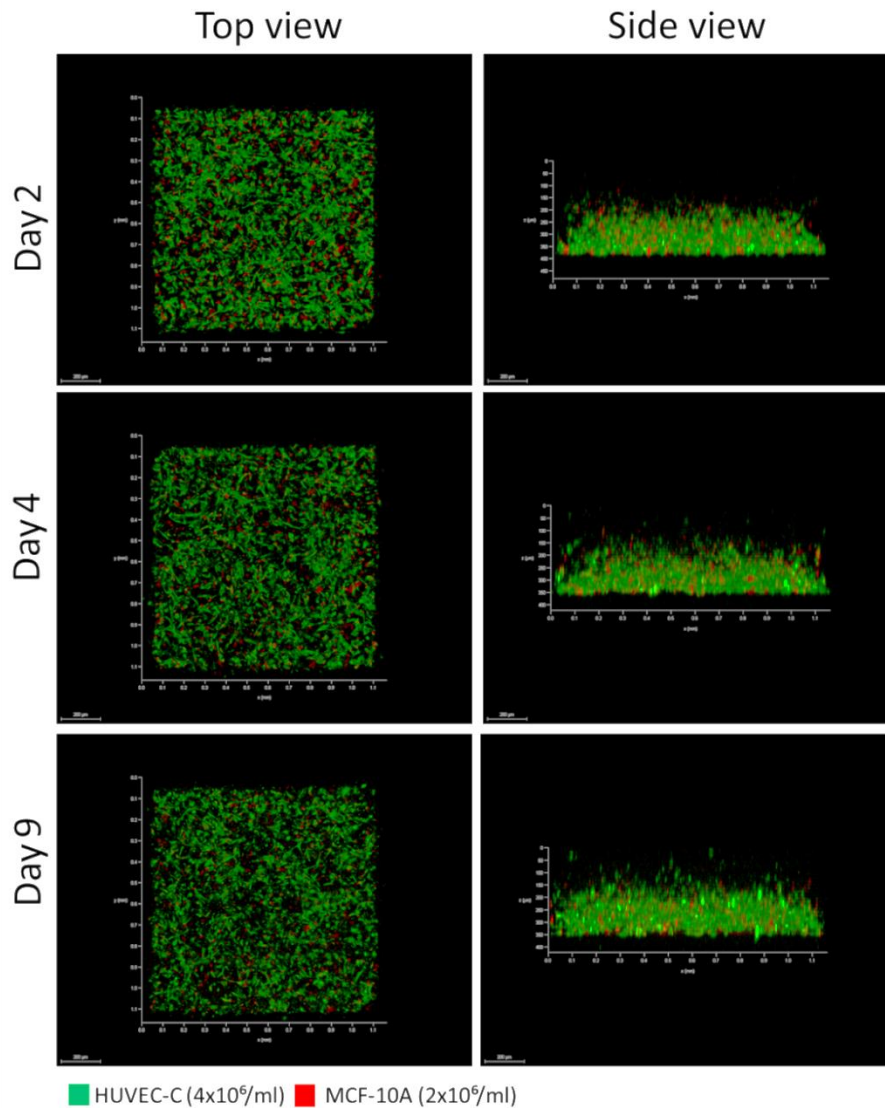


Figure 4.34. Confocal images of $4 \times 10^4/\text{ml}$ HUVEC-C and $2 \times 10^6/\text{ml}$ MCF-10A in fibrin gel in fibrin gel day.

The results showed that endothelial cells were generated more contact by presenting lumen like structure at day 4 in the absence of fibroblasts (Figure 4.34). It indicates that the presence of fibroblasts might result in distinct effect on vasculature depending on the ratio of endothelial and epithelial cells. In Figure 4.32 and In Figure 4.33 show the conditions 1.4:1 and 2:1 ratios of endothelial: epithelial cells in the presence of fibroblasts at the lateral channels. Use of more higher ratio of endothelial cells and low concentration of fibroblast at the lateral channels resulted in more alignment of endothelial cells at day 4.

We tested 1:1 ratio of endothelial: epithelial cells at the beginning for both conditions in the presence or absence of fibroblasts at the lateral channels.

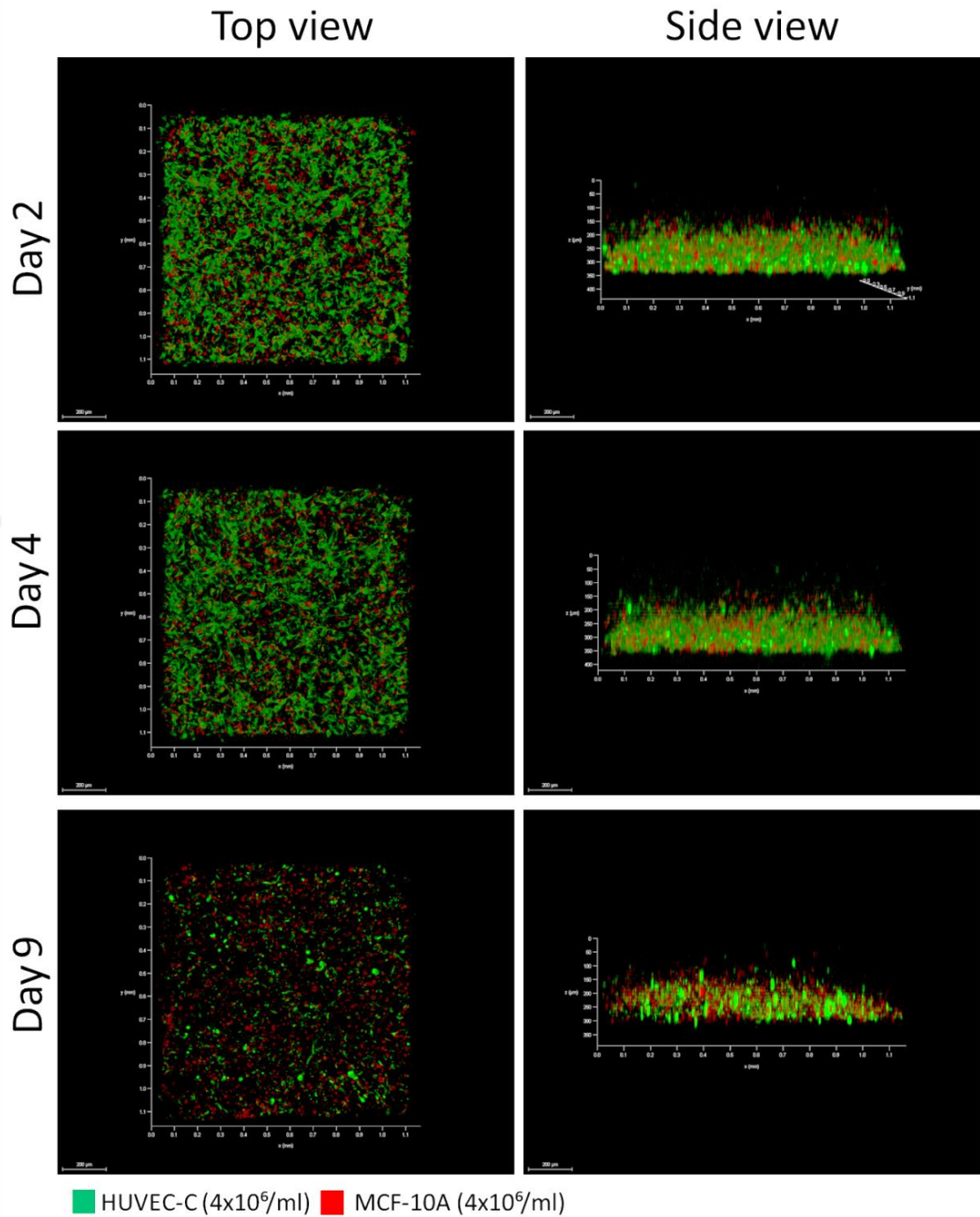


Figure 4.35. Confocal images of $4 \times 10^6/\text{ml}$ HUVEC-C and $4 \times 10^6/\text{ml}$ MCF-10A in fibrin gel in fibrin gel and $1 \times 10^6/\text{ml}$ 3T3-L1 at the lateral channels.

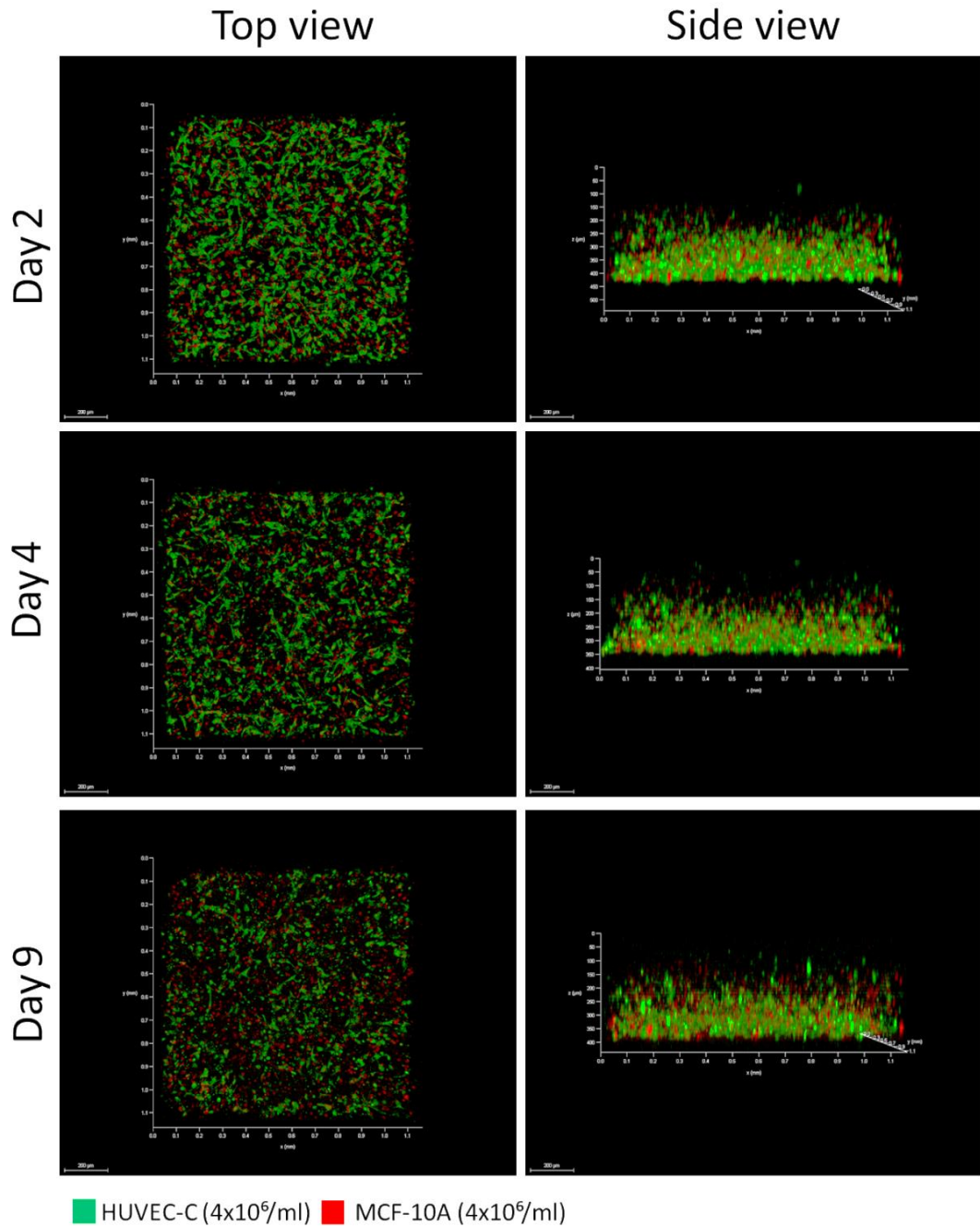


Figure 4.36. Confocal images of 4×10^6 /ml HUVEC-C and 4×10^6 /ml MCF-10A in fibrin gel day by day.

The varieties ratios (1.4:1, 2:1, 1:1) were tested for the combination of both endothelial and epithelial cells in the absence or presence of endothelial cells. The results showed that 2:1 ratio provided more convenient beginning concentration for co-culture of endothelial and epithelial cells to observe more connection and alignment of endothelial cells in the fibrin gel structure.

4.2.4. Tri-culture of b.End3, 3T3-L1 and MCF-10A Cells in Fibrin gel for Generation of Breast Tissue

In the literature, there is not any information about the concentrations of distinct cells in breast. 2D studies have been realized in 8-well chamber slides coated with matrigel in containing human endothelial cells HUVEC-C, normal or preneoplastic MCF10AT1-EIII8, MCF10A, to observe breast stromal-epithelial interactions concluded the requirement of organ specific fibroblast to provide the epithelial morphogenesis³⁵.

First of all, engineering of target breast tissue is started to optimize. For this purpose, different cell lines and cell concentrations are used to find more appropriate combination.

Table 3. Cell lines for breast and lung tissue.

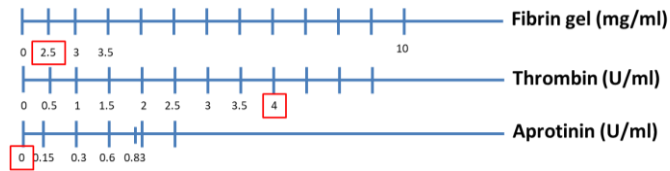
	Epithelial cell	Endothelial cell	Fibroblast
Breast tissue	MCF-10A	HUVEC-C or b.End3	3T3-L1
Lung tissue	BEAS-2B	HUVEC-C or b.End3	WI38

For this purpose, b.End3 or HUVEC-C (endothelial), 3T3-L1 (fibroblast), MCF-10A (epithelial) cell lines are used in the experiments with different cell concentrations and methods. The formation of the MVN is a critical step of engineering target tissues to functionalize the target tissues. The aim was the achievement of MVN formation in the co-culture conditions.

b.End3 cell line was preferred rather than HUVEC-C cell line. Because, it provides to work with high passage number and high cell concentration compare to HUVEC-C. In co-culture results of endothelial and epithelial cells showed that ratios of cells are crucial control the organization of cells for engineering target tissue. However, the gel componenets and the concentration of fibrin might effect on formation of more branching of endothelial cells providing lumen like structure. In the light of results and

discussions, we decided to decrease the concentration of fibrinogen from 3.5 mg/ml to 2.5 mg/ml.

Table 4. The gel components containing high concentration of fibrinogen without aprotinin.



10 μ M Green, 25 μ M Blue, 5 μ M Deep red tracker was used as dyes for b.End3, MCF-10A cells, 3T3-L1 cells respectively a day before experiment. Fibrinogen concentration was set as 2.5 mg/ml and cells were dissolved in 4U/ml thrombin containing medium. The concentrations of cells were determined according to Figure 4.20. Endothelial concentration was set to 3×10^6 /ml as a non-inhibited concentration to form vascularization. The total concentration of other cells was set to 1.8×10^6 /ml. Final concentrations of cells are set to 3×10^6 /ml or 1.5×10^6 /ml (b.End3), 0.125×10^6 /ml or 0.25×10^6 /ml (3T3-L1), 0.25×10^6 /ml or 0.5×10^6 /ml or 1×10^6 /ml (MCF-10A).

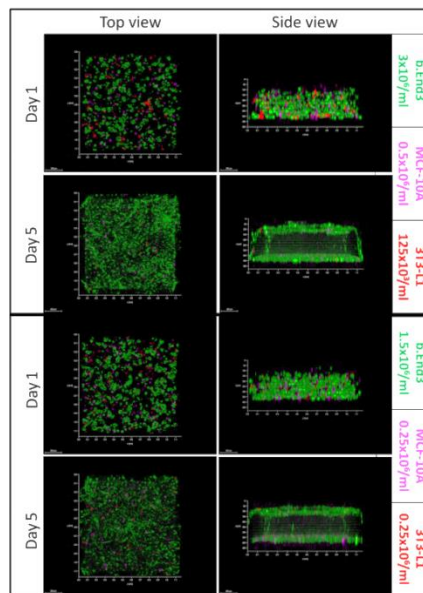


Figure 4.37. Comparison of high and low concentrations of co-culture conditions for b.End3, 3T3-L1, MCF-10A cells in fibrin gel for day 1 and day 5.

(Cont. on next page)

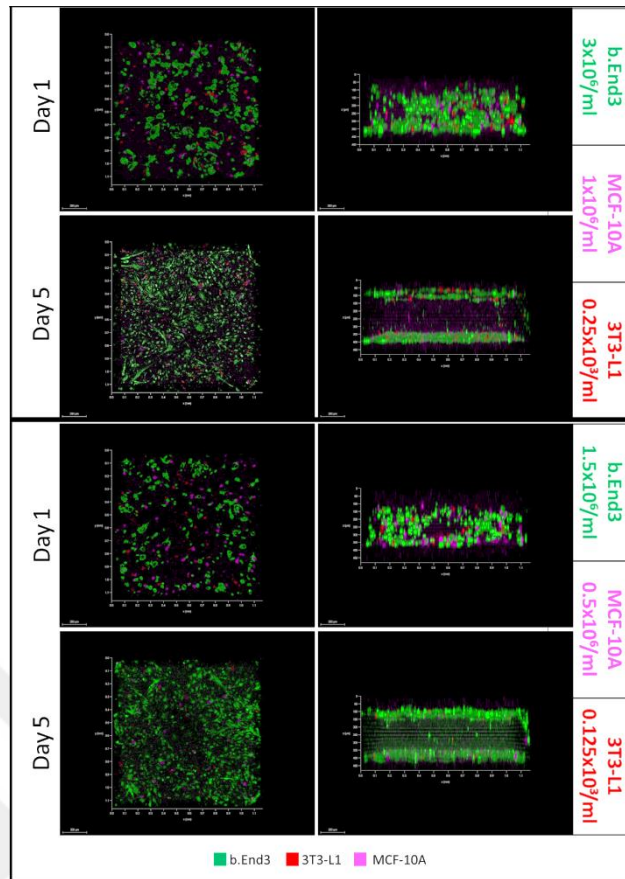


Figure 4.37. (cont.)

Numbers of endothelial cells were increased day by day. More lumen formation was observed at the conditions which contained high concentration of 3T3-L1 cells. But the connections of cells between PDMS and glass sides disappeared at the end of the fourth day. In addition, the lumen formation and vascularization were not observed at the fourth day. Images were taken by 10X objective.

We did not see the MVN at day 5. The formation of two phase was observed for all conditions. There might be difference before day5 after 24 hours.

In the approaches for engineering of MVN in lab-on-a-chip, collagen type 1 was used in 0.2mg/ml concentration to enhance the lumen formation during the vasculogenesis process ²⁶. We changed the content of fibrin gel by increasing the fibrinogen concentration adding collagen type 1 (0.5mg/ml) to induce lumen formation developing tubular structures. In addition to fibrinogen and collohaen, we added also the matrigel (1.15mg/ml) to induce the organization of epithelial cells.

Table 4. The gel components containing collagen and matrigel with aprotinin.

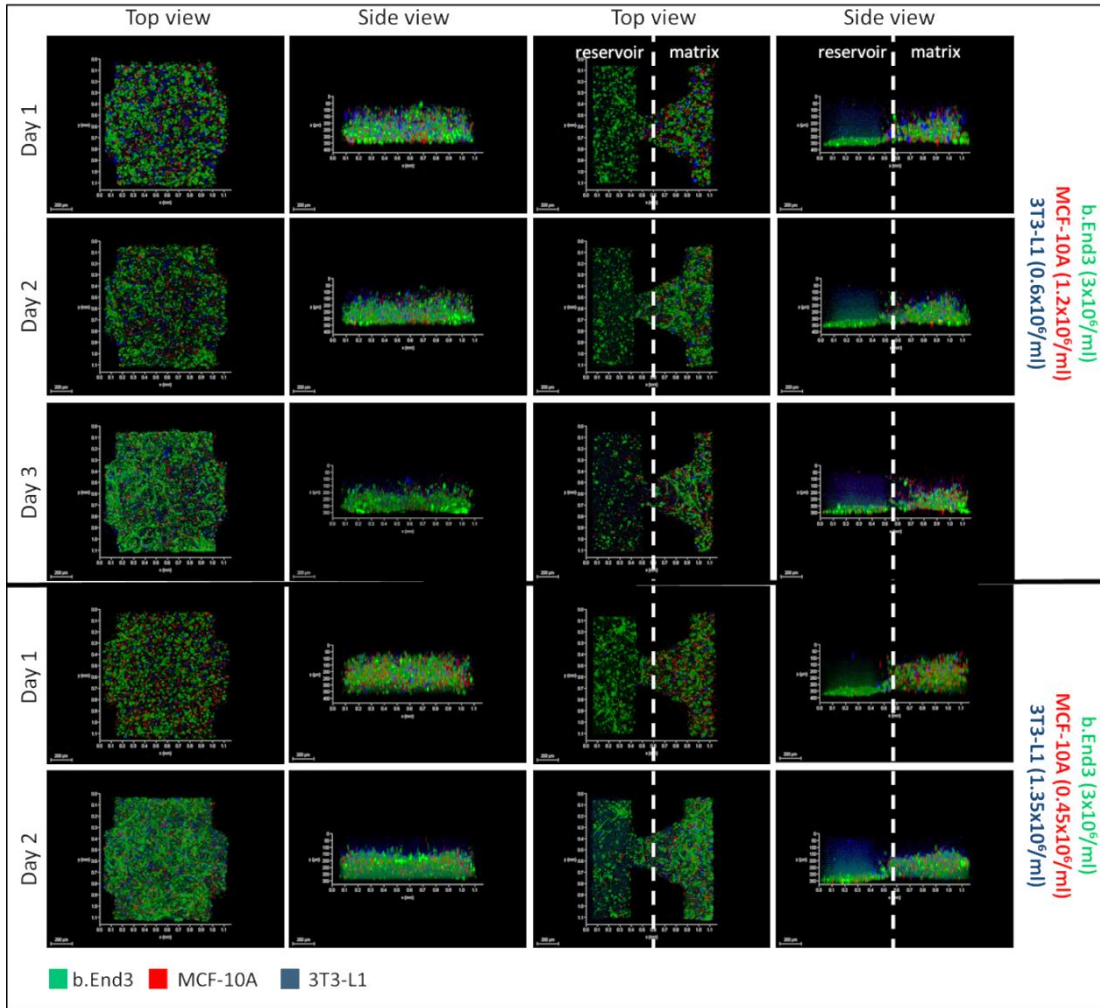
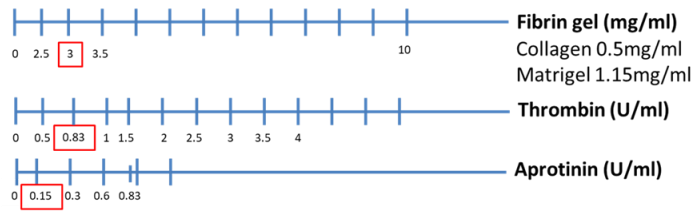


Figure 4.38. Confocal images of b.End3, 3T3-L1, and MCF-10A cells in fibrin gel with the different cell concentrations.

10 μM Green, 25 μM Blue, 5 μM Deep red tracker was used as dyes for b.End3, 3T3-L1, and MCF-10A cells, respectively a day before experiment. Fibrinogen, matrigel and collagen concentrations were set as 3 mg/ml, 1.15 mg/ml and 0.5 mg/ml.

Cells were dissolved in 2 U/ml thrombin containing medium and final concentration of thrombin was set to 0.83 U/ml. $1.8 \times 10^6/\text{ml}$ cell concentration was

obtained the optimum concentration to prevent the vascularization of the endothelial cells. Different cell concentration was used in the presence of MCF-10A and 3T3-L1 as $1.8 \times 10^6/\text{ml}$ total cell concentration (Figure 4.38, Figure 4.39 and Figure 4.40). Figure 4.38 shows the results with different cell concentration day by day. In addition, b.End3 (endothelial) cells were loaded into reservoirs also. The aim of the endothelial cells' supplement is enabling the connection between the other endothelial cells in the matrix channel to form perfusable MVN. White dashed lines show the border between matrix channels and lateral medium channels that contains additional endothelial cells.

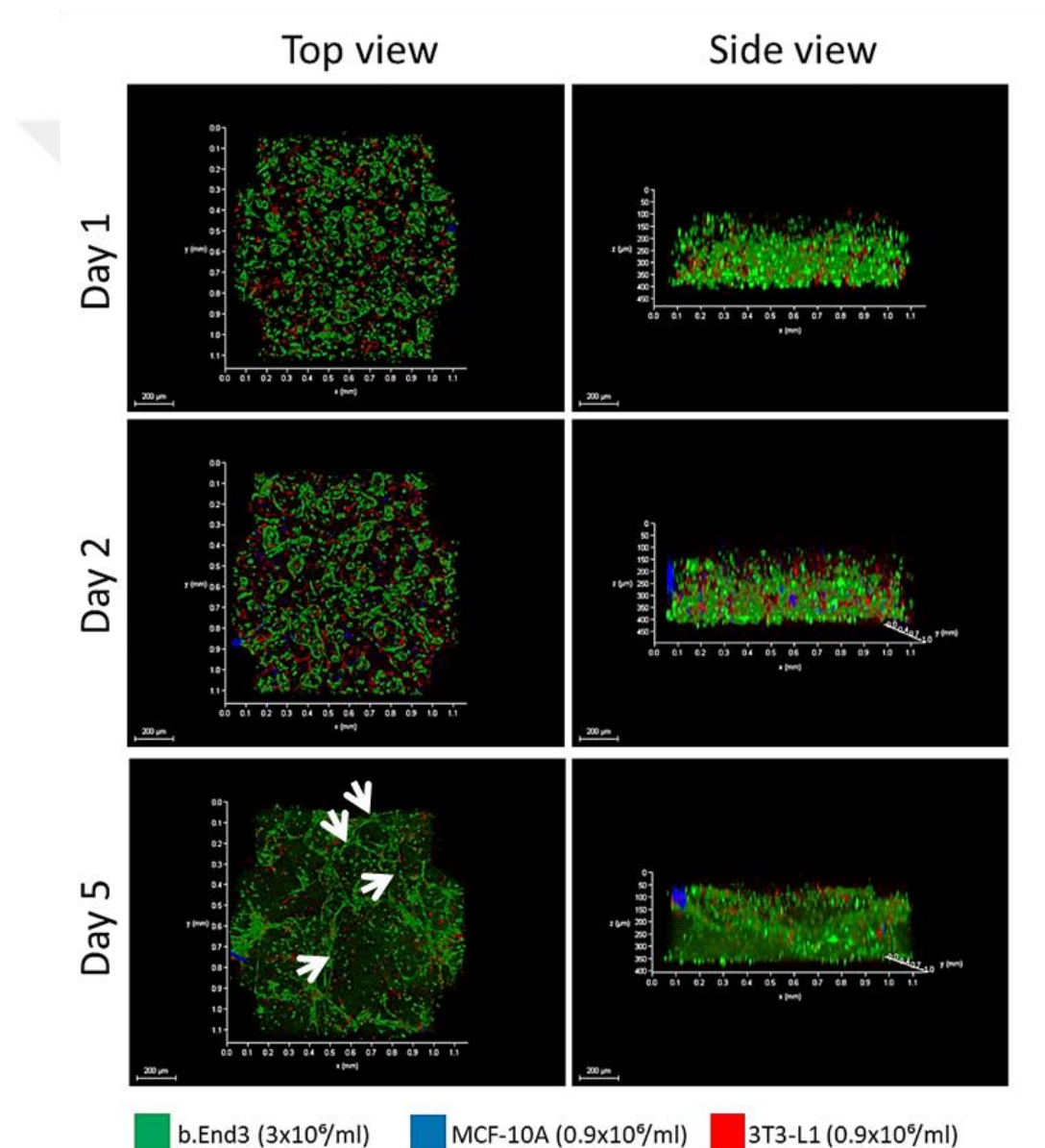


Figure 4.39. Confocal photos of $3 \times 10^6/\text{ml}$ b.End3, $0.9 \times 10^6/\text{ml}$ MCF-10A, and $0.9 \times 10^6/\text{ml}$ 3T3-L1 in fibrin gel day by day.

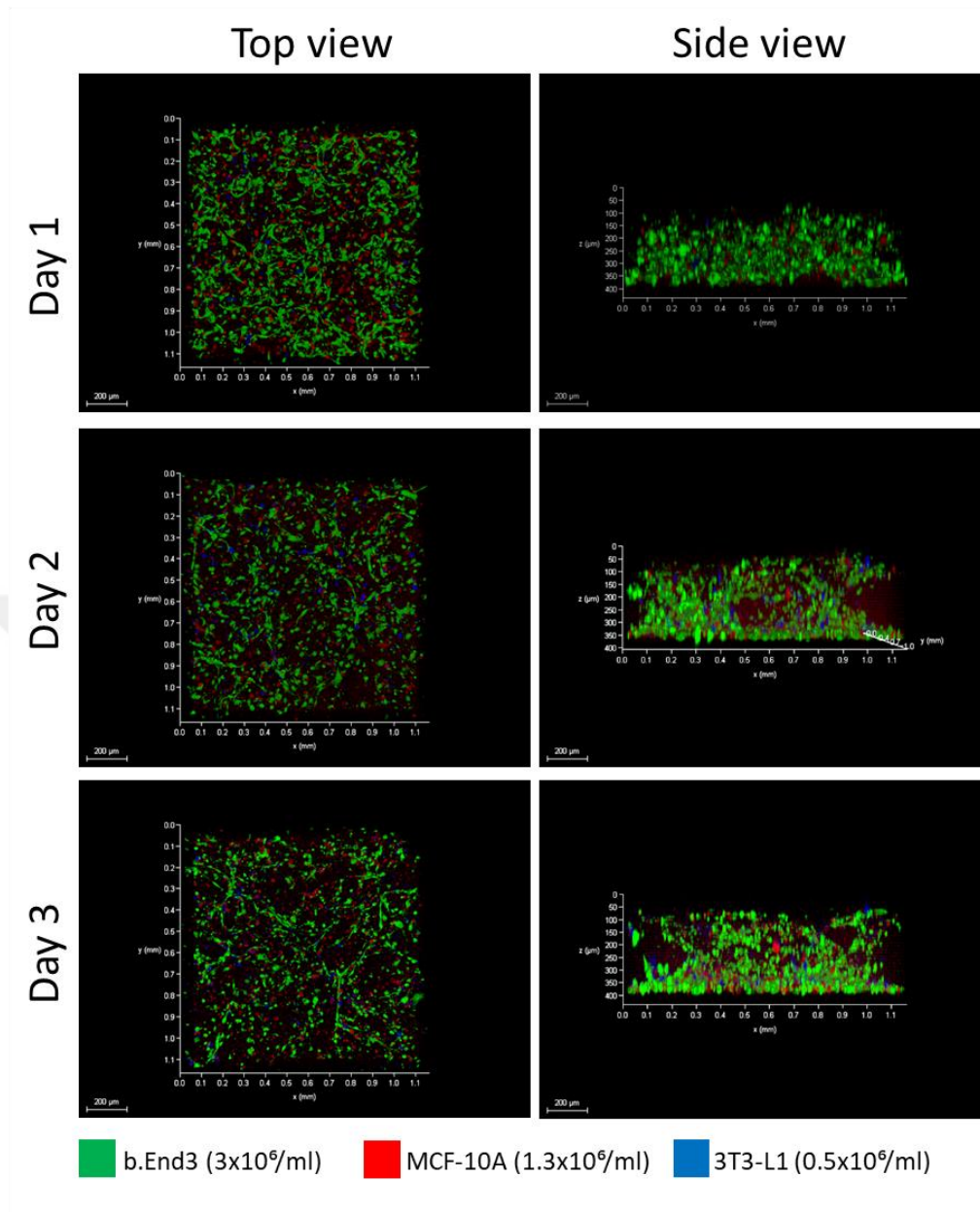


Figure 4.40. Confocal photos of $3 \times 10^6/\text{ml}$ b.End3, $1.3 \times 10^6/\text{ml}$ MCF-10A, and $0.5 \times 10^6/\text{ml}$ 3T3-L1 in fibrin gel day by day.

The results showed that the higher concentration of fibroblast resulted in more compact and close of endothelial cells to each other. When we compare to the images in Figure 4.39 and Figure 4.40, the formation of lumen structure started to form at day 2 in the higher concentration of epithelial cells (Figure 4.40). In addition, both of the concentration might be used for engineering target tissue in vasculature structure. We observed the lumens which were shown with white arrows at day5 for Figure 4.39.

But the condition of higher epithelial cells is more preferable when we consider the time.

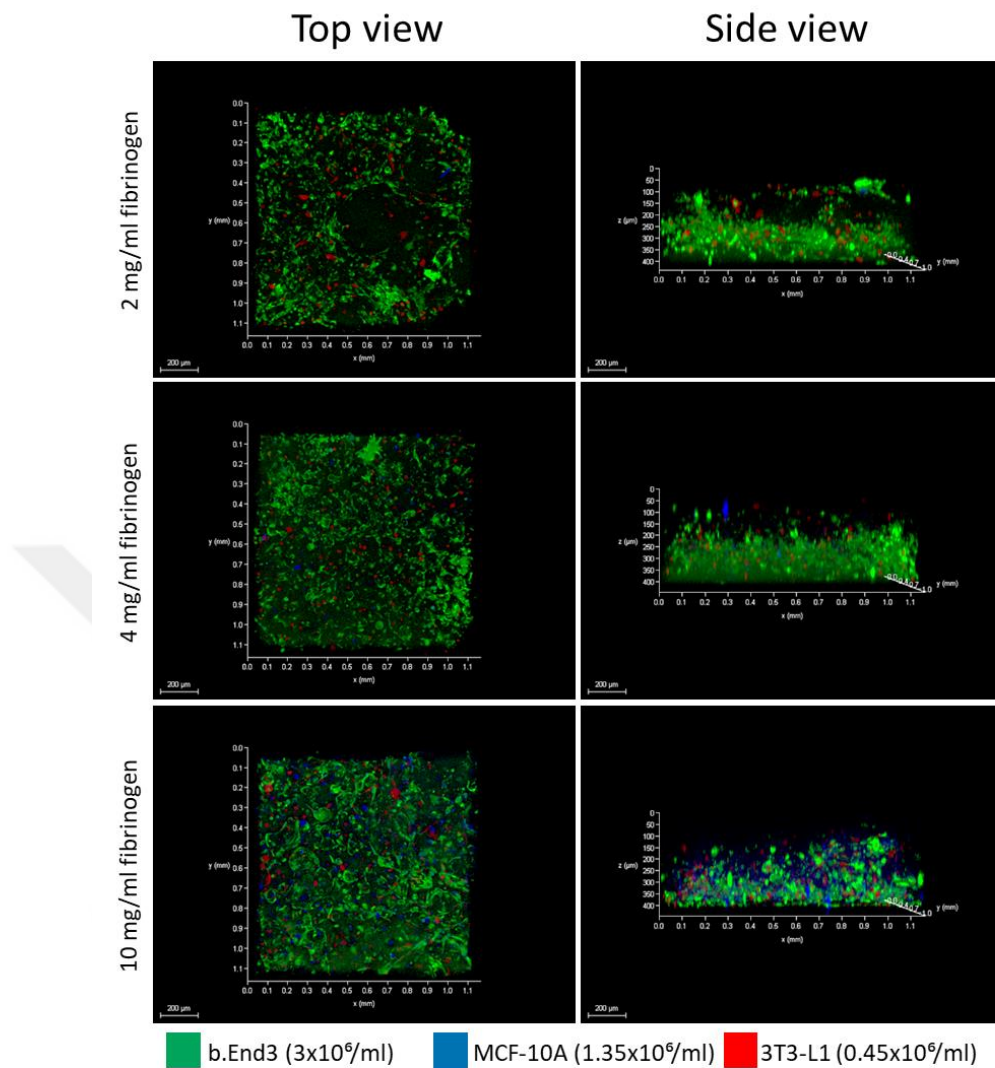


Figure 4.41. Confocal photos of 3×10^6 /ml b.End3, 1.35×10^6 /ml MCF-10A, and 0.45×10^6 /ml 3T3-L1 in fibrin gel with different gel concentration day by day.

10 μ M Green, 25 μ M Blue, 5 μ M Deep red tracker was used as dyes for b.End3, MCF-10A, 3T3-L1 cells, respectively a day before experiment. Fibrin gel was prepared using fibrinogen, matrigel and collagen as 3 mg/ml, 1.15 mg/ml and 0.5 mg/ml of concentrations, respectively for 2 mg/ml and 4 mg/ml. 1XPBS with Ca^{++} and Mg^{++} was used for dissolution of fibrinogen. 4mg/ml and 10mg/ml fibrin gel experiments. Cells were dissolved in 3U/ml thrombin containing medium according to third fibrin gel protocol. 1.8×10^6 /ml cell concentration was obtained the optimum concentration to prevent the vascularization of the endothelial cells. Different cell concentration was used in the presence of MCF-10A and 3T3-L1 as 1.8×10^6 /ml total cell concentration.

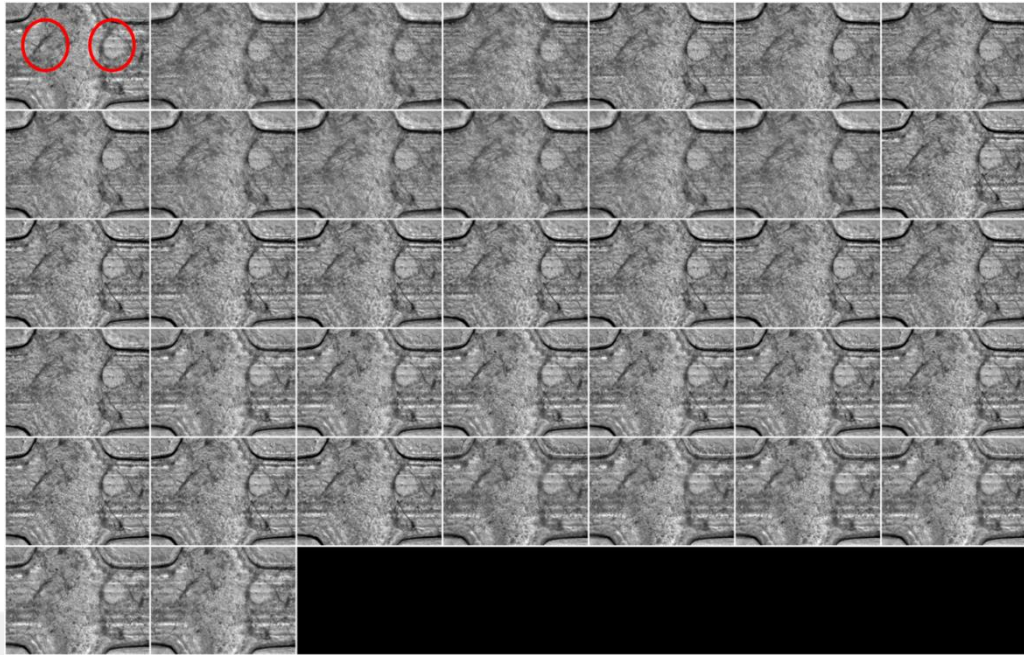


Figure 4.42. Brightfield Z-stack images of target tissue in 2 mg/ml fibrin gel at day 4.

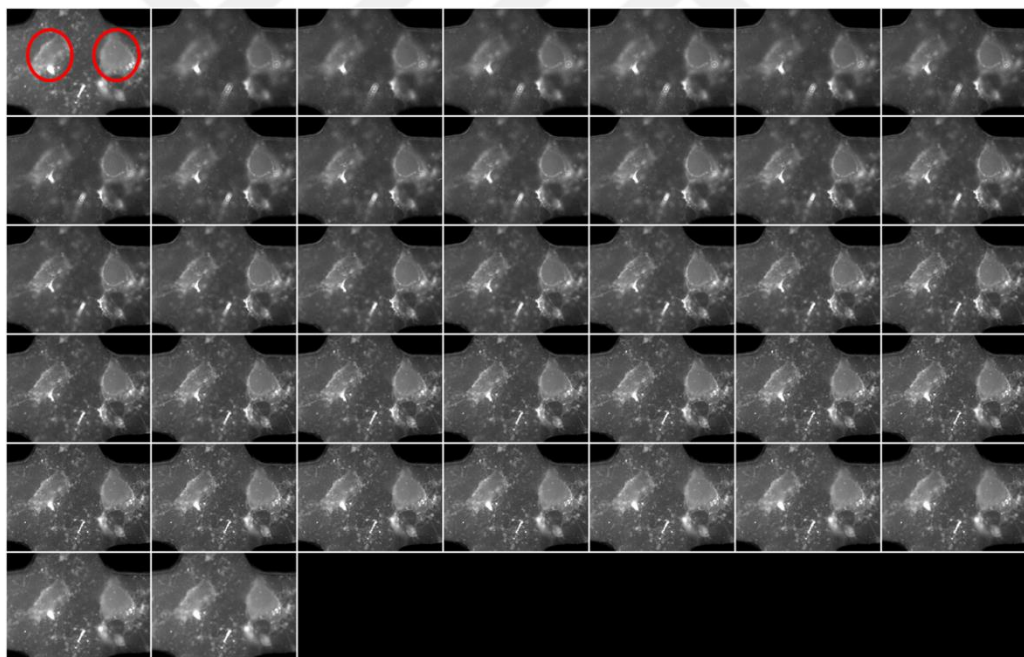


Figure 4.43. Fluorescence Z-stack images of endothelial cells in 2 mg/ml fibrin gel at day 4.

Figure 4.42, Figure 4.42, Figure 4.43 show the Z-stack images of 2mg/ml fibrin gel condition at day 4. Dextran 70 kDa (1:150) was introduced into media channel when the inlet and outlet of the matrix channel firstly stuck with tape (Figure 4.21). Red circles show the lumen structure.

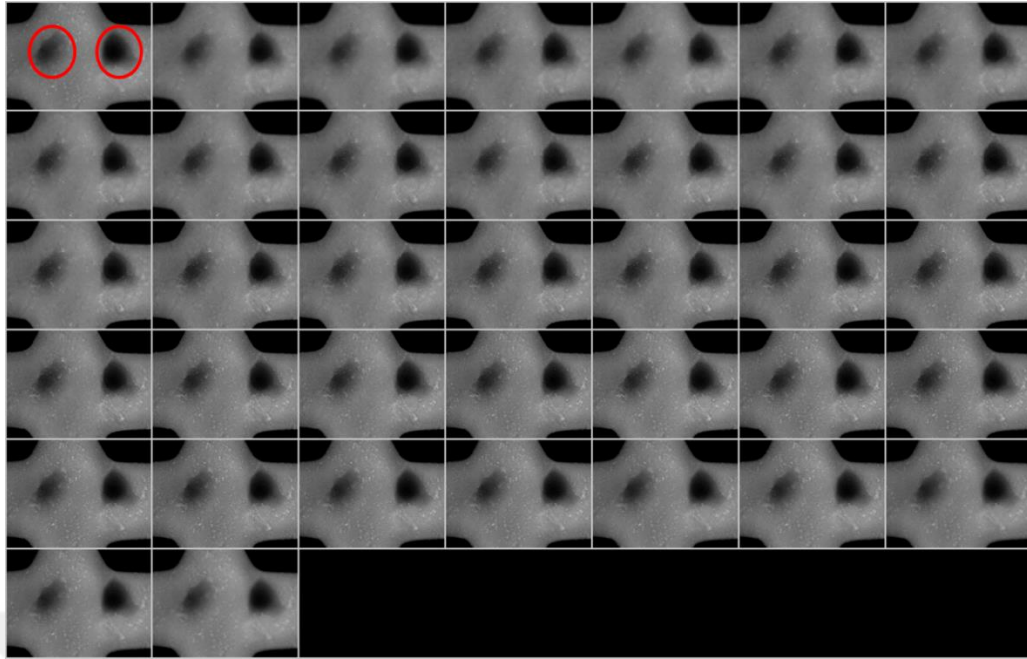


Figure 4.44. Fluorescence Z-stack images of dextran 70kDa in 2 mg/ml fibrin gel at day 4.

4.2.5. Testing the Effect of Different Mediums and Combination of Cells for Induction of Microvascular Sprouting

There are important molecules related with vessel wall and maturation network such as vascular endothelial growth factor (VEGF), platelet derived growth factor (PDGF-B) in the TGF- β family. Ang-1 takes a role in the vessel stabilization in the presence of mesenchymal stem cells²³. VEGF and Ang-1 were checked for the concentrations of proteins.

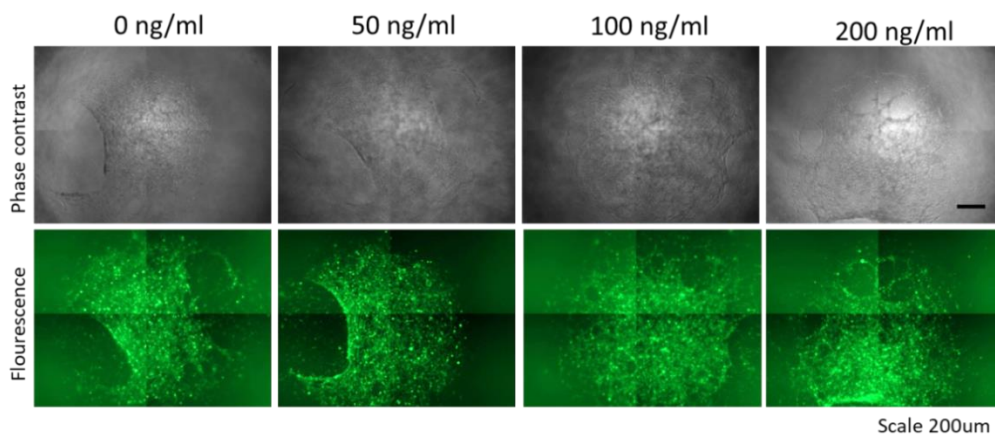


Figure 4.45. Test of different VEGF doses in vasculature.

Final concentration of b.End3 cells were set to 3×10^6 /ml. The results showed that the 100 ng/ml and 200ng/ml provided the similar effect to observe lumen structure. Larger lumen structure observed in 200ng/ml VEGF condition compare to 100ng/ml.

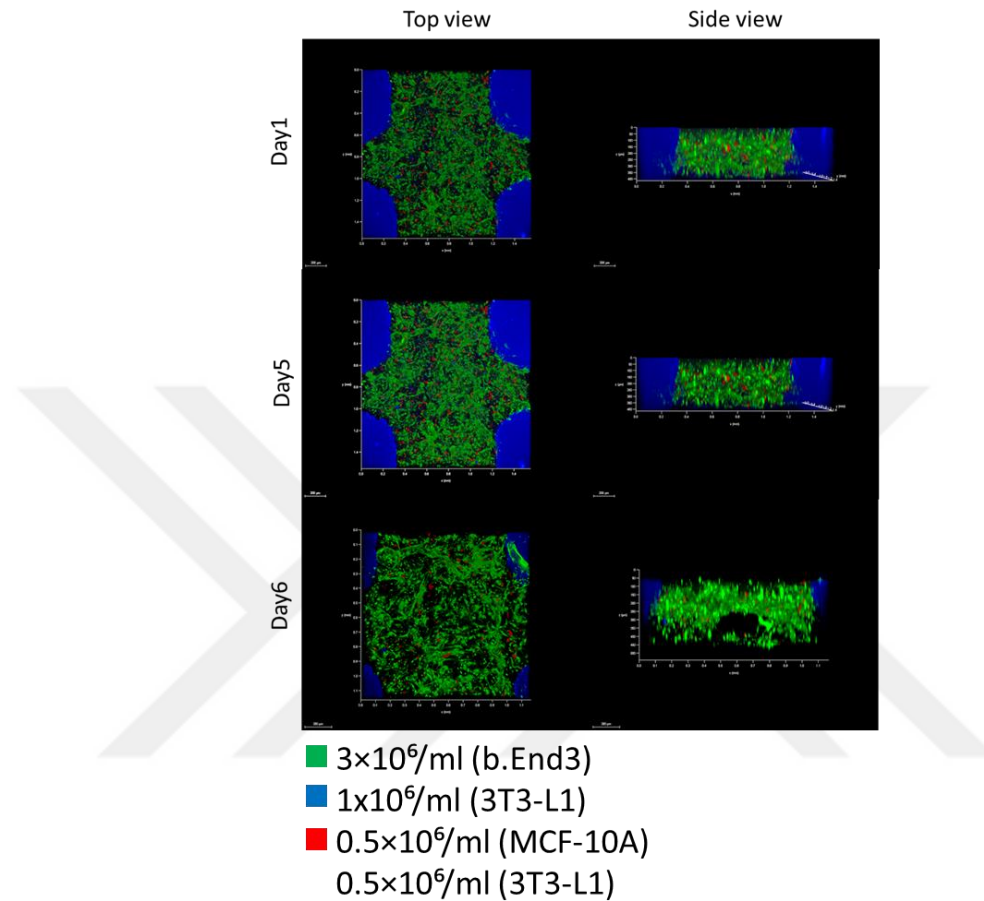


Figure 4.46. 50ng/ml VEGF and 100ng/ml Ang-1.

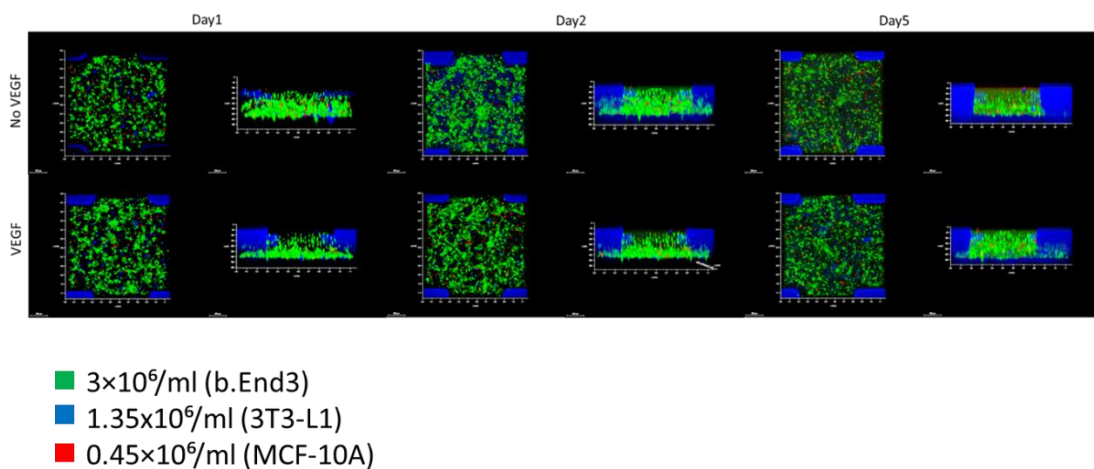


Figure 4.47. 0 and 100ng/ml VEGF in the absence of MSCs.

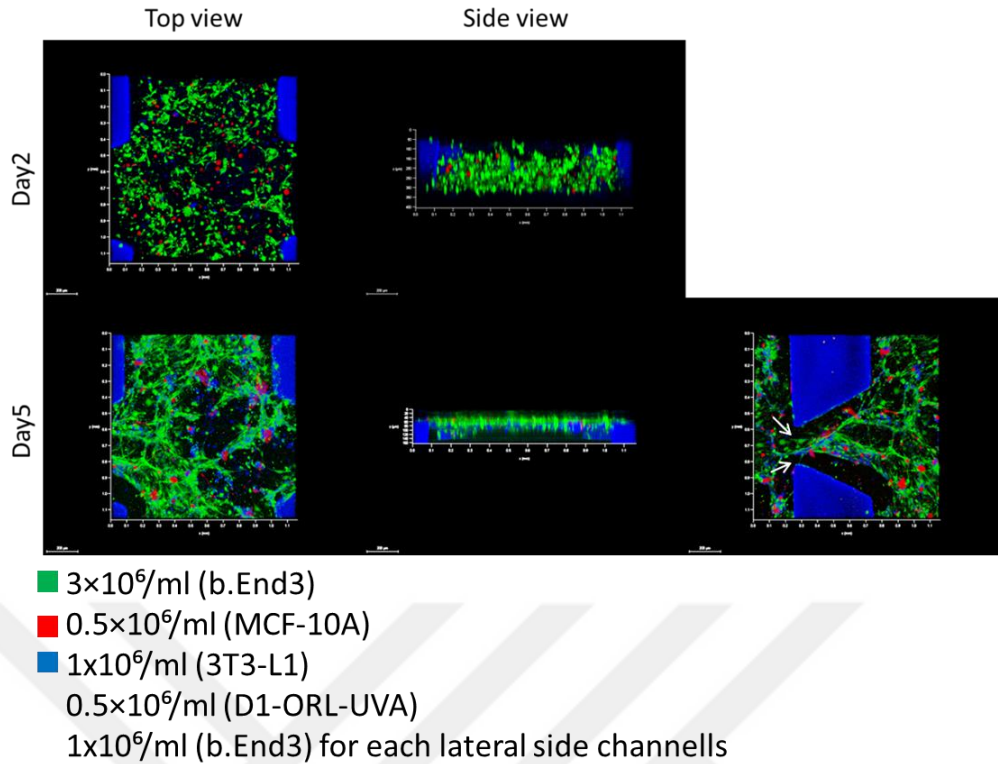


Figure 4.48. 50ng/ml VEGF conditions with endothelial cells at the lateral channels.

The results showed that the presence of MSCs did not effect the MVN formation negatively. In addition, MSCs did not provide the sprouting of endothelial cells into the lateral side channels with application of VEGF and Ang-1. As another result we did not see the any significant change with VEGF application in the presence or absence of MSC. Therefore, we decided not to use the VEGF and Ang-1.

4.2.5.1. Laminin Coated and Non-Coated Surfaces to Test Vascular Sprouting in Breast Tissue

For this purpose, laminin was used as a coating protein to provide the better attachment of endothelial cells onto lateral media channels. At another study, APTES was used to coating material by combining with collagen³⁶. APTES was used with laminin protein to enhance both the attachment to the PDMS surface by induction of sprouting of cell from the matrix into the lateral medium channels.

10 μM Green tracker was used as dye for tracking of only b.End3 a day before experiment. Higher concentration of MCF-10 was also tested in APTES coated or uncoated LOC devices. The height of left one is 295um and right one is 160 um. 5

degree cycle of rotator system was applied for 24 hours for the right one and it is incubated in the plate for 24 hours. Fibrin gel mixture was prepared with endothelial cells ($3 \times 10^6/\text{ml}$), epithelial cells (MCF-10A: $1.35 \times 10^6/\text{ml}$), fibroblasts ($0.45 \times 10^6/\text{ml}$) and loaded into middle matrix channel. 3D structure of breast is more sensitive to destruct in 2% matrigel containing media with higher height LOC compare to lower height one. Use of APTES resulted in contraction of gel not providing sprouting of endothelial cells. Use of uncoated surface and the rotator system did not result in endothelial cells' sprouting. We observed more compact entire structure in uncoated LOC devices. It might be the toxic side effect of APTES.

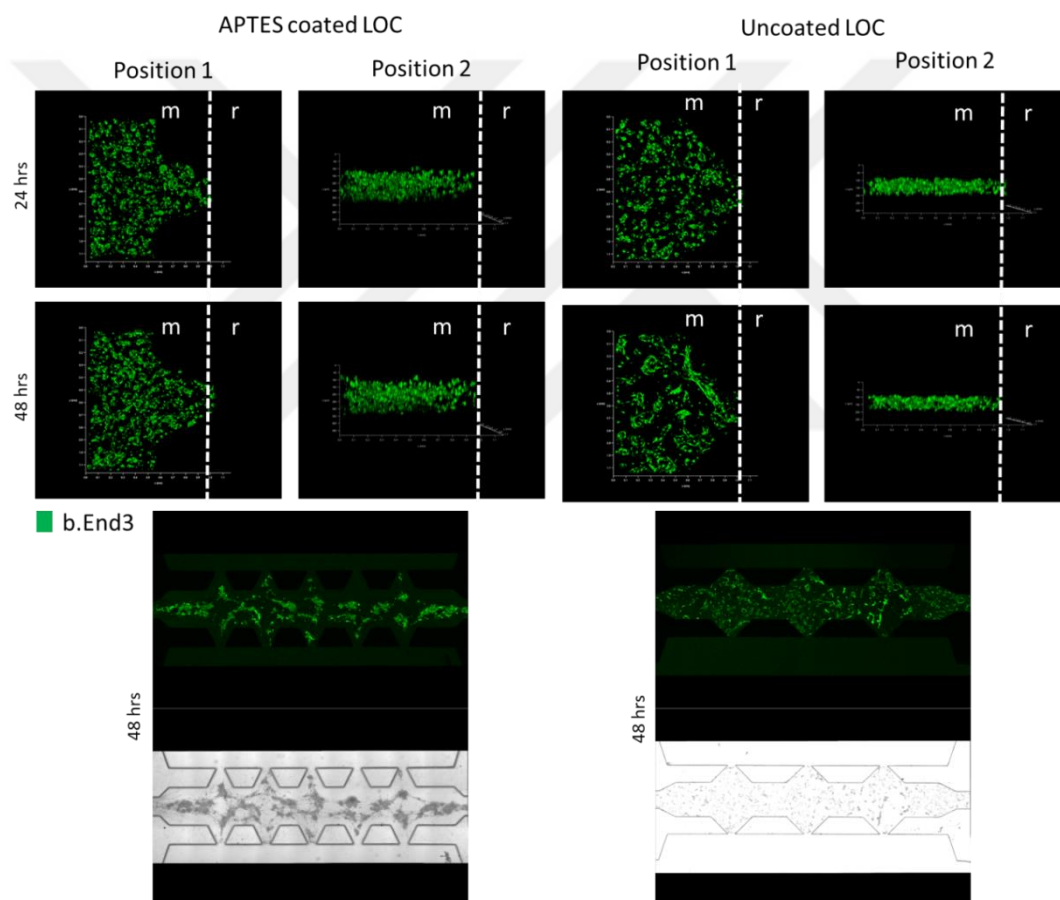


Figure 4.49. Breast tissue with 2% matrigel containing media in APTES coated or uncoated LOC devices (m: matrix, r: reservoir).

4.2.5.2. Test of Low Height and Thin Post Gaps of LOC for MVN Formation and Sprouting of Endothelial Cells

100 μm height and 1mm width LOC devices having one post or three posts to supply formation of vascularization in an easy manner compare to high height of LOC devices. First day, 100 ng/ml VEGF was added into lateral media channels and the day after media was replaced with 100 ng/ml VEGF and 200 ng/ml Ang-1 supplemented media.

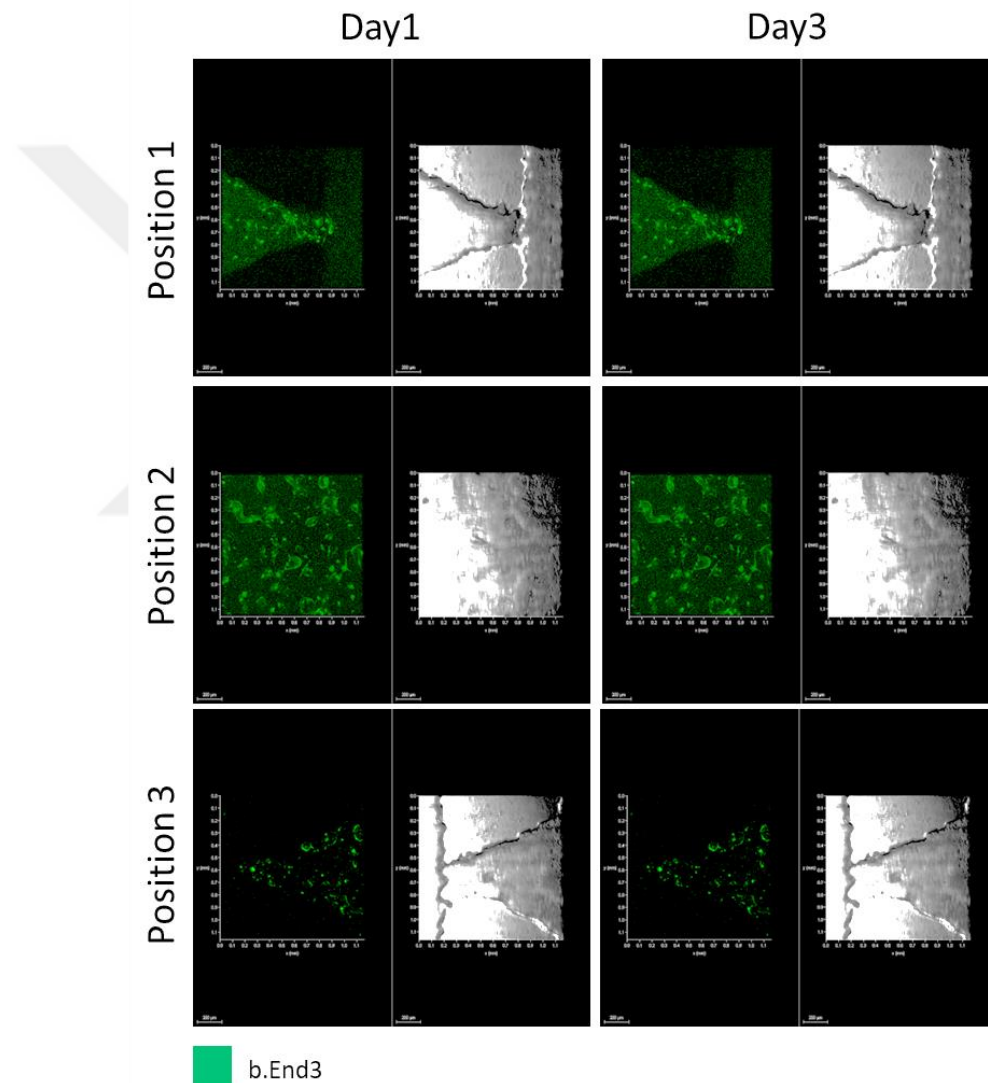


Figure 4.50. Confocal images of mimicking breast tissue in fibrin gel in one post LOC devices for day 1, day 3.

10 μM Green, tracker was used as dye for tracking of b.End3 cells a day before experiment. Fibrinogen concentration was set as 3 mg/ml and cells were dissolved in

0.83U/ml thrombin containing medium. Collagen and matrigel were also mixed with the cells. Their concentrations were 0.5 mg/ml and 1.15 mg/ml, respectively. Final concentrations of cells are 3×10^6 /ml (b.End3), 1.35×10^6 /ml (3T3-L1), 0.45×10^6 /ml (MCF-10A). 3D printed LOC devices were used in here. Height of matrix channel is $100 \mu\text{m}$, and width is 1mm having one post. Images were taken by 10X objective with confocal microscope.

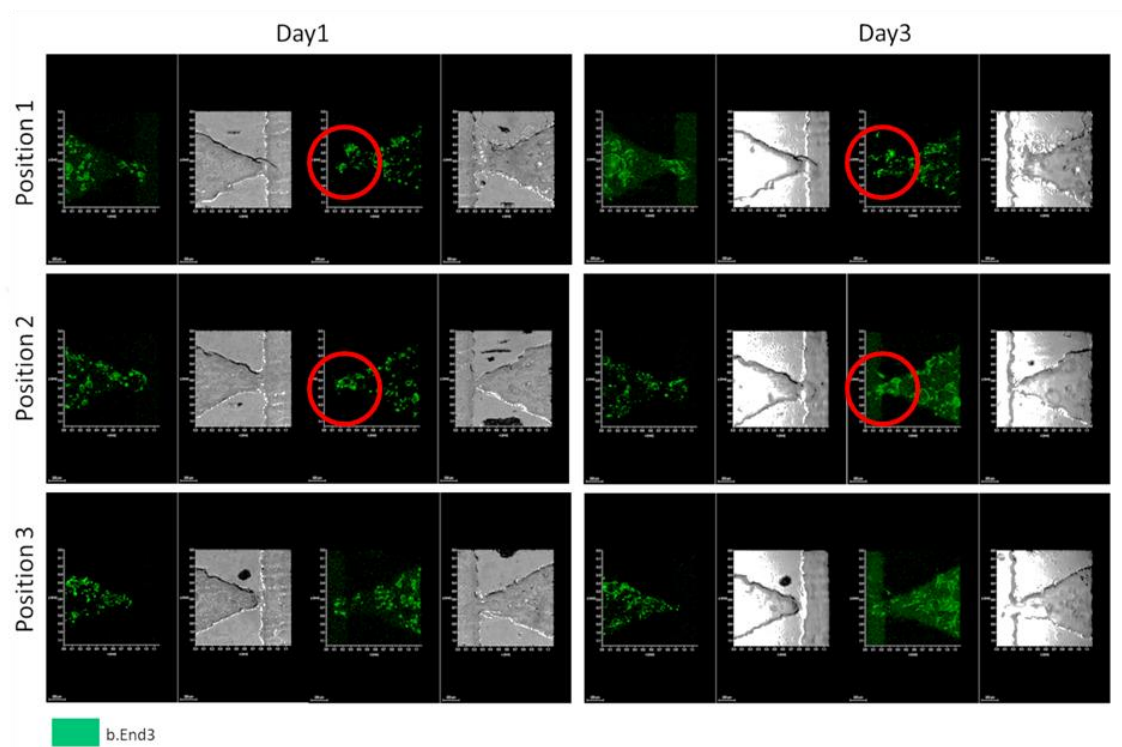


Figure 4.51. Confocal images of mimicking breast tissue in fibrin gel in three posts LOC devices for day 1, day 3.

$10 \mu\text{M}$ Green, tracker was used as dye for tracking of b.End3 cells a day before experiment. Fibrinogen concentration was set as 3 mg/ml and cells were dissolved in 0.83U/ml thrombin containing medium. Collagen and matrigel were also mixed with the cells. Their concentrations were 0.5 mg/ml and 1.15 mg/ml, respectively. Final concentrations of cells are 3×10^6 /ml (b.End3), 1.35×10^6 /ml (3T3-L1), 0.45×10^6 /ml (MCF-10A). 3D printed LOC devices were used in here. Height of matrix channel is $100 \mu\text{m}$, and width is 1mm having three posts. Images were taken by 10X objective with confocal microscope. Red circular areas show the some positions at the post gaps for sprouting of endothelial cells.

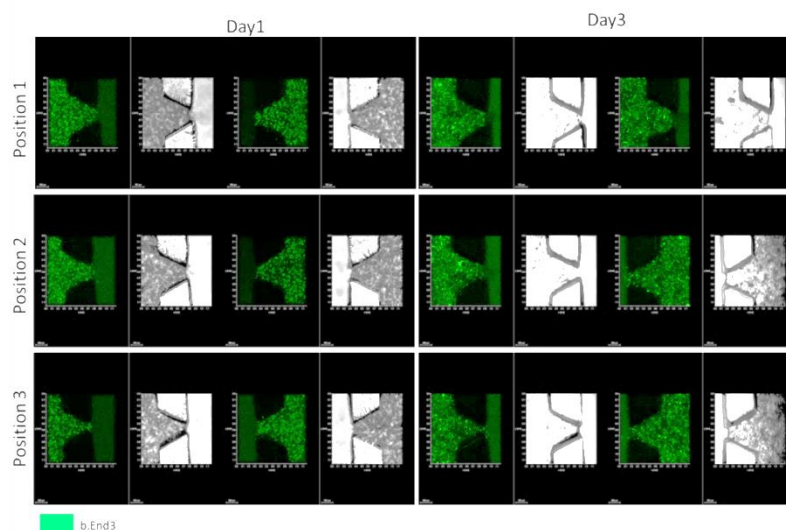


Figure 4.52. Confocal photos of mimicking breast tissue in fibrin gel in five posts and high height LOC devices for day 1, day 3.

10 μ M Green, tracker was used as dye for tracking of b.End3 cells a day before experiment. Fibrinogen concentration was set as 3 mg/ml and cells were dissolved in 0.83U/ml thrombin containing medium. Collagen and matrigel were also mixed with the cells. Their concentrations were 0.5 mg/ml and 1.15 mg/ml, respectively. Final concentrations of cells are 3×10^6 /ml (b.End3), 1.35×10^6 /ml (3T3-L1), 0.45×10^6 /ml (MCF-10A). 3D printed LOC devices were used in here. Height of matrix channel is 296 μ m, and width is 1mm having three posts. Images were taken by 10X objective with confocal microscope.

The results showed that the low height of LOC device containing three post gaps let observe the sprouting in Figure 4.51 compare to Figure 4.50 and Figure 4.50. But the sprouting was not enough to expand the channel throughout.

4.2.5.3. The Effect of Matrigel Containing Media on Structure of Breast Epithelial Cells

One aim of the study is to confirm that the tissues engineered in lab-on-a-chip devices mimic the key features of the *in vivo* tissues in terms of structure. For this purpose, different media ingredients were tested on epithelial cells to observe the acinar structure that is the unique morphology of cells.

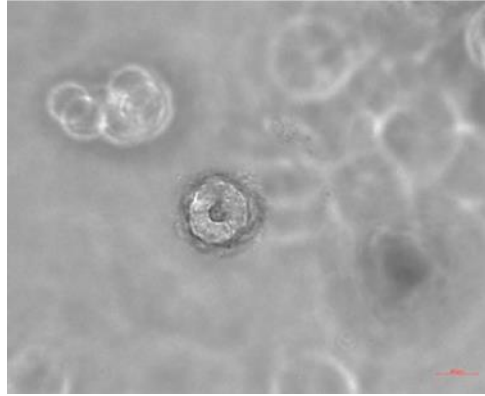


Figure 4.53. Acinus structure of MCF-10A epithelial cells in matrigel containing media at day 6.

Cells were incubated in media that is supplemented with matrigel. MCF-10A cells are seeded into fibrin gel mixture like co-culture experimental setup. Cell concentration is $0.45 \times 10^6/\text{ml}$. Photos were taken by 40X objective with fluorescence microscope. (Scale bar: $20\mu\text{m}$)

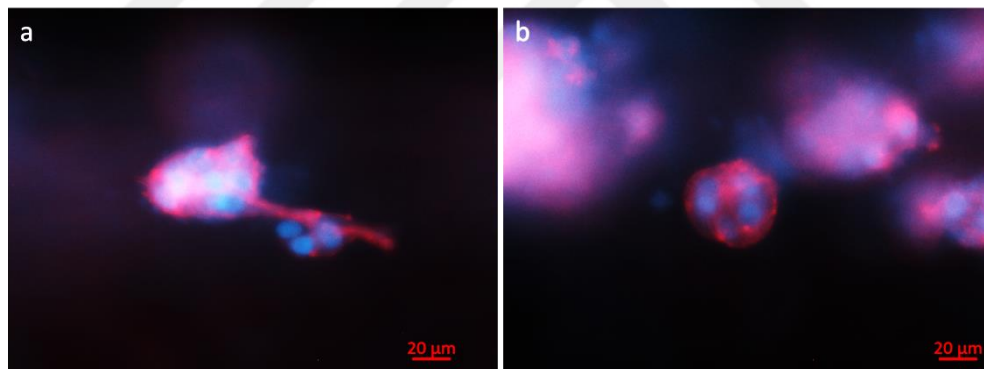


Figure 4.54. Lobular unit (a) and acinar structure (b) of MCF-10A cells.

Cells were incubated in media that is supplemented with matrigel. MCF-10A cells are seeded into fibrin gel mixture like co-culture experimental setup. Cell concentration is $0.45 \times 10^6/\text{ml}$. Media replaced with fresh one for each two days. Cells are cultured into chip for 12 days. Cells were fixed with 4% PFA for 30 minutes at the room temperature in LOC device at day 13. And then, the sample was rinsed with 1X PBS for three times. Blocking steps (0.1% BSA in 1X PBS) and DAPI (1:200) and actin (phalloidin555 1:50) staining were generated. DAPI staining was shown in blue color

and phalloidin 555 staining was shown in red color. Scale bar is 20 μm . Images were taken by 40X objective with fluorescence microscope.

4.2.5.4. Low Height and Thin Post Gaps of LOC for Generation of MVN in Lung Tissue

For this purpose, b.End3 (endothelial cells), WI38 (fibroblasts), BEAS-2B (epithelial cells) cell lines are used in the experiments with different cell concentrations. We used same cells' concentrations as breast target tissue for each type of cells (fibroblast, endothelial cells, and epithelial cells) to construct lung target tissue. Concentration of endothelial cells was fixed and the concentrations of other type of cells were calculated by direct proportion from the literature ³⁷.

Table 5. Cell concentrations ³⁷.

Lung cells Lung %	Endothelial 39%	Interstitial 29%	Type 2 Epithelial 18%	Type 1 Epithelial 11%	Macrophages 3%
	b.End3	WI38	Beas-2B		
	$3 \times 10^6/\text{ml}$	$2 \times 10^6/\text{ml}$	$2.25 \times 10^6/\text{ml}$		

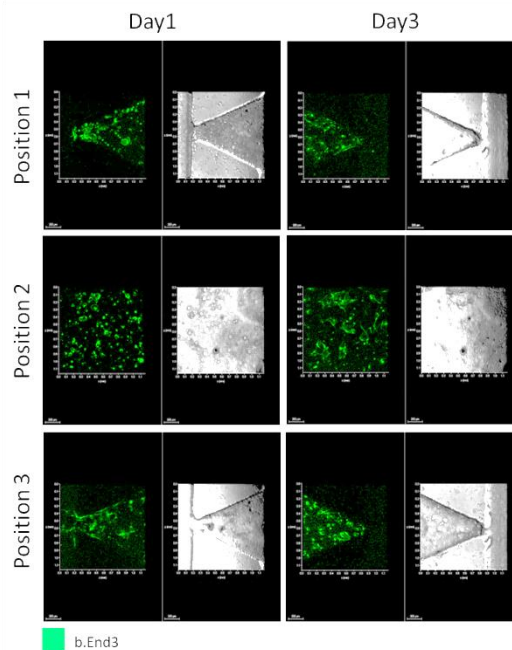


Figure 4.55. Confocal images of mimicking lung tissue in fibrin gel in one post LOC devices for day 1, day 3.

10 μ M Green, tracker was used as dye for tracking of b.End3 cells a day before experiment. Fibrinogen concentration was set as 3 mg/ml and cells were dissolved in 0.83U/ml thrombin containing medium. Collagen and matrigel were also mixed with the cells. Their concentrations were 0.5 mg/ml and 1.15 mg/ml, respectively. Final concentrations of cells are 3×10^6 /ml (b.End3), 2×10^6 /ml (WI38), 2.25×10^6 /ml (Beas-2B). 3D printed LOC devices were used in here. Height of matrix channel is 100 μ m, and width is 1mm having one post. Photos were taken by 10X objective with confocal microscope.

10 μ M Green, tracker was used as dyes for b.End3 cells a day before experiment. Fibrinogen concentration was set as 3 mg/ml and cells were dissolved in 0.83U/ml thrombin containing medium. Collagen and matrigel were also mixed with the cells. Their concentrations were 0.5mg/ml and 1.15mg/ml, respectively. Final concentrations of cells are 3×10^6 /ml (b.End3), 2×10^6 /ml (WI38), 2.25×10^6 /ml (Beas-2B). 3D printed LOC devices were used in here. Height of matrix channel is 100 μ m, and width is 1mm having three post. Images were taken by 10X objective.

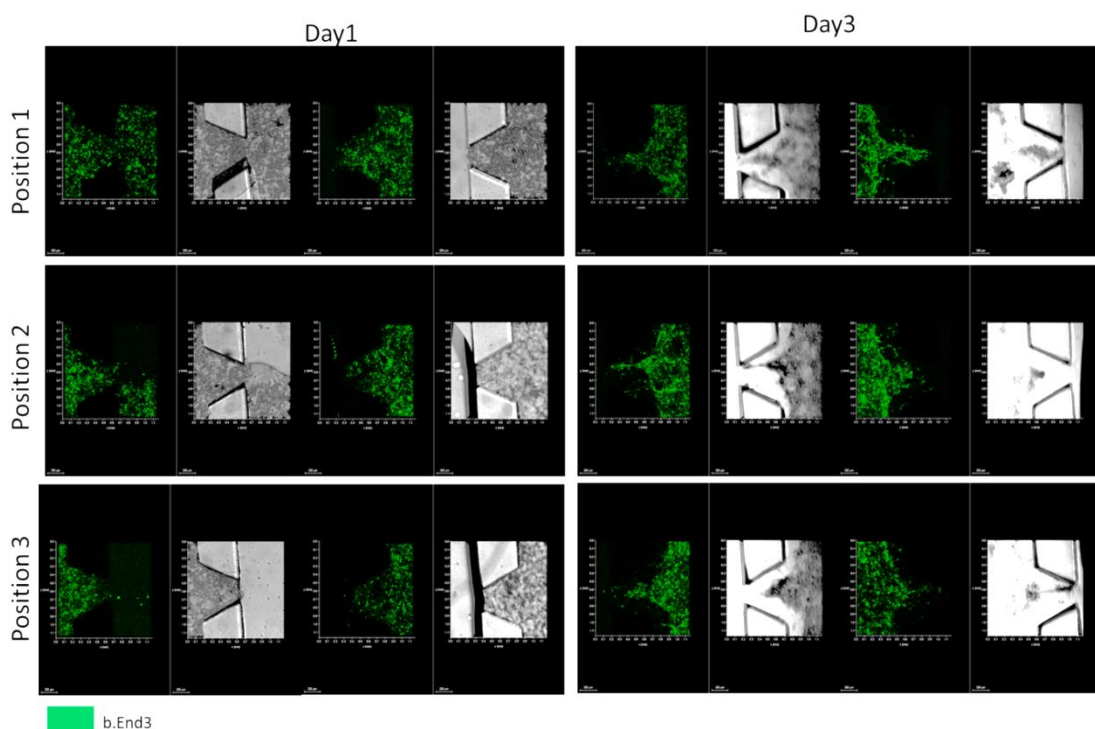


Figure 4.56. Confocal images of mimicking lung tissue in fibrin gel in five posts LOC devices for day 1, day 3.

10 μ M Green tracker was used as dye for tracking of b.End3 cells a day before experiment. Fibrinogen concentration was set as 3 mg/ml and cells were dissolved in 0.83U/ml thrombin containing medium. Collagen and matrigel were also mixed with the cells. Their concentrations were 0.5 mg/ml and 1.15 mg/ml, respectively. Final concentrations of cells are 3×10^6 /ml (b.End3), 2×10^6 /ml (WI38), 2.25×10^6 /ml (Beas-2B). Height of matrix channel is 295 μ m, and width is 1mm having five post. Photos were taken by 10X objective with confocal microscope.

4.2.5.5 Test of the Formation of MVN in the Presence of Mesenchymal Stem cells (MSCs) in the Matrix for Lung Tissue

To optimize the optimum cell concentrations at the beginning of the co-culture, doubling times of cells were considered. We used different concentrations of cells to achieve mimicking *in vivo* cell numbers by considering doubling time of each cells ³⁷. We also tested different LOC devices to determine the convenient platform. In addition, we tested the presence of mesenchymal stem cells in engineering tissue. We calculated the cell concentration with direct proportion from the literature ²³.

Table 6. Cell concentrations and doubling times.

LUNG	Intended final conc. at day3	Beginning con. at day1	Doubling time	Culture for formation of vascular network
b.End3	3×10^6 /ml	1×10^6 /ml	24 hours	3-4 days
Beas-2B	2.25×10^6 /ml	0.8×10^6 /ml	26 hours	3-4 days
WI38	2×10^6 /ml	0.66×10^6 /ml	~24 hours	3-4 days
D1-ORL-UVA	3×10^4 /ml	1.5×10^4 /ml	30-40 hours	3-4 days

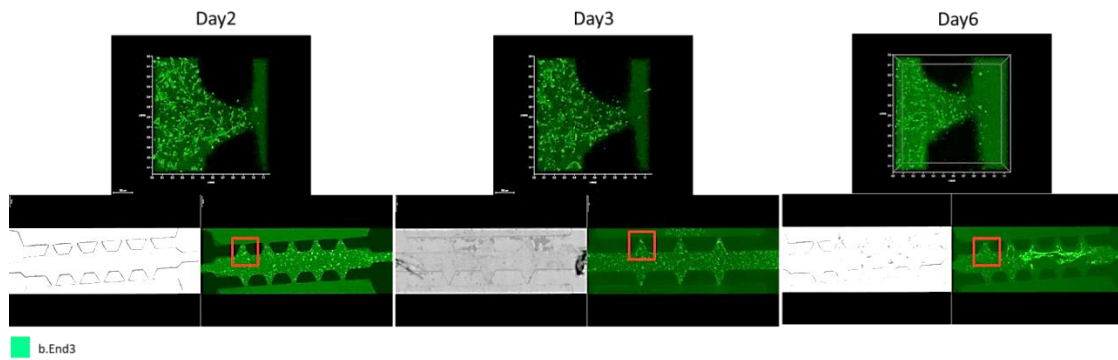


Figure 4.57. Confocal images of mimicking lung tissue in fibrin gel in five posts LOC devices for day 2, 3 and 6 in the presence of MSCs.

10 μ M Green tracker was used as dye for tracking of b.End3 cells a day before experiment. Fibrinogen concentration was set as 3 mg/ml and cells were dissolved in 0.83U/ml thrombin containing medium. Collagen and matrigel were also mixed with the cells. Their concentrations were 0.5mg/ml and 1.15mg/ml, respectively. Final concentrations of cells are 1×10^6 /ml (b.End3), 0.66×10^6 /ml (WI38), 0.8×10^6 /ml (Beas-2B) and 1.5×10^4 /ml (D1-ORL-UVA). Height of matrix channel is 295 μ m, and width is 1mm having five posts. Images were taken by 10X objective with confocal microscope.

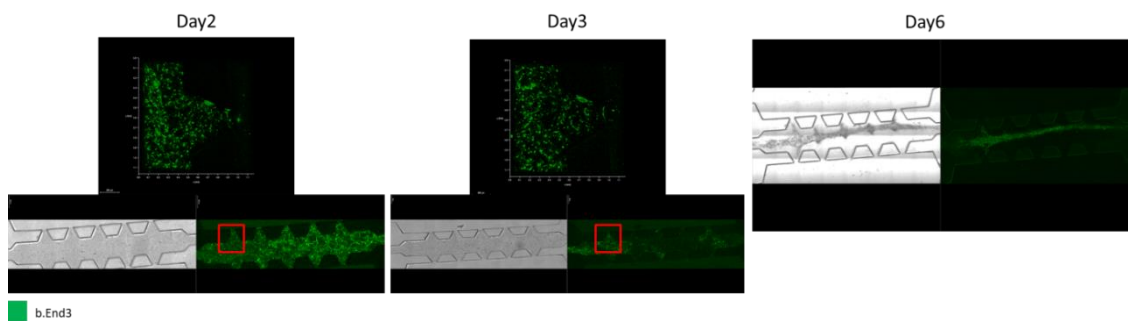


Figure 4.58. Confocal images of mimicking lung tissue in fibrin gel in five posts LOC devices for day 2, 3 and 6 in the absence of MSCs.

10 μ M Green tracker was used as dye for tracking of b.End3 cells a day before experiment. Fibrinogen concentration was set as 3 mg/ml and cells were dissolved in 0.83U/ml thrombin containing medium. Collagen and matrigel were also mixed with the cells. Their concentrations were 0.5 mg/ml and 1.15 mg/ml, respectively. Final concentrations of cells are 1×10^6 /ml (b.End3), 0.66×10^6 /ml (WI38), 0.8×10^6 /ml (Beas-

2B). Height of matrix channel is 295 μm , and width is 1mm having five posts. Images were taken by 10X objective with confocal microscope.

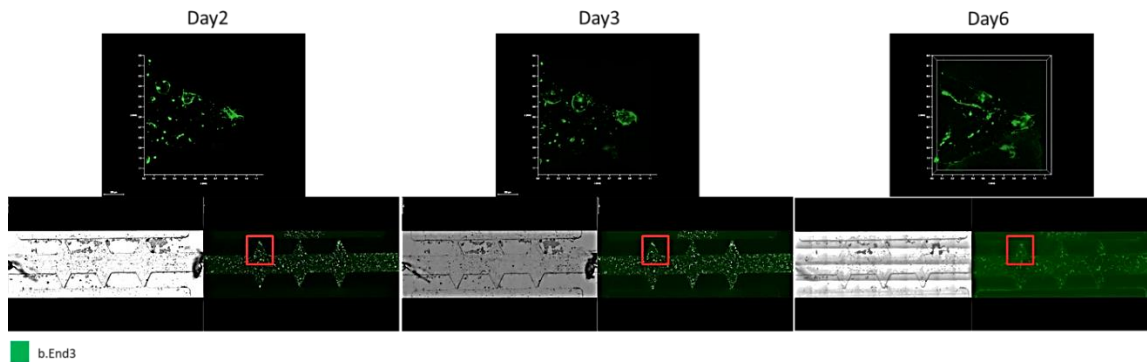


Figure 4.59. Confocal images of mimicking lung tissue in fibrin gel in five posts LOC devices for day 2, 3 and 6 in the presence of MSCs.

10 μM Green tracker was used as dyes for b.End3 cells a day before experiment. Fibrinogen concentration was set as 3 mg/ml and cells were dissolved in 0.83U/ml thrombin containing medium. Collagen and matrigel were also mixed with the cells. Their concentrations were 0.5mg/ml and 1.15mg/ml, respectively. Final concentrations of cells are $1 \times 10^6/\text{ml}$ (b.End3), $0.66 \times 10^6/\text{ml}$ (WI38), $0.8 \times 10^6/\text{ml}$ (Beas-2B) and $1.5 \times 10^4/\text{ml}$ (D1-ORL-UVA). Height of matrix channel is 100 μm , and width is 1mm having three posts. Images were taken by 10X objective with confocal microscope.

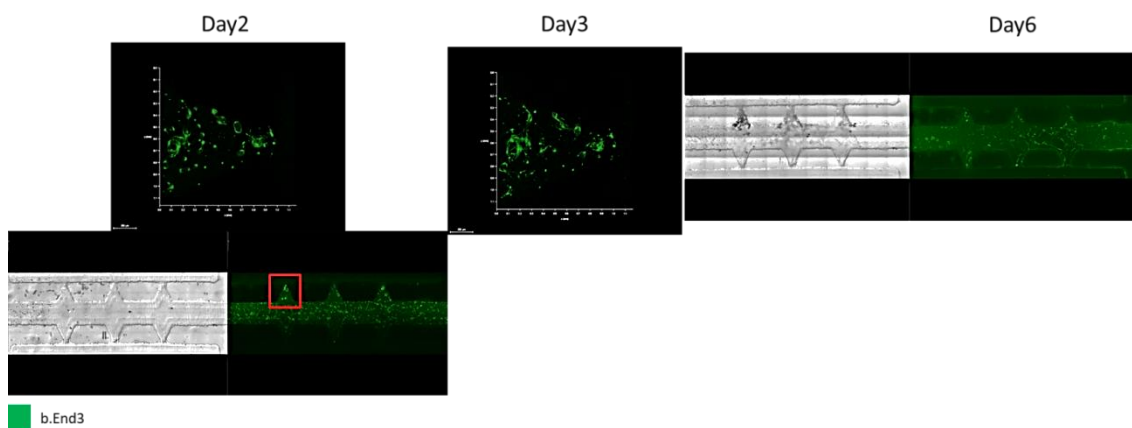


Figure 4.60. Confocal images of mimicking lung tissue in fibrin gel in five posts LOC devices for day 2, 3 and 6 in the absence of MSCs.

10 μM Green tracker was used as dye for tracking of b.End3 cells a day before experiment. Fibrinogen concentration was set as 3 mg/ml and cells were dissolved in 0.83U/ml thrombin containing medium. Collagen and matrigel were also mixed with the cells. Their concentrations were 0.5 mg/ml and 1.15 mg/ml, respectively. Final concentrations of cells are $1 \times 10^6/\text{ml}$ (b.End3), $0.66 \times 10^6/\text{ml}$ (WI38), $0.8 \times 10^6/\text{ml}$ (Beas-2B) and $1.5 \times 10^4/\text{ml}$ (D1-ORL-UVA). Height of matrix channel is 100 μm , and width is 1mm having three posts. Images were taken by 10X objective with confocal microscope.

Table 7. Cell concentrations from different sources.

	b.End3	WI38/3T3-L1	Beas-2B/ MCF-10A	D1-ORL-UVA
Wisco number	$3 \times 10^6/\text{ml}$	$2 \times 10^6/\text{ml}$	$2.25 \times 10^6/\text{ml}$	$3 \times 10^7/\text{ml}$
Wisco_NoMSCs	$3 \times 10^6/\text{ml}$	$2 \times 10^6/\text{ml}$	$2.25 \times 10^6/\text{ml}$	-
Jeon number	$3 \times 10^6/\text{ml}$	$8.4 \times 10^5/\text{ml}$	$8.4 \times 10^5/\text{ml}$	$1.2 \times 10^5/\text{ml}$

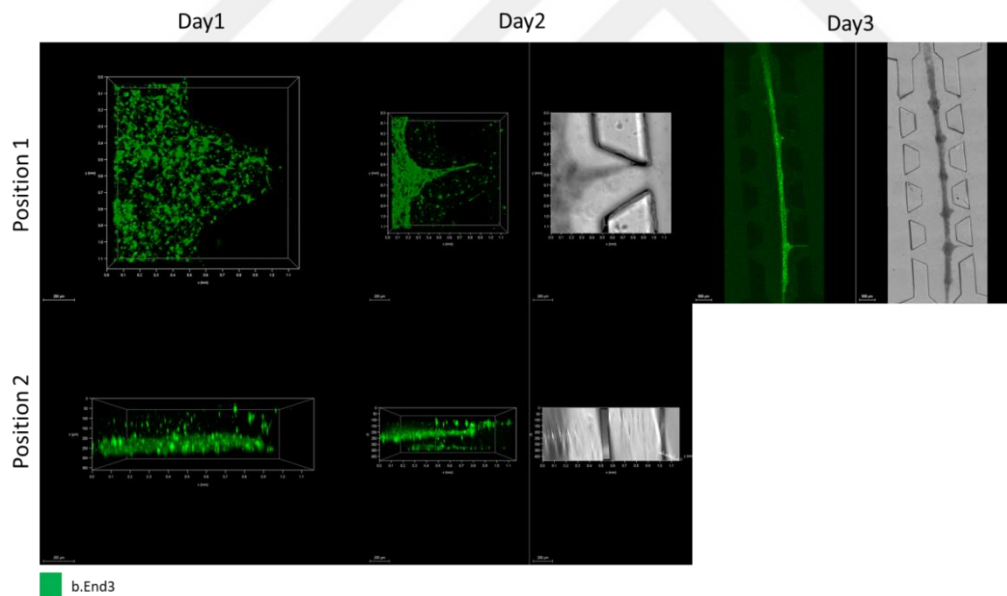


Figure 4.61. Confocal images of lung tri-culture in fibrin gel according to Wisco numbers in high height of LOC device.

10 μM Green tracker was used as dye for tracking of b.End3 cells a day before experiment. Fibrinogen concentration was set as 3 mg/ml and cells were dissolved in 0.83U/ml thrombin containing medium. Collagen and matrigel were also mixed with the cells. Their concentrations were 0.5 mg/ml and 1.15 mg/ml, respectively. Final

concentrations of cells are $3 \times 10^6/\text{ml}$ (b.End3), $2 \times 10^6/\text{ml}$ (WI38), $2.25 \times 10^6/\text{ml}$ (Beas-2B) and $3 \times 10^4/\text{ml}$ (D1-ORL-UVA). Height of matrix channel is $295 \mu\text{m}$, and width is 1mm having five posts. Images were taken by 10X objective with confocal microscope.

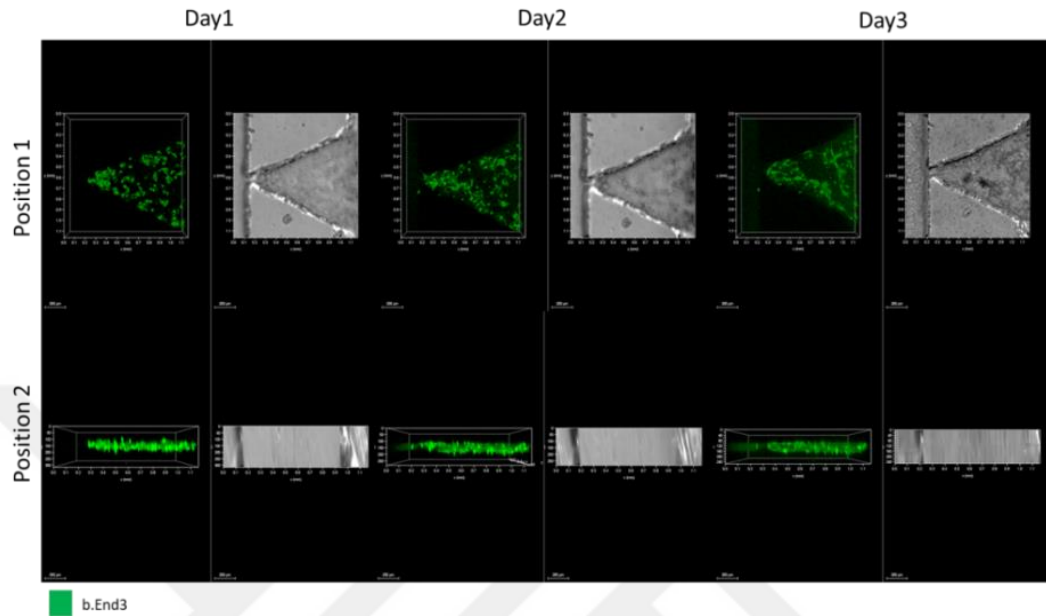


Figure 4.62. Confocal images of lung tri-culture in fibrin gel according to Wisco numbers in low height of LOC device.

$10 \mu\text{M}$ Green tracker was used as dye for tracking of b.End3 cells a day before experiment. Fibrinogen concentration was set as 3 mg/ml and cells were dissolved in 0.83 U/ml thrombin containing medium. Collagen and matrigel were also mixed with the cells. Their concentrations were 0.5 mg/ml and 1.15 mg/ml , respectively. Final concentrations of cells are $3 \times 10^6/\text{ml}$ (b.End3), $2 \times 10^6/\text{ml}$ (WI38), $2.25 \times 10^6/\text{ml}$ (Beas-2B) and $3 \times 10^4/\text{ml}$ (D1-ORL-UVA). Height of matrix channel is $100 \mu\text{m}$, and width is 1mm having three posts. Images were taken by 10X objective with confocal microscope.

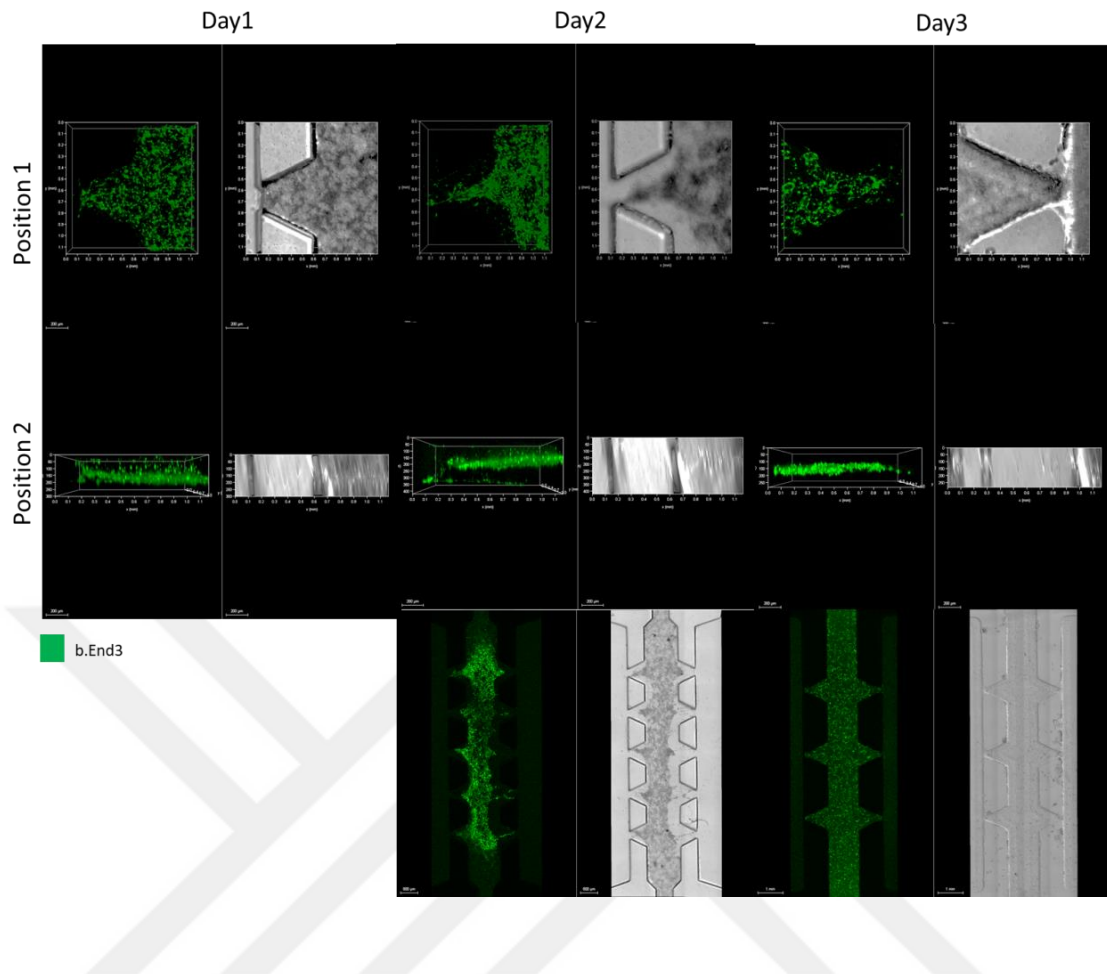


Figure 4.63. Confocal images of lung tri-culture in fibrin gel according to Wisco numbers in high height of LOC device in the absence of MSCs.

10 μ M Green tracker was used as dye for tracking of b.End3 cells a day before experiment. Fibrinogen concentration was set as 3 mg/ml and cells were dissolved in 0.83U/ml thrombin containing medium. Collagen and matrigel were also mixed with the cells. Their concentrations were 0.5mg/ml and 1.15mg/ml, respectively. Final concentrations of cells are 3×10^6 /ml (b.End3), 8.4×10^5 /ml (WI38), 8.4×10^5 /ml (Beas-2B). Height of matrix channel is 295 μ m, and width is 1mm having five posts. Images were taken by 10X objective with confocal microscope.

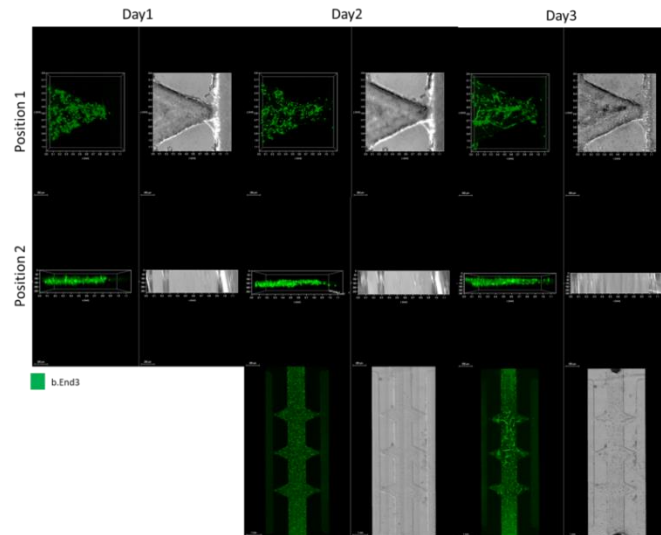


Figure 4.64. Confocal images of lung tri-culture in fibrin gel according to Wisco numbers in low height of LOC device in the absence of MSCs.

10 μ M Green tracker was used as dye for tracking of b.End3 cells a day before experiment. Fibrinogen concentration was set as 3 mg/ml and cells were dissolved in 0.83U/ml thrombin containing medium. Collagen and matrigel were also mixed with the cells. Their concentrations were 0.5mg/ml and 1.15mg/ml, respectively. Final concentrations of cells are 3×10^6 /ml (b.End3), 2×10^6 /ml (WI38), 2.25×10^6 /ml (Beas-2B). Height of matrix channel is 100 μ m, and width is 1mm having three posts. Images were taken by 10X objective with confocal microscope.

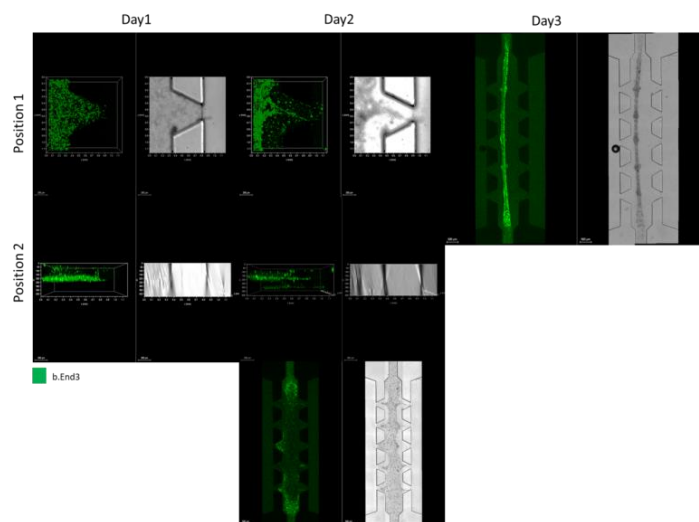


Figure 4.65. Confocal images of lung tri-culture in fibrin gel according to Jeon numbers in high height of LOC device.

10 μM Green, tracker was used as dye for tracking of b.End3 cells a day before experiment. Fibrinogen concentration was set as 3 mg/ml and cells were dissolved in 0.83U/ml thrombin containing medium. Collagen and matrigel were also mixed with the cells. Their concentrations were 0.5 mg/ml and 1.15 mg/ml, respectively. Final concentrations of cells are $3 \times 10^6/\text{ml}$ (b.End3), $8.4 \times 10^5/\text{ml}$ (WI38), $8.4 \times 10^5/\text{ml}$ (Beas-2B) and $1.2 \times 10^5/\text{ml}$ (D1-ORL-UVA). Height of matrix channel is 295 μm , and width is 1mm having five posts. Photos were taken by 10X objective with confocal microscope.

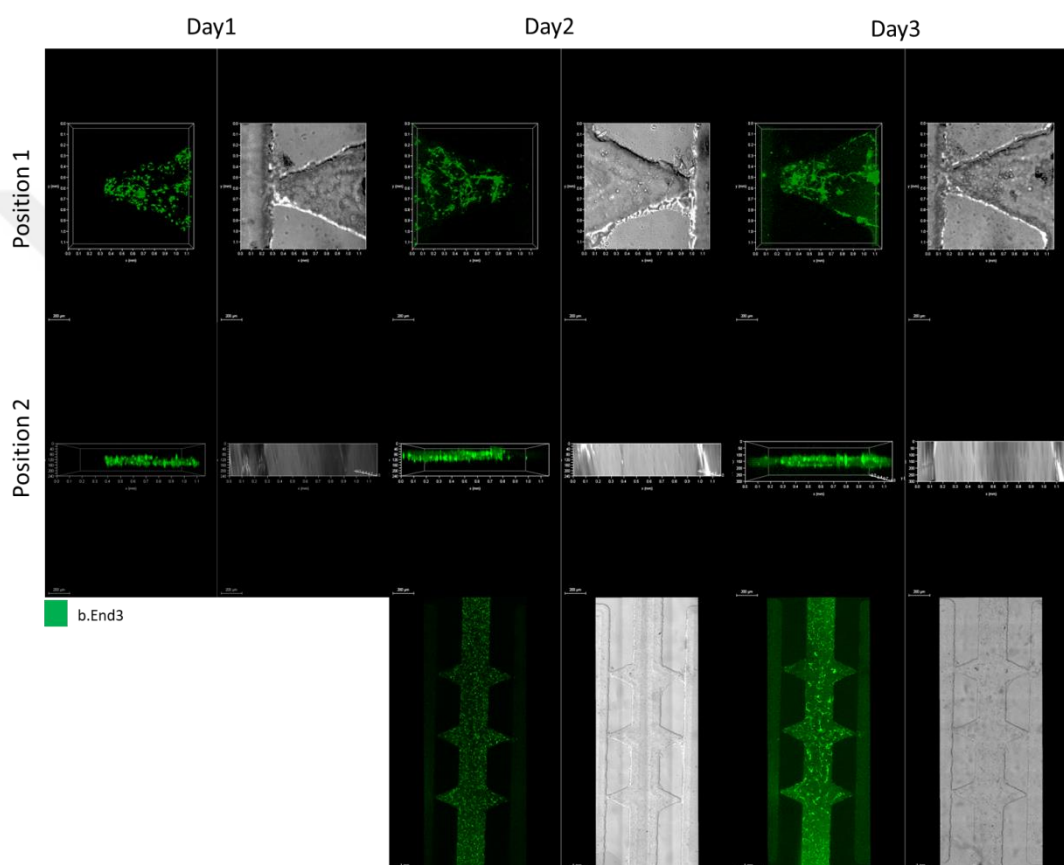


Figure 4.66. Confocal images of lung tri-culture in fibrinogen according to Jeon numbers in low height of LOC device.

10 μM Green, tracker was used as dye for tracking of b.End3 cells a day before experiment. Fibrinogen concentration was set as 3 mg/ml and cells were dissolved in 0.83U/ml thrombin containing medium. Collagen and matrigel were also mixed with the cells. Their concentrations were 0.5 mg/ml and 1.15 mg/ml, respectively. Final concentrations of cells are $3 \times 10^6/\text{ml}$ (b.End3), $8.4 \times 10^5/\text{ml}$ (WI38), $8.4 \times 10^5/\text{ml}$ (Beas-2B) and $1.2 \times 10^5/\text{ml}$ (D1-ORL-UVA). Height of matrix channel is 100 μm , and width is 1mm having five posts. Photos were taken by 10X objective with confocal microscope.

The results showed that use of MSCs in matrices effected the conservation of tissue structure without degradation. In addition, shrinkage of gel was observed regardless of height of LOC devices. For this reason, we decided to use optimized cell concentration like breast tissue.

4.2.5.6 Use of Matrigel and Collagen Containing Fibrin Gel for Generation of Lung Tissue

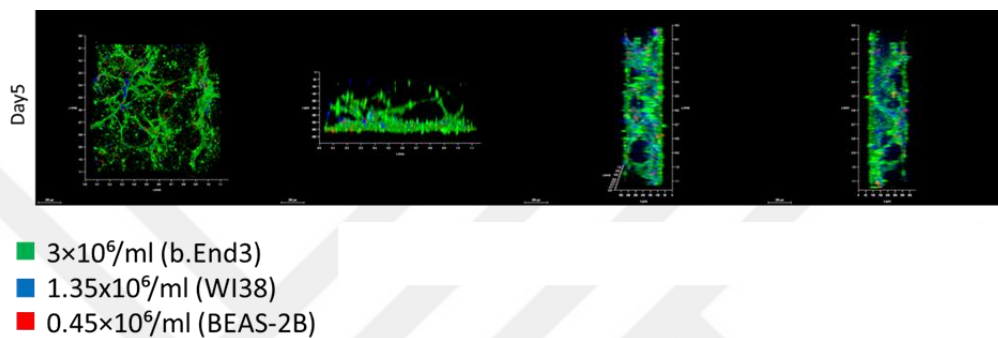


Figure 4.67. Confocal images of lung tissue in matrigel and collagen containing fibrin gel.

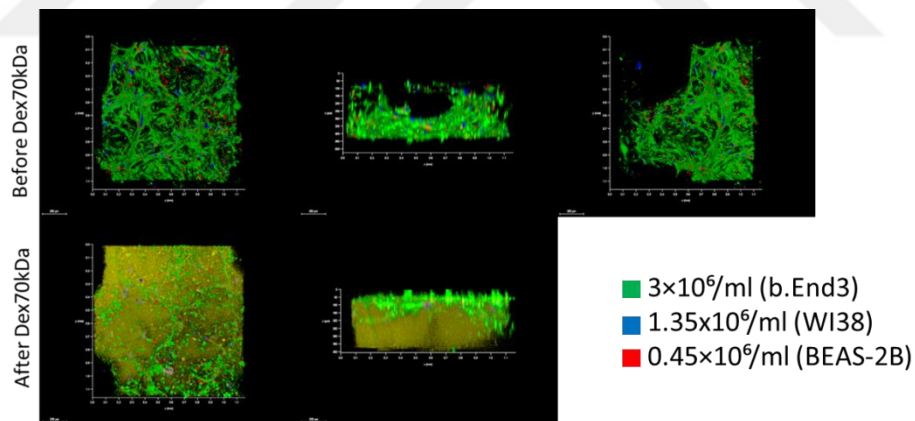


Figure 4.68. Confocal images after application of dextran 70kDa of lung tissue in matrigel and collagen containing fibrin gel.

The ratio of 3: 1.35: 0.45 for endothelial cells: fibroblasts: epithelial cells supported the MVN generation. And the structure was conserved in long term. We also tested the permeability of tissue mimics by using 70 kDa dextran molecules which was applied at day 5.

4.2.5.7. The Effect of Matrigel Containing Media on Structure of Lung Epithelial Cells

One aim of the study is to confirm that the tissues engineered in lab-on-a-chip devices mimic the key features of the *in vivo* tissues in terms of structure. For this purpose, different media ingredients were tested on epithelial cells to observe the acinar structure that is the unique morphology of cells.

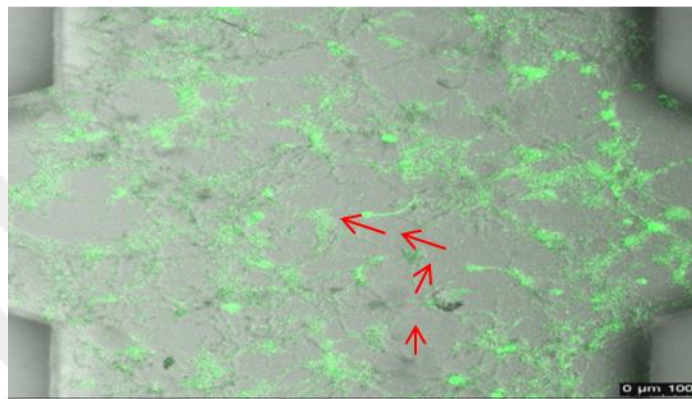


Figure 4.69. Images of alveolar ducts.

Figure 4.69 shows the merge image of phase contrast and fluorescence BEAS-2B cells. Only BEAS-2B cells were cultured in fibrin gel like co-culture conditions. Matrigel supplemented media was used for culture. Medium refreshed for each two days. Images were taken at day 4 by 10X objectives with confocal microscope. Beas-2B cells were organized as mimicking alveolar duct structure that was shown by red arrows in fibrin gel.

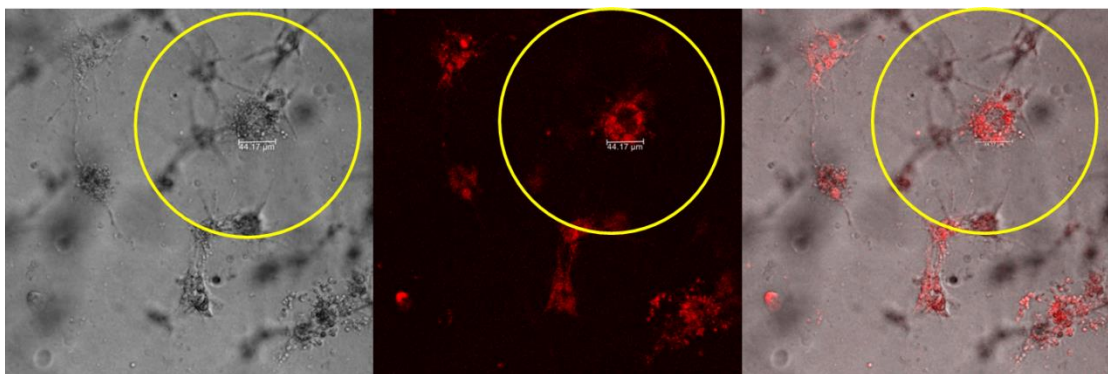


Figure 4.70. Structure of Beas-2B epithelial cells in fibrin gel at day 7.

4.3. Invasion of Different Cell Lines in Fibrin Gel and GFR

Matrigel and Mixture of Fibrin and GFR-matrigel (FM)

We tested our gel component for only containing fibrin at 3mg/ml concentration. But we observed the shrinkage of the gel in Figure 4.71. Black dashed lines show the We decided to change the content with mixing GFR-matrigel to reduce contraction. We also used GFR-matrigel environment to compare the effect of different matrices.

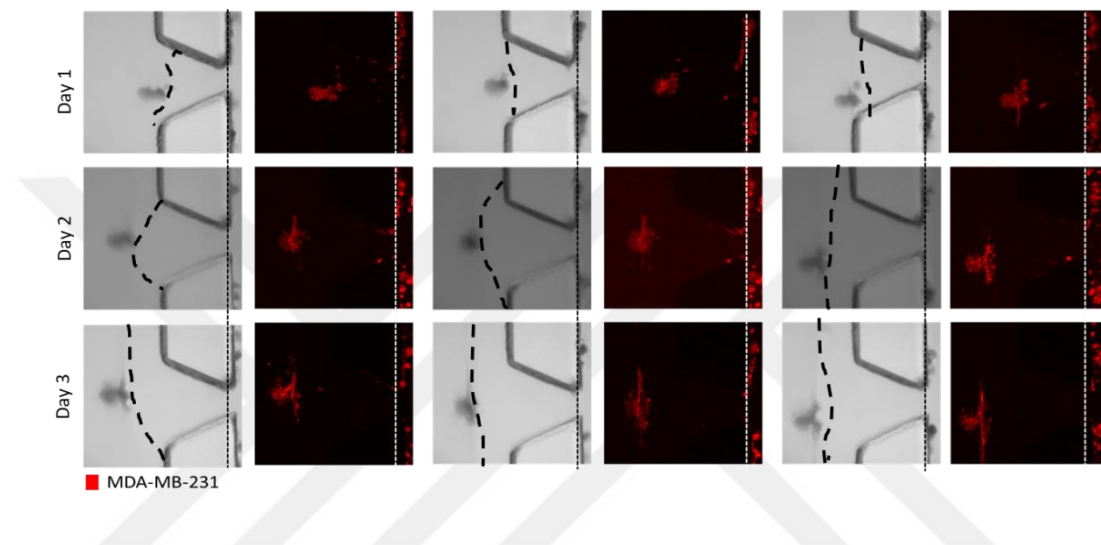


Figure 4.71. Invasion of breast cancer cells in only containing fibrin gel structure.

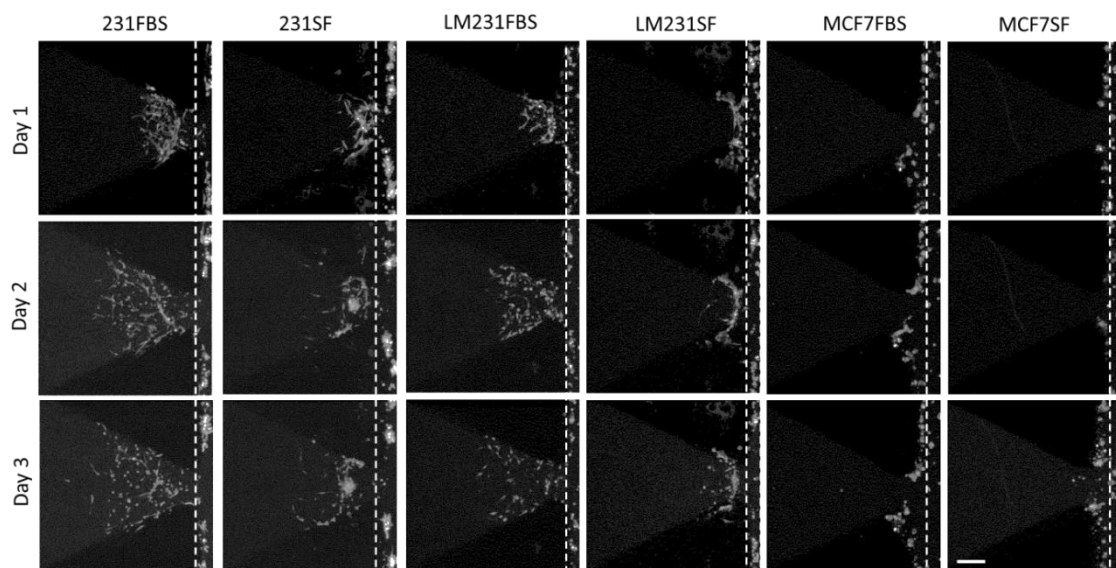


Figure 4.72. Invasion capacity of cells in GFR-matrigel.

We used MDA-MB-231, LM-231 and MCF7 cell lines towards to serum or without conditions through the GFR matrigel or mixture of fibrin and GFR matrigel matrices (Figure 4.72 and Figure 4.73, FBS: Fetal bovine serum, SF: Serum free).

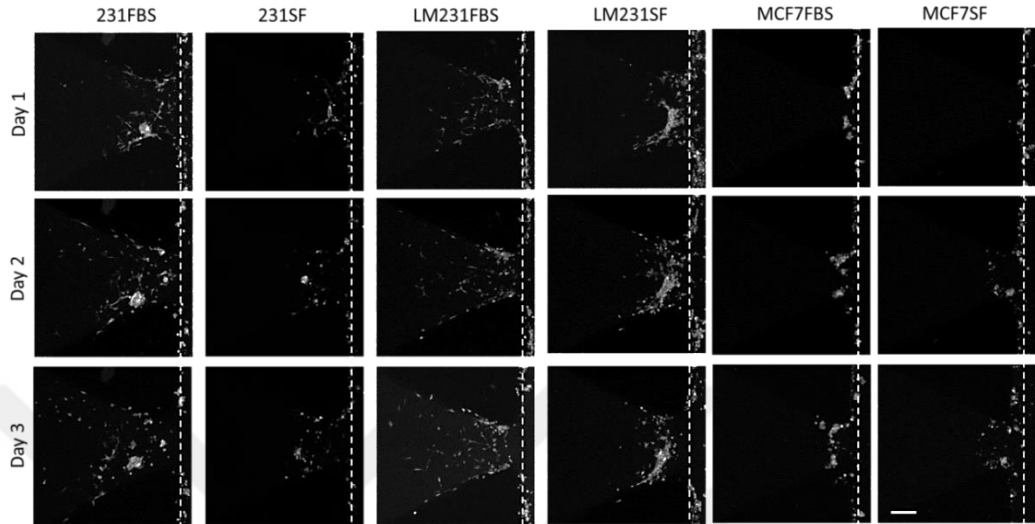


Figure 4.73. Invasion capacity of cells in mixture of fibrinogen and GFR matrigel.

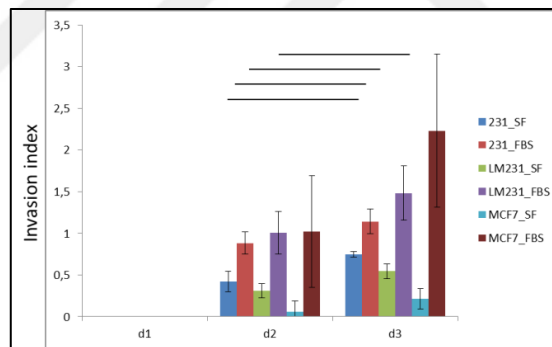


Figure 4.74. Invasion index of different cells into GFR-matrigel.

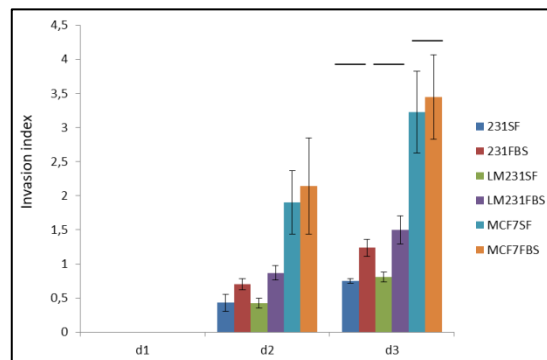


Figure 4.75. Invasion index of different cells into FM.

The results show that there is a significant differences between serum and serum free conditions for both each cell type and different matrices ($p < 0.005$). There is not any significant differences between MDA-MB-231 and LM-MDA-MB-231 (lung metastatic) cell lines for both of each matrices. There is a significant differences between breast cancer cell lines and MCF-7 as a negative control in GF-matrigel but not for mixture of fibrin and GFR-matrigel. The student T-test was done for statistical analysis. It indicates the confirmation of our lab-on-a-chip system that can be used for the observation of invasion.

4.3.1. Invasion of Cells into Breast and Lung Tissue Mimics Laden

GFR-Matrigel

Two different gel content (GFR-matrigel, 1 GFR-matrigel: 1 Fibrin) was tested in the experiments. Final concentrations were set to 3mg/ml for each gel. For breast tissue, MCF-10A (1×10^6) and 3T3-L1 (1×10^6) cells were used in the matrix. In addition, Beas-2B (1×10^6) and WI-38 (1×10^6) cells were used in the matrices. For monoculture of each condition, cell concentration was set to 2×10^6 /ml to eliminate the concentration differences when we compare the results with co-culture of cells. For the naming of all images first cell name shows the cells are laden in matrix and the second cell name shows the invaded cell name into the matrix (Scales: 200 μ m).

The results show that there is not any significant differences between MDA-MB-231 and LM-MDA-MB-231 (lung metastatic) cell lines but MDA-MB-231 cells more invaded compare to MDA-MB-LM231 cells. It can be because of having heterotypic cell population in MDA-MB-231. Epithelial cells (MCF-10A) were invaded into Beas-2B and MCF-10A. This is not expected results but the reason can be the induction of migration to the same cell type in a paracrine signaling way.

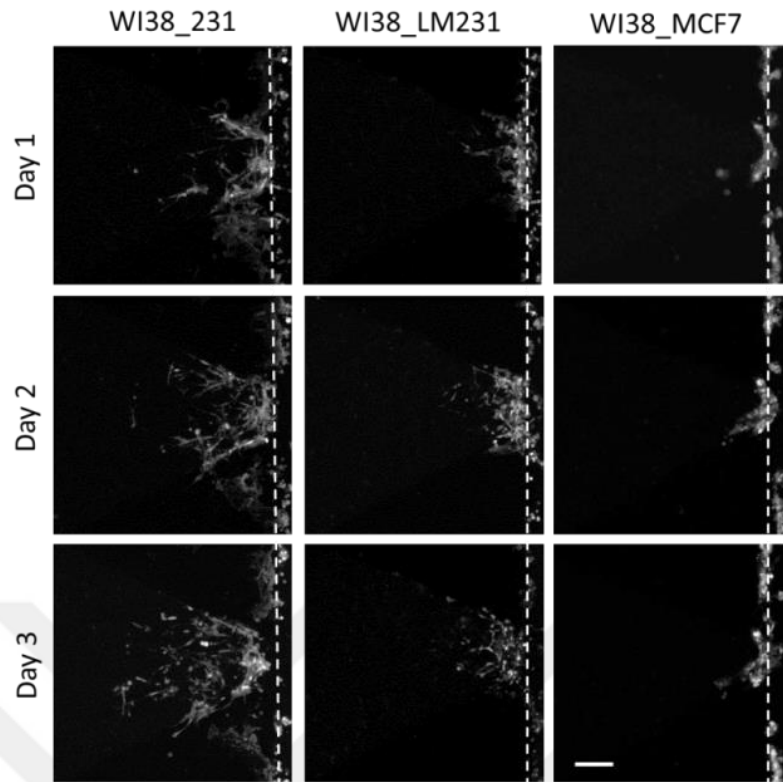


Figure 4.76. Invasion of cells into lung fibroblast laden within GFR-matrigel.

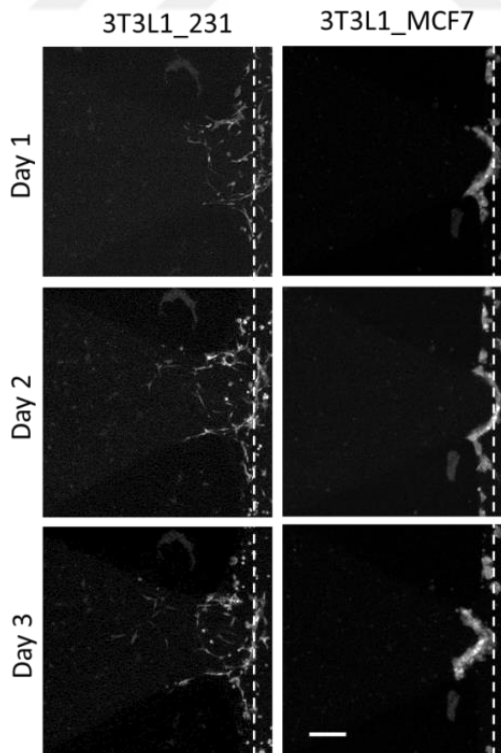


Figure 4.77. Invasion of cells into breast fibroblast laden within GFR-matrigel.

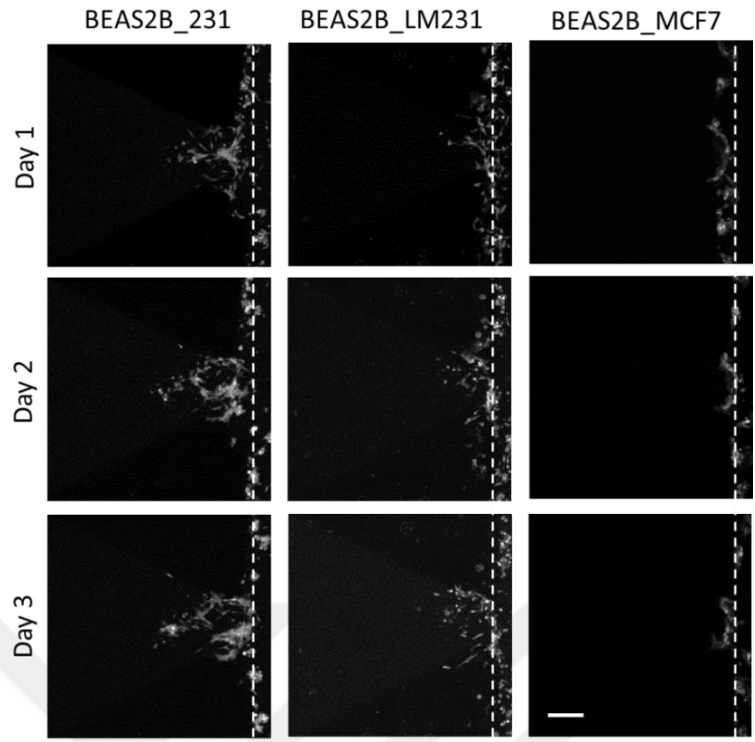


Figure 4.78. Invasion of cells into lung epithelial cell laden within GFR-matrigel.

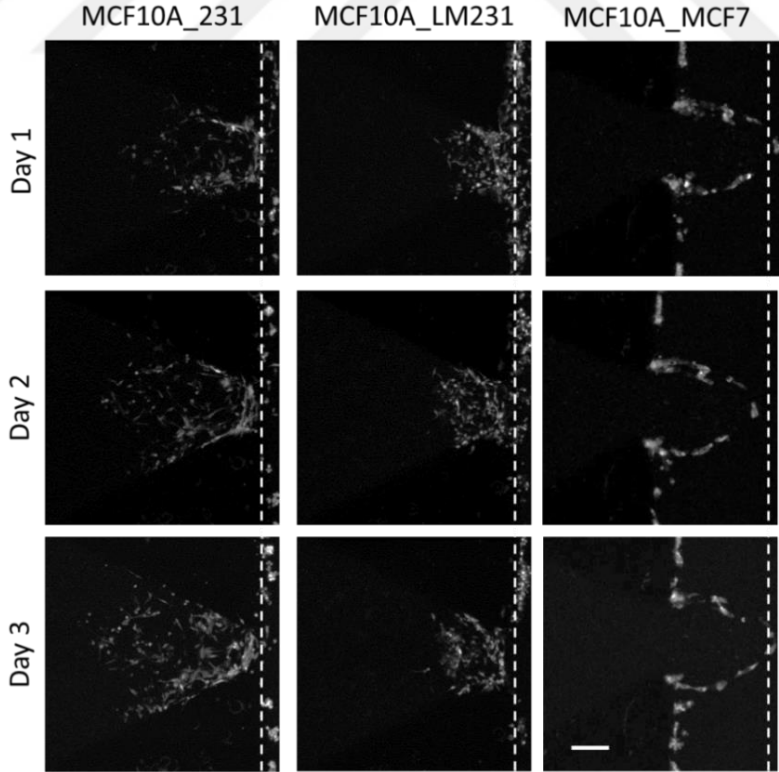


Figure 4.79. Invasion of cells into breast epithelial cell laden within GFR-matrigel.

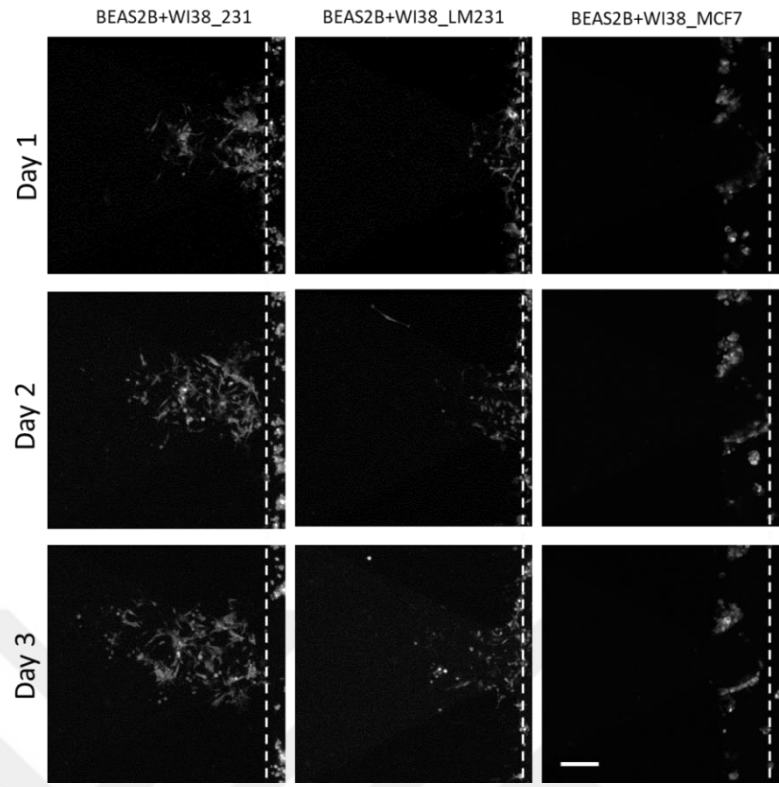


Figure 4.80. Invasion of cells into lung tissue mimic laden within GFR-matrigel.

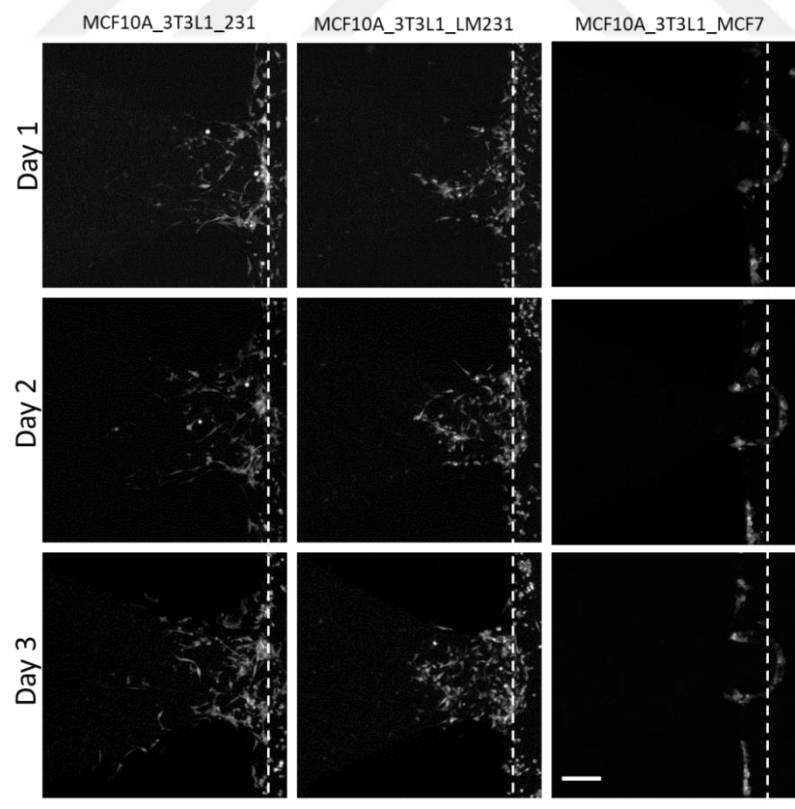


Figure 4.81. Invasion of cells into breast tissue mimic laden within GFR-matrigel.

4.3.2. Invasion of Cells into Breast and Lung Tissue Mimics Laden Mixture of Fibrin Gel and GFR-Matrigel (FM)

Two different gel content (GFR-matrigel, 1 GFR-matrigel: 1 Fibringel) was tested in the experiments. Final concentrations were set to 3mg/ml for each gel. For lung tissue, Beas2B (1×10^6) and WI38 (1×10^6) cells were used in the marix. Two different gel content (GFR-matrigel, 1 GFR-matrigel: 1 Fibringel) was tested in the experiments. Final concentrations were set to 3mg/ml for each gel. For breast tissue, MCF-10A (1×10^6) and 3T3-L1 (1×10^6) cells were used in the marix. In addition, Beas-2B (1×10^6) and WI-38 (1×10^6) cells were used in the marices. For monoculture of each condition, cell concentration was set to 2×10^6 /ml to eliminate the concentration differences when we compare the results in co-culture of cells. For the naming of all images first cell name shows the cells are laden in matrix and the second cell name shows the invaded cell name into the matrix.

The results show that there is not any significant differences between MDA-MB-231 and MDA-MB-LM231 (lung metastatic) cell lines but MDA-MB-231 cells more invaded compare to MDA-MB-LM231 cells. It can be because of having heterotypic cell population in MDA-MB-231. Epithelial cells (MCF-10A) were invaded into Beas-2B and MCF-10A. This is not expected results but the reason can be the induction of migration to the same cell type in a paracrine signaling way.

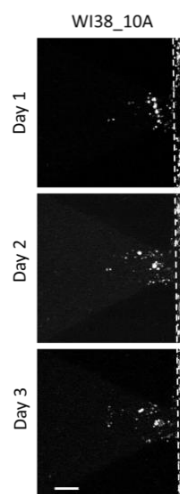


Figure 4.82. Invasion of cells into lung fibroblast cell laden within FM.

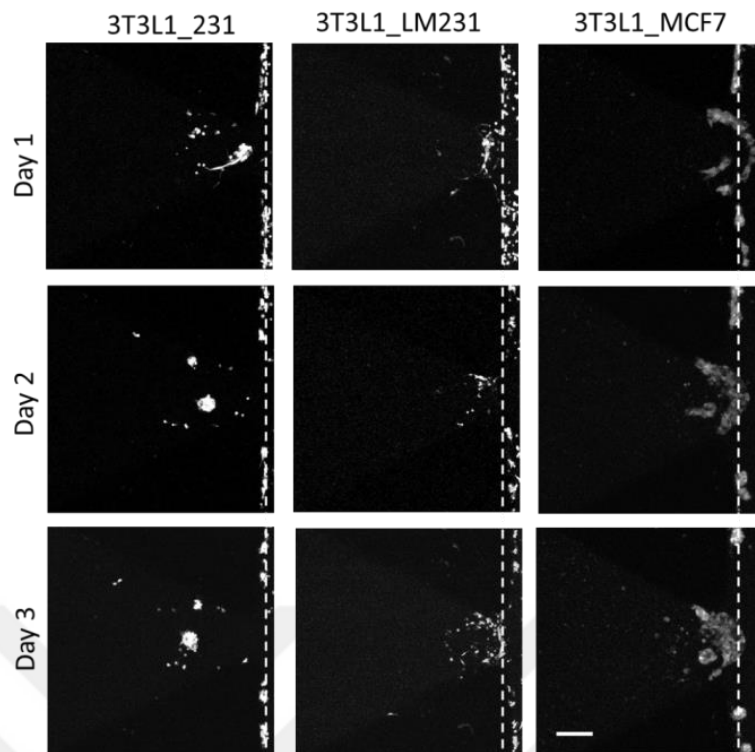


Figure 4.83. Invasion of cells into breast fibroblast cell laden within FM.

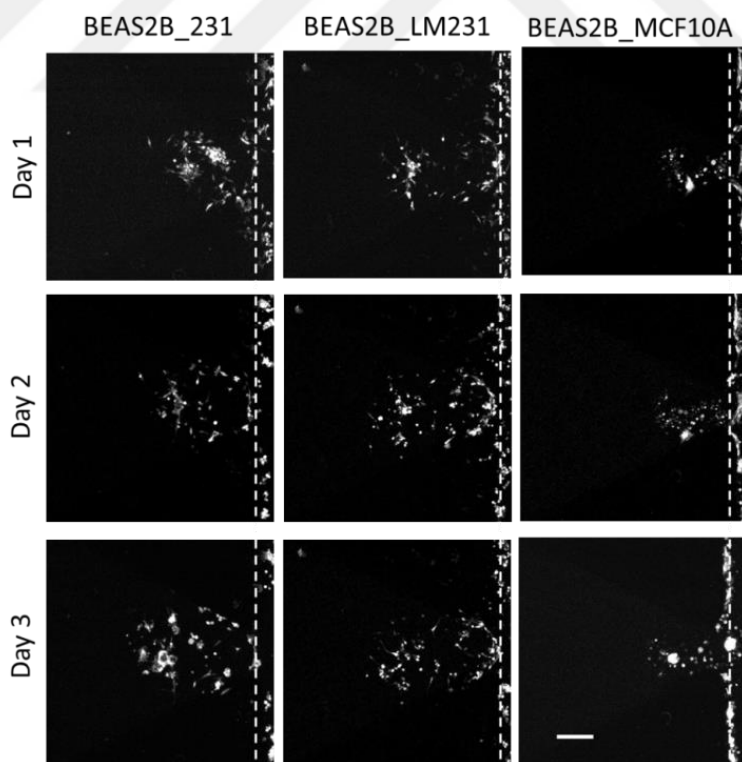


Figure 4.84. Invasion of cells into lung epithelial cell laden within FM.

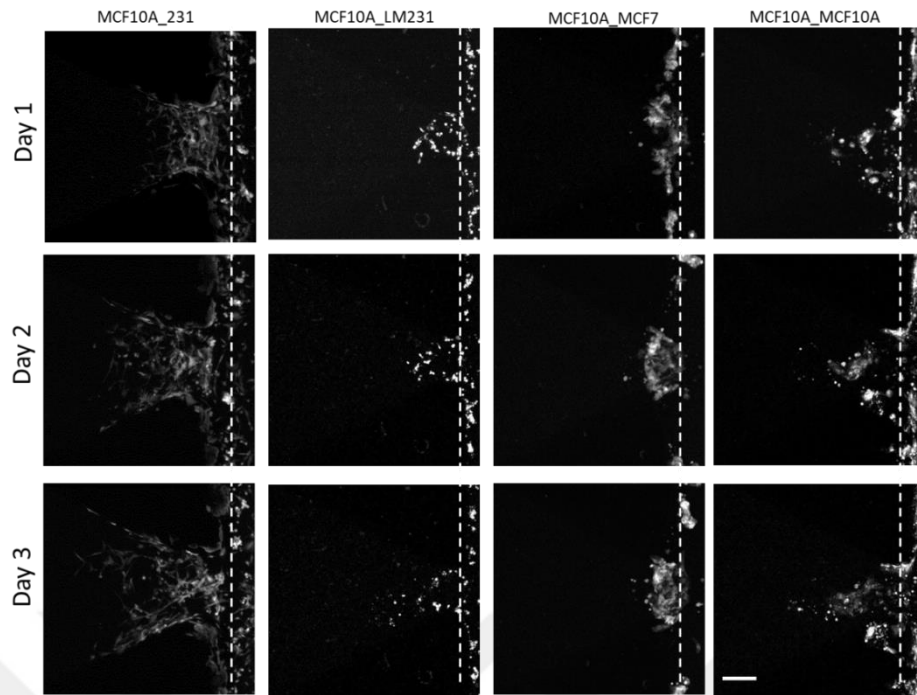


Figure 4.85. Invasion of cells into breast epithelial cell laden within FM.

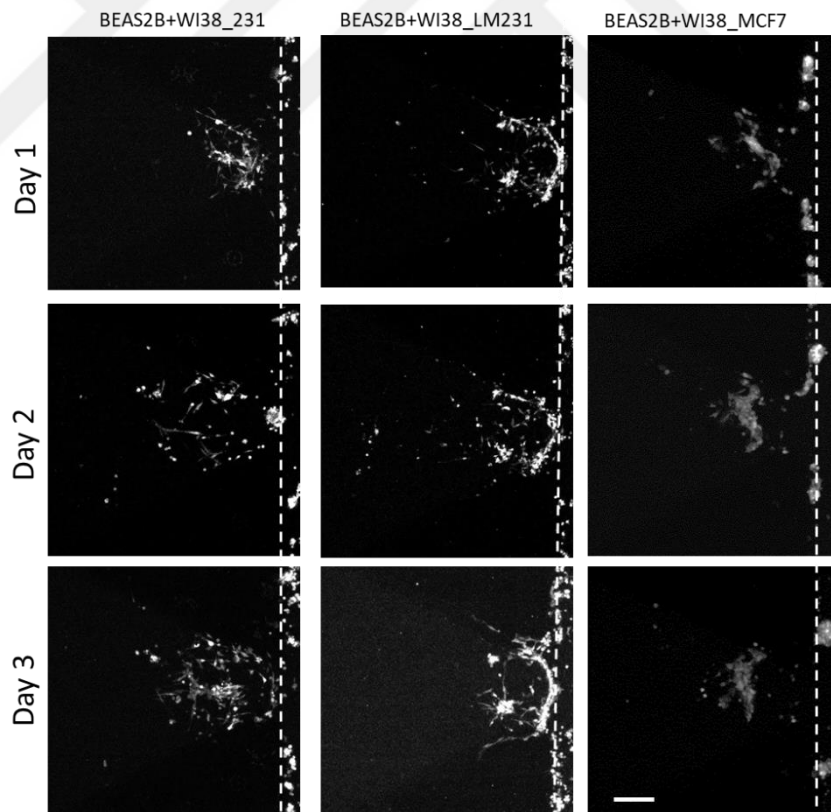


Figure 4.86. Invasion of cells into lung tissue mimic laden within FM.

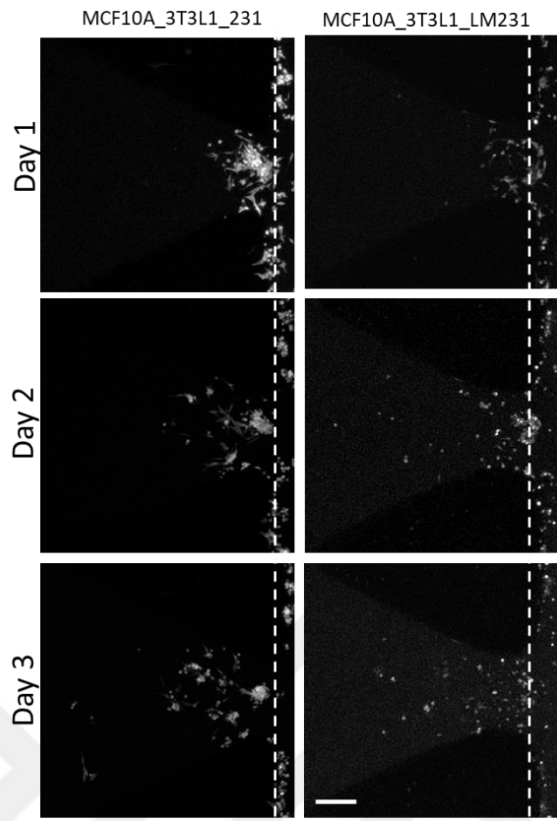


Figure 4.87. Invasion of cells into breast tissue mimic laden within FM.

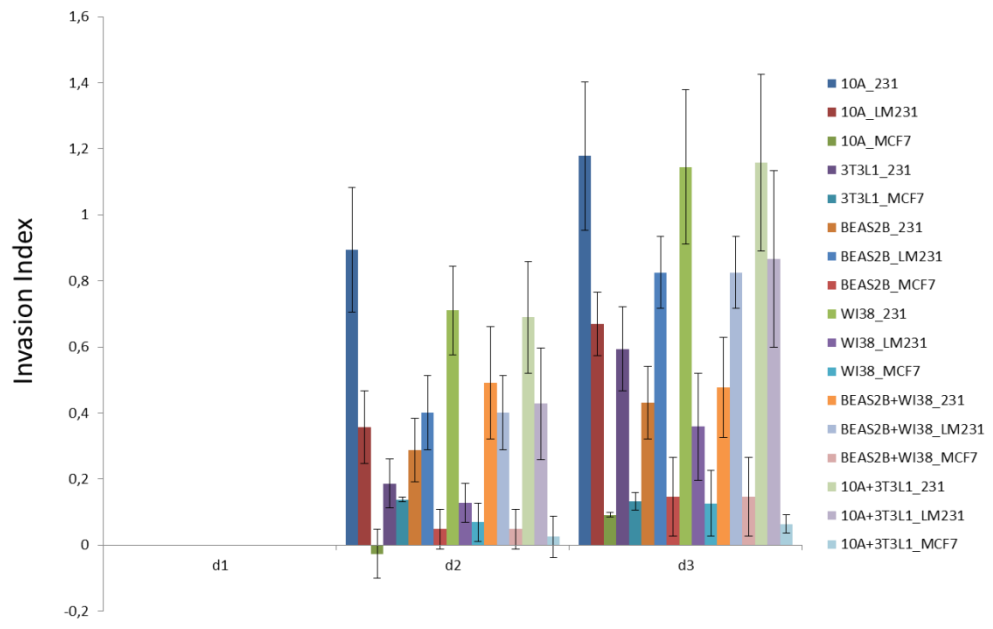


Figure 4.88. Invasion index of distinct cells into epithelial cells, fibroblasts or breast and lung tissue mimics laden within GFR-matrigel separately day by day.

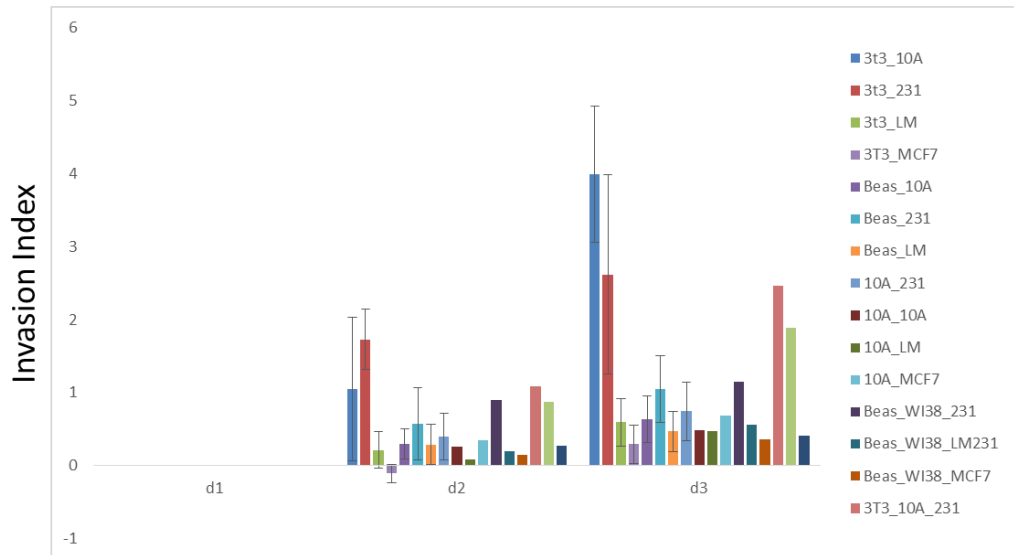


Figure 4.89. Invasion index of distinct cells into epithelial cells, fibroblasts or breast and lung tissue mimics laden within FM separately day by day.

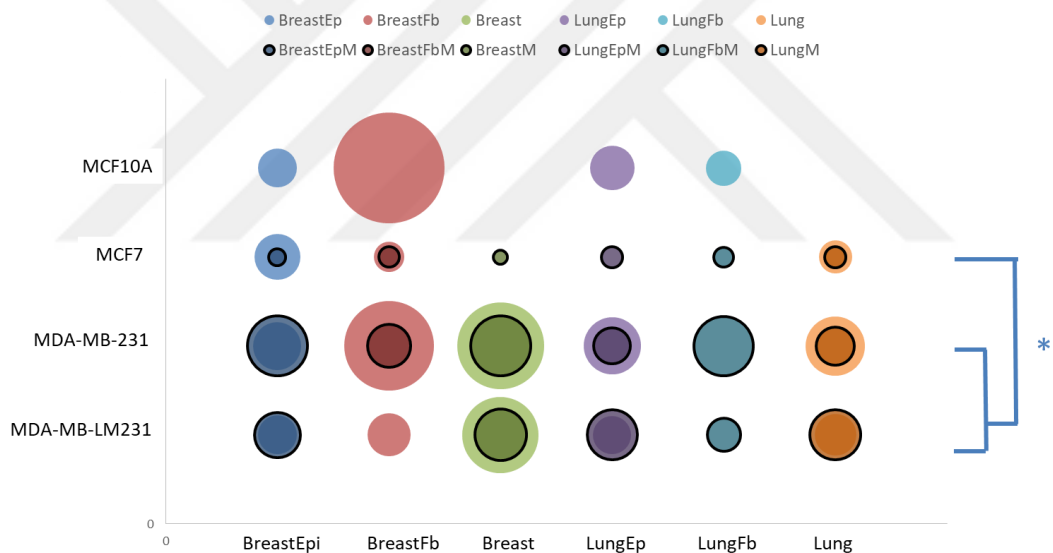


Figure 4.90. Summary of invasion into distinct matrices.

Figure 4.90 shows the summary of invasion results (BreastEp: MCF-10, BreastFb: 3T3-L1, LungEp: Beas-2B, LungFb: WI-38, BreastM: MCF-10A and 3T3-L1 cells laden in GFR-Matrigel, BreastFb: MCF-10A and 3T3-L1 cells laden in mixture of fibrin and GFR-Matrigel, LungM: Beas-2B and WI-38 cells laden in GFR-matrigel, LungFb: Beas-2B and WI-38 cells laden mixture of fibrin and GFR-Matrigel). The groups were linked in the graph to show the non significant differences between MDA-MB-231 and MDA-MB-LM231, but there is a significant differences compare to MCF-7

for each tissue mimics. Invasion of MDA-MB-231 and MD-MB-LM231 cells did not show differences for both only epithelial/fibroblasts and tissue mimics laden matrices (GFR-matrigel and mixture of it with fibrin gel). The reason might be more heterogeneous population of MDA-MB-231 cells. Bone metastatic breast cancer cell line can be used to observe more tissue specific invasion for lung tissue mimics.

4.4. Extravasation of Different Cell Lines into Breast and Lung Tissue Mimics

4.4.1. Formation of Endothelial Monolayer

Endothelial monolayer formation is the critical step to mimic blood vessel. Here, the formation of endothelial monolayer was used as an alternative approach rather than formation of MVN. For the further steps target breast (containing MCF-10A and 3T3-L1) and lung tissues (containing Beas-2B and WI38) will be used as homing to observe the extravasation of breast cancer cells and lung metastatic breast cancer cells. Extravasation chip was consisting of three channels; homing channel, media channel and a narrow channel for culturing endothelial cells that can mimic a blood vessel.

Before the extravasation assays, extravasation LOCs were coated with chemicals and proteins, respectively to ensure the attachment of endothelial cells for the generation of intact monolayer. Here, we used APTES as a pre-coating material and a linker by combining with laminin (LAM) as a component of basement membrane. LAM-coated surface allowed the formation of an intact endothelial monolayer structure (Figure 4.92).

Control of endothelial cells' distribution within the EMC is important for the generation of monolayer with the appropriate surface for cell attachment. Here, we used dextran to inhibit the cluster formation and the results showed that use of dextran provided homogeneous distribution of endothelial cells (Figure 4.91).

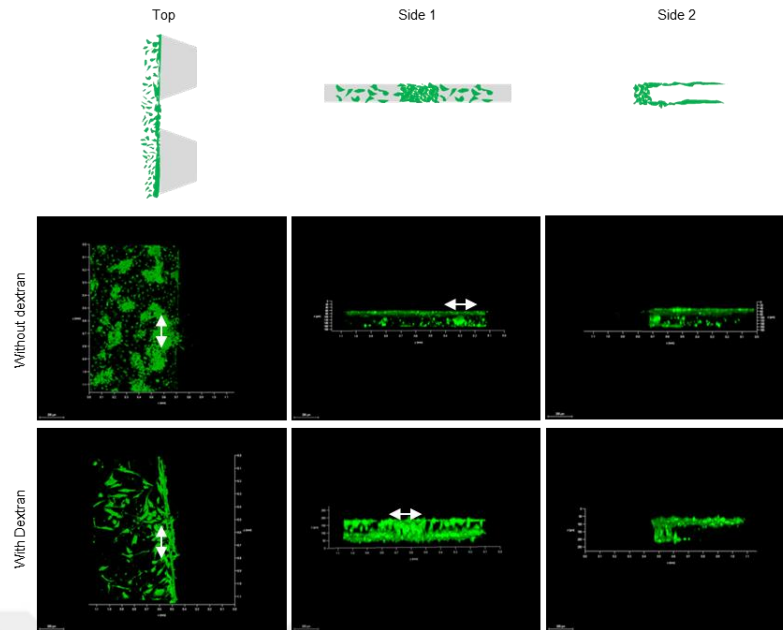


Figure 4.91. Dextran ensured homogeneous distribution of endothelial cells.

Confocal images showing the distributions of endothelial cells with or without dextran from different views (top, side 1 and side 2). The endothelial monolayer between the post gaps are represented with two-sided arrows (Scale bar: 200 μ M).

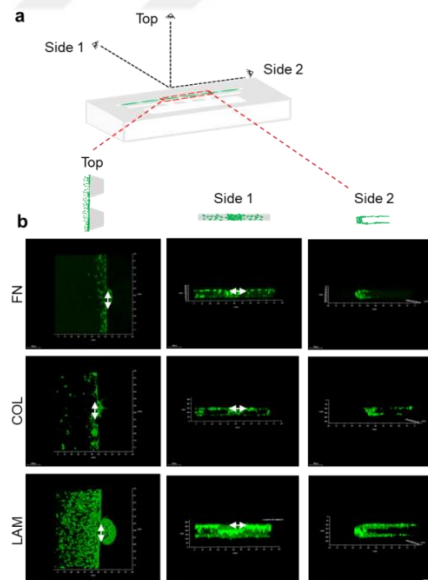


Figure 4.92. Laminin coating resulted in efficient intact endothelial monolayer formation. (a) Representative 3D images of extravasation LOC showing endothelial cells (green) on laminin (LAM) coated surfaces from different views (top, side 1 and side 2). (b) The endothelial monolayer between the post gaps are represented with two-sided arrows (Scale bar: 200 μ M).

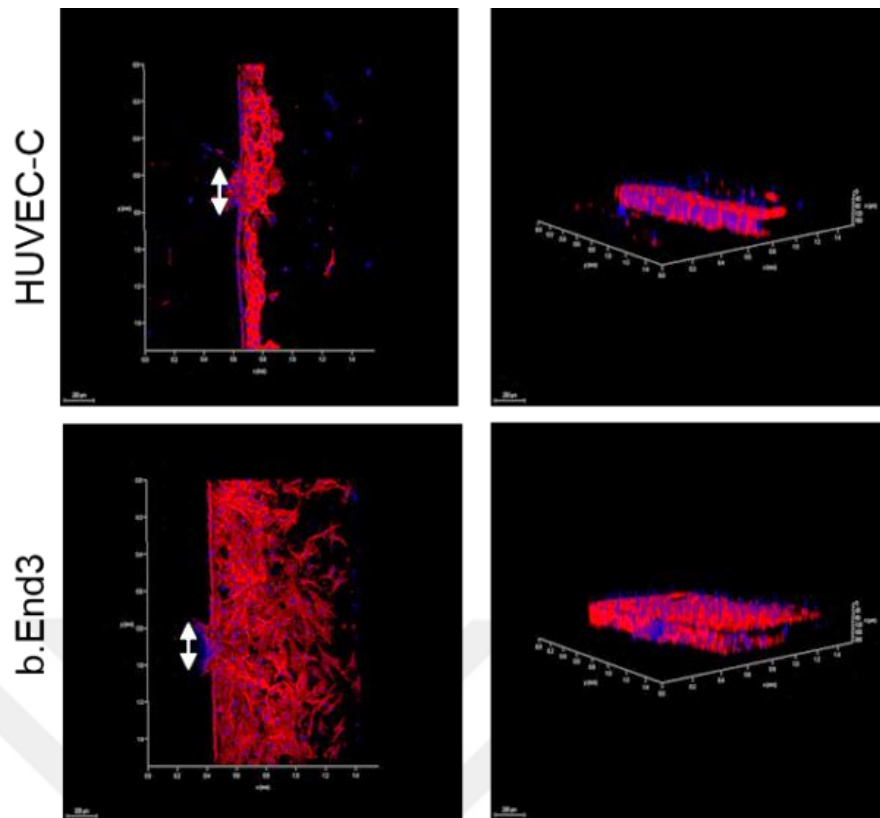


Figure 4.93. Staining of endothelial monolayer composed of different sources of endothelial cells.

4.4.1.1. Characterization of Endothelial Monolayer

Intact endothelial monolayer formation was further demonstrated by permeability assay. Diffusion of 70-kDa dextran in the absence or presence of endothelial monolayer was analyzed. The endothelial barrier function was quantified to confirm the size-selective transendothelial transport of cancer cells. The 70 kDa dextran used here to measure endothelial monolayer integrity is equal to the molecular weight of serum albumin which is 69 kDa³⁸. It is also much lower than vascular permeability values that was previously obtained on the microfluidic platform which were almost 2 cm/s and 2.8 cm/s respectively^{39,40}. Besides, the permeability difference between endothelial monolayer with HUVEC-C cells and without any cells is relatively corresponding to the same ratio previously described in another study⁴¹. Accordingly, the endothelial monolayer generated in LOC seems rather size-selective and well-organized to see extravasation of cells clearly.

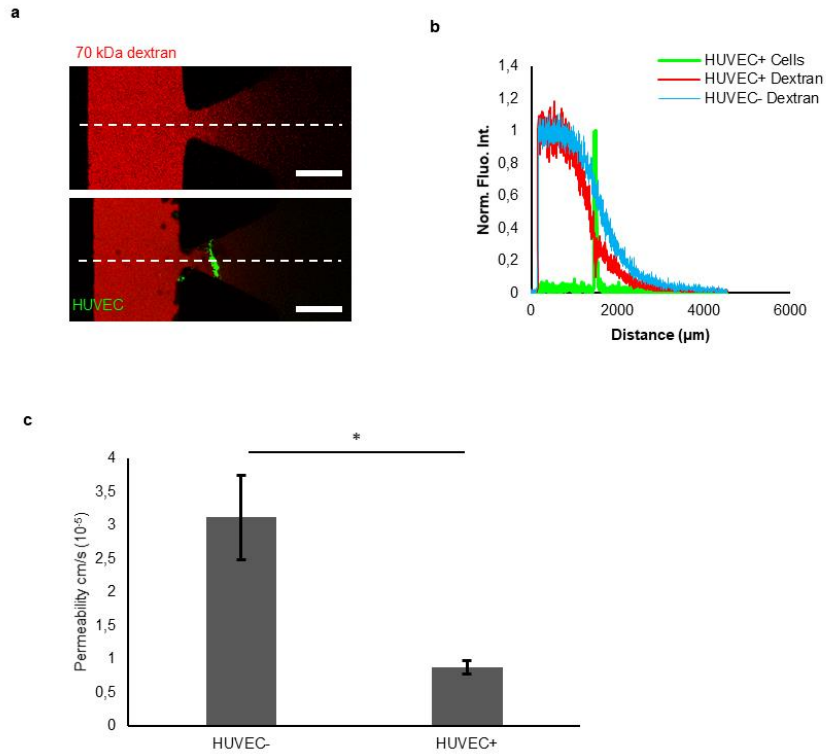


Figure 4.94. (a) Confocal images of 70 kDa dextran, (b) fluorescence intensity of 70 kDa dextran, (c) permeability of 70 kDa dextran in the absence and the presence of HUVEC (Scale bar: 500 μM).

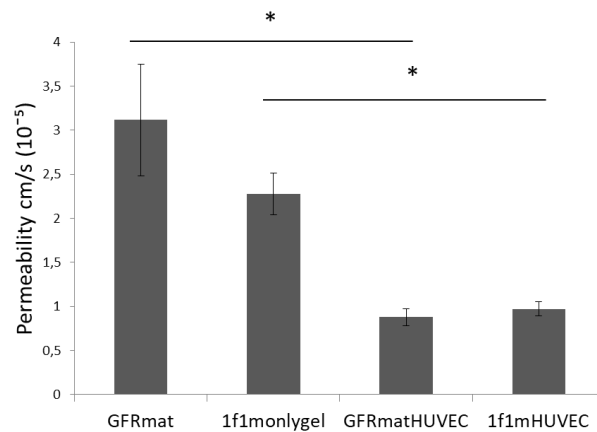


Figure 4.95. Permeability values of different gel component with or without endothelial cells.

The results showed that the mixture of fibrin and matrigel provides the convenient conditions having the similar range with GFR-matrigel. There are not significant differences between distinct gels with or without endothelial cells. But, there is a significant difference in the presence of endothelial monolayer for each gel

($p < 0.005$). The generation of endothelial monolayer resulted in the decrease of permeability value.

4.4.1.2. Extravasation into Lung Tissue Mimics

GFR-matrigel was used to generate lung tissue microenvironment. And the concentrations of cells are $1 \times 10^6/\text{ml}$ for WI-38 and Beas2B, $3.85 \times 10^6/\text{ml}$ for b.End3. WI38 and Beas2B were seeded into matrix and cultured for 24 hours. And the day after, endothelial cells were seeded and incubated at the vertical position for 24 hours to generate endothelial monolayer. At the end of the incubation, endothelial monolayer was checked under the confocal microscope by taking images. If it is intact layer, cancer cells were seeded into endothelial channel and then cultured for 24 hours to observe the extravasation of cancer cells through the endothelial cells.

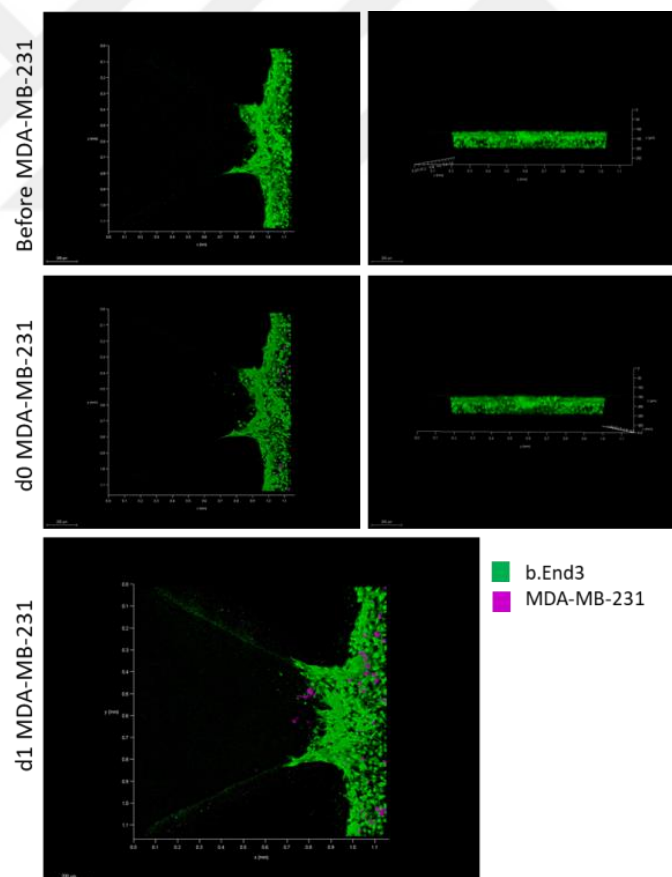


Figure 4.96. Extravasation of MDA-MB-231 breast cancer cells into generated lung tissue.

Figure 4.96 shows the merge images for Z-stack of brightfield and fluorescence images (green: endothelial cells, red: cancer cells). Circular area shows the cancer cells are associated with endothelial cells, and extravasated at day 0 and day 1, respectively.

4.4.2. Formation of MVN in Tissue Mimics

Endothelial cells ($6 \times 10^6/\text{ml}$) were labeled with tracker dyes the day before experiment. Fibroblast (WI38: $1 \times 10^6/\text{ml}$) and epithelial cells (Beas2B: $1 \times 10^6/\text{ml}$) were not labeled with tracker dyes.

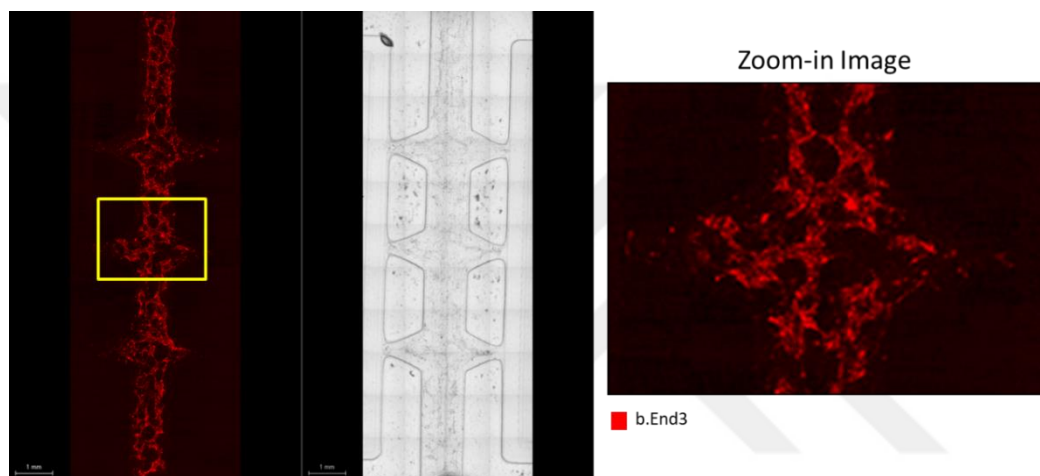


Figure 4.97. Lung tissue in fibrin and GFR matrigel mixture at day 2.

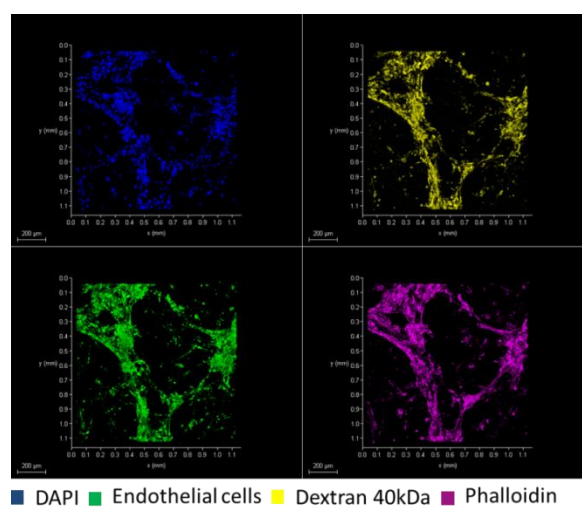


Figure 4.98. Confirmation of MVN formation at day 2.

For the formation of tissue mimics with MVN, endothelial cells (6×10^6), fibroblasts (1×10^6) and epithelial cells (1×10^6) were used in the mixture of fibrin and GFR-matrigel. $10 \mu\text{M}$ cell trackers were applied to only endothelial cells. Figure 4.97 shows the tilescan images of lung tissue at day 2 before applying dextran molecule. Figure 4.98 shows the localization of the dextran molecule (yellow) which is co-localized with endothelial cells (green). It indicates that the diffusion of dextran through the endothelial cells. DAPI and Phalloidin staining was also represented with blue and magenta colors, respectively,

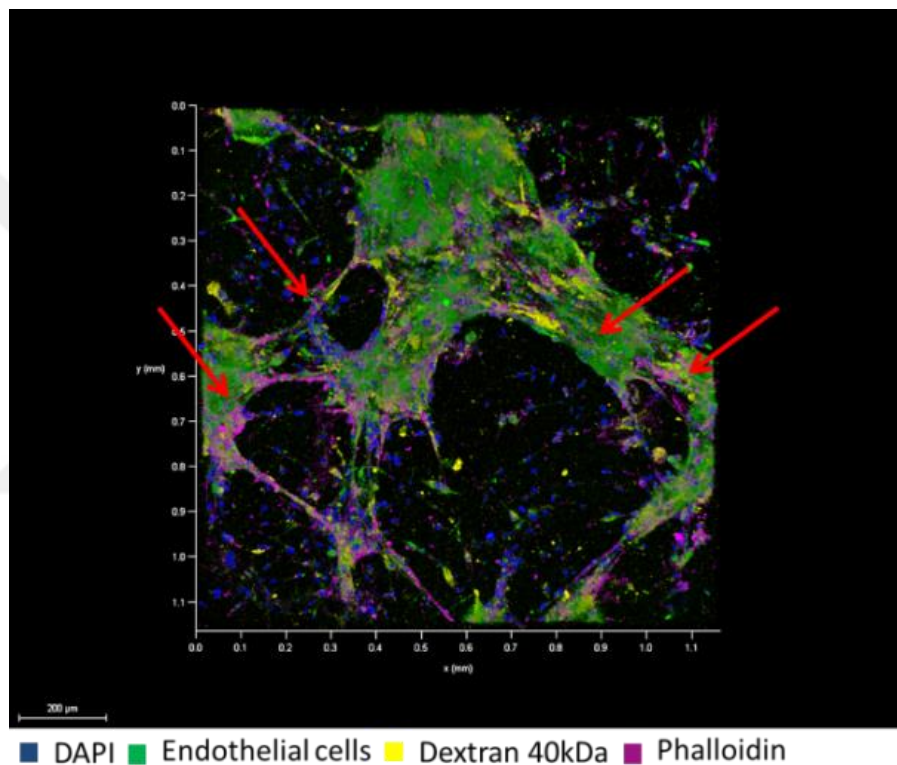


Figure 4.99. Lung tissue laden within fibrin and GFR matrigel mixture after dextran loading and staining.

Dextran 40kDa was applied into chip and incubated overnight with dextran at 37°C incubator in the humidity conditions. At the end of the incubation, sample was fixed with 4% PFA at $+4^\circ\text{C}$ for overnight. And then it was rinsed with 1XPBS for three times. Figure 4.99 shows the staining of lung tissue with phalloidin and DAPI after fixation. Red arrows indicate the areas with MVN. And the co-localization of green and yellow colors indicates the confirmation of MVN formation (Green: Endothelial cells, Yellow: Dextran 40kDa, Purple: phalloidin 647, Blue: DAPI).

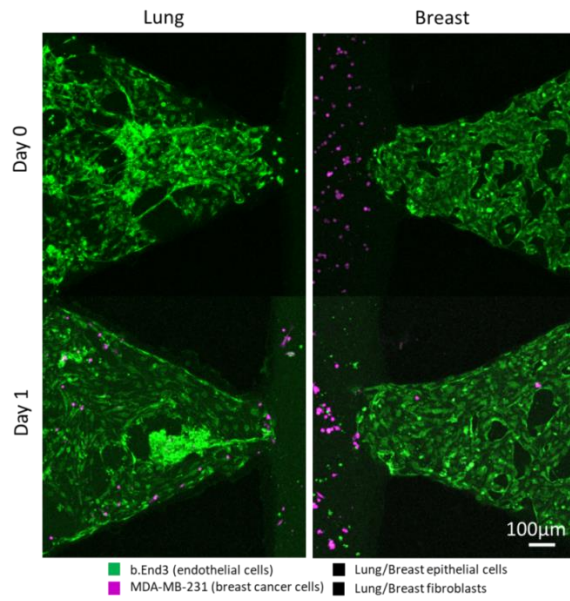


Figure 4.100. Extravasation of breast cancer cells into lung and breast tissue mimics with MVN.

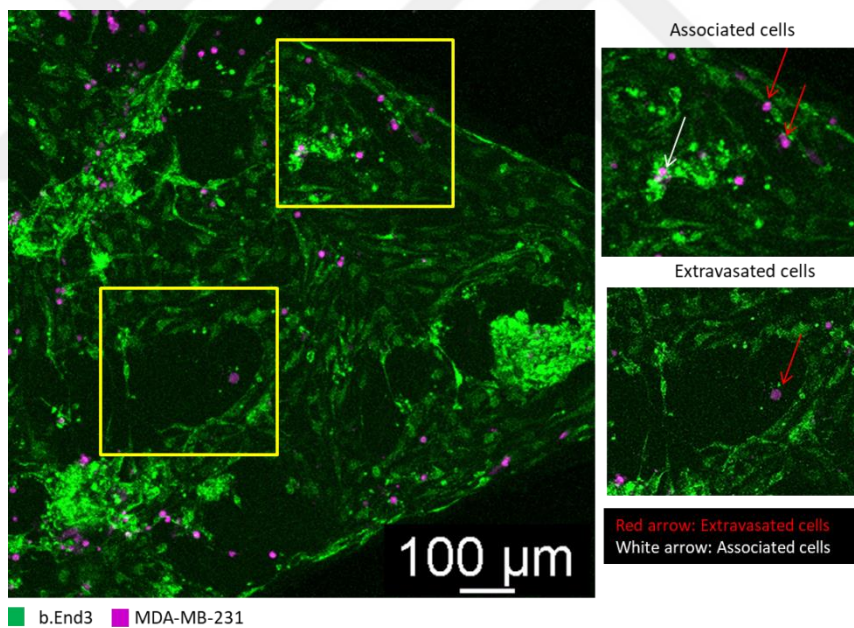


Figure 4.101. Analysis of extravasation in MVN tissue mimics.

Figure 4.100 and Figure 4.101 shows the extravasation of cells after 24 hours for tissue mimics and extravasated, associated and intravasated cells for analysis. Figure 4.101 shows the extravasation of breast cancer cells for breast and lung tissues. The results showed that more extravasated cells were observed in lung tissue mimics while more intravasated cells were counted in breast tissue. It indicates that the generation of the

lung tissue mimics was achieved when we compare the extravasation values in breast tissue as a control tissue mimic.

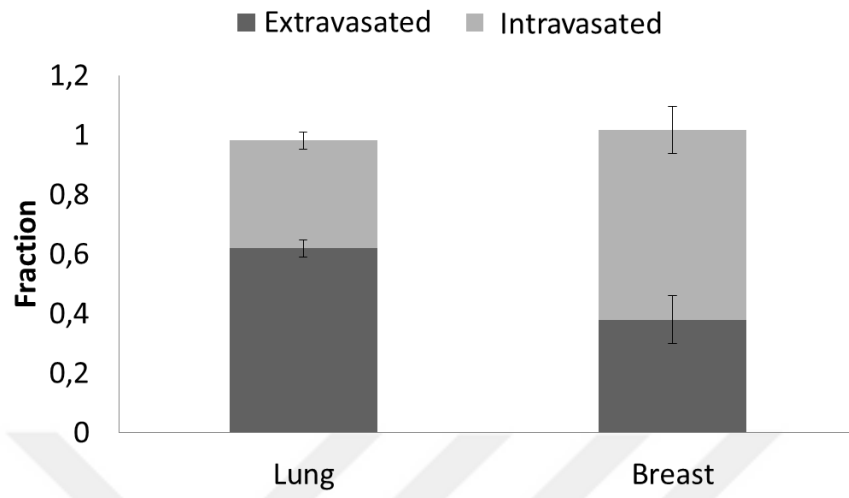


Figure 4.102. Extravasation of breast cancer cells for breast and lung tissue mimics.

CHAPTER 5

CONCLUSION

Vascularization is a critical step in tissue engineering research, which leads to generation of both functional, oxygenated healthy tissue. The control of extracellular matrix with the proliferation of cells is a challenge for the generation of a new tissue. Metastasis is the main reason for the cancer related death so the improvement of new diagnostic tools and discovery of therapeutics might affect the millions of cancer patients in the world. There is not any tool in the literature to predict the homing choices of cancer. For this reason, we focused on improving a lab-on-a-chip platform to predict the homing choices of cancer that is composed of lung and breast tissue mimics with microvascular network or endothelial monolayer structure. We optimized methods to observe homing choices related steps: invasion and extravasation. Firstly, we tested the distinct matrices such as only fibrin gel, GFR-matrigel or mixture of them with changing concentrations of fibrin gel, its' catalizator thrombin and with or without aprotinin as an enzyme inhibitor.

In this research, the different kinds of ECM materials and the mixture of them were tested for the generation of tissue mimics. Fibrinogen is a coagulant glycoprotein having a coiled-coiled structure that was formed by three crosslinked polypeptide chain. The crucial role of fibrin that presents bioactive molecules like fibronectin and FXIII by providing an environment for the attachment of distinct kinds of cells such as endothelial cells, fibroblasts and inflammatory cells ⁴². Other ECM materials such as matrigel, collagen and natural plasma cloth have been studied in angiogenesis and vasculogenesis research. Comparative studies show that fibrin provides higher values in terms of number of microvessels, both vascular and vascular wall area among the collagen and matrigel sharing the highest values with natural plasma clot ⁴³. In the light of the information in literature, we mainly used fibrin in generation of microvasculature tissue mimics. But the main disadvantage of fibrin is its' highly degradable nature. This degradation rate can be changed depending on the penetration of protease inhibitors or proteases such as matrix metalloproteinases released by cells and host tissue ⁴². We tried different approaches such as use of aprotinin as a proteinase inhibitor and mixture of fibrin and GFR-matrigel to inhibit. The results show that the invasion of cancer cells was inhibited in the presence of aprotinin in only fibrin gel. We did not use aprotinin to

observe the invasion and extravasation with engineering tissue mimics to evaluate the results comparably. The gel content optimized in the presence of collagen and matrigel with fibrin to both inhibit degradation and enhance the formation of microvascular network by using fibroblasts, epithelial and endothelial cells in tissue mimics. Scaffold both only fibrin gel and matrigel (1.15 mg/ml)-collagen (0.5 mg/ml) supplemented fibrin gels supported the formation of MVN. In addition, the component concentrations of scaffold were optimized for fibrin and thrombin. The ratio of fibrin and thrombin affects the both pore size and stiffness of the matrices that is resulted in changing diffusion of nutrients, proliferation rate and cell migration^{28,44}. We tested the ratio of 0.88 (3.5 mg/ml fibrin: 4 U/ml thrombin), 0.75 (3 mg/ml fibrin: 4 U/ml thrombin), 6 (3 mg/ml fibrin: 0.5 U/ml thrombin), 3.6 (3 mg/ml fibrin: 0.83 U/ml thrombin) for fibrin to thrombin. The ratio of 0.83 U/ml supported better MVN generation, which is nearly equal to 2 kPa of stiffness while the pore size is equal to 8 μm that is inferencial value from the literature²⁸. The results indicate that our optimized fibrin gel content with the ratio of 3.6 provided the more porous structure compare to other tested ratio and only matrigel containing gel whose average pore size is 2 μm ⁴⁵.

The tri-culture conditions were optimized for tissue mimics. The ratio of endothelial cell: fibroblast: epithelial cell was optimized as 3: 0.45: 1.45 to support the formation of MVN better within 3 days without degradation of matrix.

The deposition of fibrinogen takes place in supporting of growth factors' attachment that provides a scaffold with other adhesive glycoproteins as in a wound healing process. Therefore, this structure enhances adhesion, proliferation and migration in both angiogenesis and growth of tumor cell. The inappropriate fibrin deposition might be observed in the stroma of several tumor types but not fibrin; fibrinogen takes place within stroma in breast cancer conversely. Endogeneous synthesis of fibrinogen polypeptides from MCF-7 human breast cancer cell line was shown in the stroma of breast cancer that affects the migration of breast cancer cells⁴⁶. Our optimized fibrin gel can be also studied in further tumor microenvironment researches, which provide to understand *in vivo* like conditions effect on cell growth dissemination of tumor, and metastasis.

We optimized the method for the generation of endothelial monolayer which ensures the observation of extravasation step of metastasis. Characterization of monolayer was confirmed with the diffusion of dextran molecule. The integrity of GFR-matrigel and the mixture of it with fibrin gel were tested in terms of the diffusion of 70

kDa dextran molecule. There is not any significant difference between distinct gels. This indicates that the gel mixture of fibrin and GFR-matrigel can be also used in generation of endothelial monolayer.

Invasion of MDA-MB-231 and MD-MB-LM231 cells did not show differences for both only epithelial/fibroblasts and tissue mimics laden matrices (GFR-matrigel and mixture of it with fibrin gel). The reason might be more heterogenous population of MDA-MB-231 cells. Bone metastatic breast cancer cell line can be used to observe more tissue specific invasion for lung tissue mimics.

Tissue mimics were generated within MVN and then MDA-MB-231 was used to observe extravasation. The results show that more extravasted cells were observed in lung tissue mimics while more intravasated cells were counted in breast tissue.

For a future projection, endothelial cells can be produced by genetic manipulations which provide to have specific cells to tissues. These engineered cells and also unmanipulated endothelial cells can be used in tri-culture conditions with epithelial cells and fibroblasts to better mimic tissue microenvironment and observe the controbution of endothelial cells for both invasion and extravasation. The optimized tissue microenvironment conditions with MVN can be applied in also mimicking tumor stroma. This novel platform can present a convenient environment to study drug research in the fiels of cancer and angiogenesis.

REFERENCES

1. Hanahan, D.; Weinberg, R. A., Hallmarks of cancer: the next generation. *Cell* **2011**, *144* (5), 646-74.
2. Langley, R. R.; Fidler, I. J., The seed and soil hypothesis revisited--the role of tumor-stroma interactions in metastasis to different organs. *Int J Cancer* **2011**, *128* (11), 2527-35.
3. Weigelt, B.; Peterse, J. L.; van 't Veer, L. J., Breast cancer metastasis: markers and models. *Nat Rev Cancer* **2005**, *5* (8), 591-602.
4. Nguyen, D. X.; Bos, P. D.; Massague, J., Metastasis: from dissemination to organ-specific colonization. *Nat Rev Cancer* **2009**, *9* (4), 274-84.
5. Ali, S.; Coombes, R. C., Endocrine-responsive breast cancer and strategies for combating resistance. *Nature Reviews Cancer* **2002**, *2* (2), 101-112.
6. Debnath, J.; Muthuswamy, S. K.; Brugge, J. S., Morphogenesis and oncogenesis of MCF-10A mammary epithelial acini grown in three-dimensional basement membrane cultures. *Methods* **2003**, *30* (3), 256-268.
7. Chen, M. B.; Whisler, J. A.; Fröse, J.; Yu, C.; Shin, Y.; Kamm, R. D., On-chip human microvasculature assay for visualization and quantification of tumor cell extravasation dynamics. *Nature protocols* **2017**, *12* (5), 865-880.
8. Irmisch, A.; Huelsken, J., Metastasis: new insights into organ-specific extravasation and metastatic niches. *Experimental cell research* **2013**, *319* (11), 1604-1610.
9. Ridge, S. M.; Sullivan, F. J.; Glynn, S. A., Mesenchymal stem cells: key players in cancer progression. *Molecular Cancer* **2017**, *16* (1), 31.
10. Uccelli, A.; Moretta, L.; Pistoia, V., Mesenchymal stem cells in health and disease. *Nature reviews immunology* **2008**, *8* (9), 726-736.
11. Sun, B., Therapeutic potential of mesenchymal stromal cells in a mouse breast cancer metastasis model. *Cytotherapy* **2009**, *11*.
12. Primiceri, E.; Chiriaco, M. S.; Rinaldi, R.; Maruccio, G., Cell chips as new tools for cell biology--results, perspectives and opportunities. *Lab on a Chip* **2013**, *13* (19), 3789-3802.
13. Ozdil, B.; Onal, S.; Oruc, T.; Okvur, D. P., Fabrication of 3D Controlled in vitro Microenvironments. *MethodsX* **2014**, *1*, 60-66.
14. Qin, D.; Xia, Y.; Whitesides, G. M., Soft lithography for micro-and nanoscale patterning. *Nature protocols* **2010**, *5* (3), 491-502.
15. Huh, D.; Hamilton, G. A.; Ingber, D. E., From 3D cell culture to organs-on-chips. *Trends in cell biology* **2011**, *21* (12), 745-754.

16. Andersson, H.; Van Den Berg, A., Microfabrication and microfluidics for tissue engineering: state of the art and future opportunities. *Lab on a Chip* **2004**, *4* (2), 98-103.
17. Battiston, K. G.; Cheung, J. W.; Jain, D.; Santerre, J. P., Biomaterials in co-culture systems: towards optimizing tissue integration and cell signaling within scaffolds. *Biomaterials* **2014**, *35* (15), 4465-4476.
18. Lehmann, A. D.; Daum, N.; Bur, M.; Lehr, C.-M.; Gehr, P.; Rothen-Rutishauser, B. M., An in vitro triple cell co-culture model with primary cells mimicking the human alveolar epithelial barrier. *European journal of pharmaceutics and biopharmaceutics* **2011**, *77* (3), 398-406.
19. Song, J. W.; Cavnar, S. P.; Walker, A. C.; Luker, K. E.; Gupta, M.; Tung, Y.-C.; Luker, G. D.; Takayama, S., Microfluidic endothelium for studying the intravascular adhesion of metastatic breast cancer cells. *PloS one* **2009**, *4* (6), e5756.
20. Kim, J. B. In *Three-dimensional tissue culture models in cancer biology*, Seminars in cancer biology, Elsevier: 2005; pp 365-377.
21. Huh, D.; Matthews, B. D.; Mammoto, A.; Montoya-Zavala, M.; Hsin, H. Y.; Ingber, D. E., Reconstituting organ-level lung functions on a chip. *Science* **2010**, *328* (5986), 1662-1668.
22. Huh, D.; Leslie, D. C.; Matthews, B. D.; Fraser, J. P.; Jurek, S.; Hamilton, G. A.; Thorndike, K. S.; McAlexander, M. A.; Ingber, D. E., A human disease model of drug toxicity-induced pulmonary edema in a lung-on-a-chip microdevice. *Science translational medicine* **2012**, *4* (159), 159ra147-159ra147.
23. Jeon, J. S.; Bersini, S.; Gilardi, M.; Dubini, G.; Charest, J. L.; Moretti, M.; Kamm, R. D., Human 3D vascularized organotypic microfluidic assays to study breast cancer cell extravasation. *Proceedings of the National Academy of Sciences* **2015**, *112* (1), 214-219.
24. Bichel, L. L.; Young, E. W.; Mader, B. R.; Beebe, D. J., Tubeless microfluidic angiogenesis assay with three-dimensional endothelial-lined microvessels. *Biomaterials* **2013**, *34* (5), 1471-1477.
25. Folkman, J.; Haudenschild, C., Angiogenesis in vitro. *Nature* **1980**, *288* (5791), 551-556.
26. Kim, S.; Lee, H.; Chung, M.; Jeon, N. L., Engineering of functional, perfusable 3D microvascular networks on a chip. *Lab on a Chip* **2013**, *13* (8), 1489-1500.
27. Bang, S.; Lee, S.-R.; Ko, J.; Son, K.; Tahk, D.; Ahn, J.; Im, C.; Jeon, N. L., A low permeability microfluidic blood-brain barrier platform with direct contact between perfusable vascular network and astrocytes. *Scientific reports* **2017**, *7* (1), 1-10.
28. Chiu, C. L.; Hecht, V.; Duong, H.; Wu, B.; Tawil, B., Permeability of three-dimensional fibrin constructs corresponds to fibrinogen and thrombin concentrations. *BioResearch open access* **2012**, *1* (1), 34-40.

29. Coffin, S. T.; Gaudette, G. R., Aprotinin extends mechanical integrity time of cell-seeded fibrin sutures. *Journal of Biomedical Materials Research Part A* **2016**, *104* (9), 2271-2279.
30. Yamamoto, K.; Tanimura, K.; Mabuchi, Y.; Matsuzaki, Y.; Chung, S.; Kamm, R. D.; Ikeda, M.; Tanishita, K.; Sudo, R., The stabilization effect of mesenchymal stem cells on the formation of microvascular networks in a microfluidic device. *Journal of Biomechanical Science and Engineering* **2013**, *8* (2), 114-128.
31. Jeon, J. S.; Bersini, S.; Whisler, J. A.; Chen, M. B.; Dubini, G.; Charest, J. L.; Moretti, M.; Kamm, R. D., Generation of 3D functional microvascular networks with human mesenchymal stem cells in microfluidic systems. *Integrative Biology* **2014**, *6* (5), 555-563.
32. Weaver, V.; Bissell, M.; Fischer, A.; Peterson, O., The importance of the microenvironment in breast cancer progression: recapitulation of mammary tumorigenesis using a unique human mammary epithelial cell model and a three-dimensional culture assay. *Biochemistry and cell biology* **1996**, *74* (6), 833-851.
33. Schmeichel, K. L.; Weaver, V. M.; Bissell, M. J., Structural cues from the tissue microenvironment are essential determinants of the human mammary epithelial cell phenotype. *Journal of mammary gland biology and neoplasia* **1998**, *3* (2), 201-213.
34. Wynn, T. A.; Chawla, A.; Pollard, J. W., Macrophage biology in development, homeostasis and disease. *Nature* **2013**, *496* (7446), 445-455.
35. Shekhar, M. P.; Werdell, J.; Santner, S. J.; Pauley, R. J.; Tait, L., Breast stroma plays a dominant regulatory role in breast epithelial growth and differentiation: implications for tumor development and progression. *Cancer research* **2001**, *61* (4), 1320-1326.
36. Siddique, A.; Meckel, T.; Stark, R. W.; Narayan, S., Improved cell adhesion under shear stress in PDMS microfluidic devices. *Colloids and Surfaces B: Biointerfaces* **2017**, *150*, 456-464.
37. Wikswa, J. P.; Curtis, E. L.; Eagleton, Z. E.; Evans, B. C.; Kole, A.; Hofmeister, L. H.; Matloff, W. J., Scaling and systems biology for integrating multiple organs-on-a-chip. *Lab on a Chip* **2013**, *13* (18), 3496-3511.
38. Ono, N.; Mizuno, R.; Ohhashi, T., Effective permeability of hydrophilic substances through walls of lymph vessels: roles of endothelial barrier. *American Journal of Physiology-Heart and Circulatory Physiology* **2005**, *289* (4), H1676-H1682.
39. Jeon, J. S.; Zervantonakis, I. K.; Chung, S.; Kamm, R. D.; Charest, J. L., In vitro model of tumor cell extravasation. *PloS one* **2013**, *8* (2), e56910.
40. Zervantonakis, I. K.; Hughes-Alford, S. K.; Charest, J. L.; Condeelis, J. S.; Gertler, F. B.; Kamm, R. D., Three-dimensional microfluidic model for tumor cell intravasation and endothelial barrier function. *Proceedings of the National Academy of Sciences* **2012**, *109* (34), 13515-13520.

41. Frost, T. S.; Jiang, L.; Lynch, R. M.; Zohar, Y., Permeability of Epithelial/Endothelial Barriers in Transwells and Microfluidic Bilayer Devices. *Micromachines* **2019**, *10* (8), 533.
42. Chiti, M. C.; Dolmans, M.-M.; Donnez, J.; Amorim, C., Fibrin in reproductive tissue engineering: a review on its application as a biomaterial for fertility preservation. *Annals of biomedical engineering* **2017**, *45* (7), 1650-1663.
43. Nicosia, R. F.; Ottinetti, A., Modulation of microvascular growth and morphogenesis by reconstituted basement membrane gel in three-dimensional cultures of rat aorta: a comparative study of angiogenesis in matrigel, collagen, fibrin, and plasma clot. *In vitro cellular & developmental biology* **1990**, *26* (2), 119-128.
44. Duong, H.; Wu, B.; Tawil, B., Modulation of 3D fibrin matrix stiffness by intrinsic fibrinogen–thrombin compositions and by extrinsic cellular activity. *Tissue Engineering Part A* **2009**, *15* (7), 1865-1876.
45. Zaman, M. H.; Trapani, L. M.; Sieminski, A. L.; MacKellar, D.; Gong, H.; Kamm, R. D.; Wells, A.; Lauffenburger, D. A.; Matsudaira, P., Migration of tumor cells in 3D matrices is governed by matrix stiffness along with cell-matrix adhesion and proteolysis. *Proceedings of the National Academy of Sciences* **2006**, *103* (29), 10889-10894.
46. Simpson-Haidaris, P.; Rybarczyk, B., Tumors and fibrinogen: the role of fibrinogen as an extracellular matrix protein. *Annals of the New York Academy of Sciences* **2001**, *936* (1), 406-425.

VITA

Date and Place of Birth: 1989, İzmir/TURKEY

Education

Ph.D., Bioengineering (GPA: 3.43/4.00) | Izmir Institute of Technology | Izmir –Turkey, 2020. Thesis Title: “Engineering Target Tissue in Lab-on-a-chip Devices for Predicting Homing Choices of Metastatic Cancer”

M.Sc., Biotechnology (GPA: 3.19/4.00) | Izmir Institute of Technology | İzmir –Turkey, 2014. Thesis Title: “Invadopodia Formation on Nanometer Scale Protein Patterns”

B.Sc., Biology (GPA: 3.03/4.00) | Ege University | Izmir – Turkey, 2012

Grants

Project scholarship | The Scientific and Technological Research Council of Turkey (TÜBİTAK) 115E057 | 2015-2019.

Priority Areas Research Scholarship | The Scientific and Technological Research Council of Turkey (TÜBİTAK) BİDEB 2211-C | 2019-2021.

Scholarship | Council of Higher Education (YÖK) 100/2000, Tissue Engineering and Biomaterials| 2016-2021.

Peer-reviewed Journal Articles

Firatligil-Yildirim, B., Bati-Ayaz, G., Tahmaz, I., Bilgen, M., Pesen-Okvur, D., & Yalcin-Ozuysal, O. (2020). Homing Choices of Breast Cancer Cells Revealed by Tissue Specific Invasion and Extravasation Lab-on-a-chip Platforms. *bioRxiv*.

Onal, Sevgi, Merve Turker-Burhan, Gizem Bati-Ayaz, Hamdullah Yanik, and Devrim Pesen-Okvur. "Breast cancer cells and macrophages in a paracrine-juxtacrine loop." *Biomaterials* 267 (2020): 120412.

Bati-Ayaz, Gizem, Ali Can, and Devrim Pesen-Okvur. "Cellular distribution of invadopodia is regulated by nanometer scale surface protein patterns." *European Journal of Cell Biology* 96, no. 7 (2017): 673-684.

Bati, Gizem, and Devrim Pesen Okvur. "Invadopodia: proteolytic feet of cancer cells." *Turkish Journal of Biology* 38, no. 6 (2014): 740-747.